AN ABSTRACT OF THE THESIS OF

Danielle N. Runion for the degree of Master of Science in Soil Science presented on June 8, 2018.

Title: Effects of Biofilm on Sandy Soil Hydrology

Abstract approved: _____

Maria I. Dragila

It is known that soil biota affects water dynamics through various complex mechanisms. The impact on retention by soil biota are due to a combination of changes to pore geometry, pore clogging by biofilms, biofilms that serve to connect thin water films across many pores as the soil dries, and to changes in the properties of the biofilm during the drying process. This study explored the physical properties of biofilm in a natural sandy soil. Specifically, we studied the role that microbial exudates play in water retention during drainage and in water connectivity during evaporation. During early stages of evaporation, pores containing biofilm support capillary flow through a continuous liquid network that delivers water up to the soil surface. This enhanced connectivity by microbial exudates extends the duration of Stage I evaporation and increases the depth of the drying front. As matric potential increases, microbial stresses may result in alterations to the biofilm and how it interacts with soil moisture, subsequently changing

pore scale transport mechanisms. During drainage, soils with biofilm held more moisture than an abiotic soil in which the biofilm had been destroyed. The study confirmed that biofilms may serve an important role in sandy soils by providing a connected network for water delivery to roots in a porous media with otherwise low capillary potential.

Effects of Biofilm on Sandy Soil Hydrology

by

Danielle N. Runion

A THESIS

submitted to

Oregon State University

in partial fulfillment of
the requirements for the
degree of

Master of Science

Presented June 8, 2018
Commencement June 2019

Master of Science thesis of Danielle N. Runion presented on June 8, 2018.

APPROVED:

_____

Major Professor, representing Soil Science

_____

Head of the Department of Crop and Soil Science

_____

Dean of the Graduate School

I understand that my thesis will become part of the permanent collection of Oregon State University libraries. My signature below authorizes release of my thesis to any reader upon request.

_____

Danielle N. Runion, Author

ACKNOWLEDGEMENTS

The writer wishes to express her deepest appreciation to the following individuals who have contributed to the completion of this study:

Dr. Maria I. Dragila. Professor, Soil Physics, for sharing her passion, knowledge, guidance, and constant encouragement as a research advisor.

Dr. Ruijun Qin, Assistant Professor, Extension Agronomist, for his constant support and guidance as a committee member.

Dr. Claire L. Phillips, for her helpful suggestions, advice, and constant support as a committee member.

Dr. Todd Jarvis, Director, Institute for Water and Watersheds, for showing constant support as a graduate council representative.

Stephanie Nolasco, M.S. in Soil, for collaborating, giving advice, and working together as team throughout the research process.

Shannon Andrews, Manager 1-R&D Lab, for constant support and advice during the research process.

Gloria M. Ambrowiak, Faculty Research Assistant, for sharing her knowledge and guidance throughout my research process.

Special thanks are given to the number of graduate students, faculty in the Crop and Soil Science department, and Central Analytical Lab who offered advice, support and aided with data collection as well as lab analysis during this endeavor.

TABLE OF CONTENTS

Page

LIST OF FIGURES

LIST OF TABLES

Chapter 1: Introduction

1.1 Objective

The purpose of this study was to understand how biofilms in sandy soil affect water movement. The long-term goal is to improve agricultural management for water scarce regions. Water transport mechanisms in sandy soil are complex, and historically processes have been investigated as abiotic relationships. In fact, the soil physics community has well understood the abiotic relationship between porous media and its capillary function. Yet we know that there are other factors impacting water transport throughout the vadose zone. Understanding the mechanisms by which water dynamics are impacted by microbial exudates is important for success towards water conservation. To determine the effects of biofilms, samples of biotic soil and abiotic soil were examined and compared. The biotic soil was collected from the field in grab samples and stored in a cooler to preserve the biology until experimental use. The abiotic soil was also collected as grab samples from the same location but treated with hydrogen peroxide to eliminate all biological matter. The biotic contributions to water retention in sandy soil were measured through comparison to the water held abiotically with focus on the drying cycle, particularly evaporation and drainage. During evaporation, it was expected that microbial exudates in the biotic sample would extend the capillary fringe due to a sustained connected water phase, permitting deeper extraction of water. This would result in extraction of more water overall during the evaporation process. The moisture content in the capillary fringe was expected to be higher than the abiotic sample because water is held in extracellular polymeric substances. Additionally, biofilms may affect the pore-size distribution by cementing particles together creating microaggregates. This could change the water movement throughout the soil, and it is important to compare the abiotic to biotic pore-size distributions to explore what mechanisms are

influencing evaporation dynamics. Microbial exudates should increase water retention during drainage if biofilms of the biotic soil hold more water than is adsorbed in films of the abiotic soil. A static stepwise experiment used to map the long-term drainage process allowed for the quantification of the total water energy; thus, partitioning drainage into capillary and osmotic contributions. This confirmed how much more water is retained by osmotic forces in the biotic sample. Another goal was to examine how microbial exudates influence the hydraulic conductivity of the media.

1.2 Theory

Unsaturated soil is composed of solid, liquid, and a gas phases that in this paper are denoted by the subscripts, *s*, *w*, and *g*, respectively; in this case, the liquid phase will always be water. The unsaturated soil has a total volume (V_{tot}) which is occupied by fractions of each of these phases; depending on texture and soil water content, each phase has its own density (ρ). The bulk density (ρ_b) is the dry mass of the soil (m_s) divided by the total volume (V_{tot}).

$$\rho_b = \frac{m_s}{V_{tot}} \qquad [1]$$

The solid phase is comprised of the mineral components with an average particle density (ρ_p) of 2.65 g/cm^3 (Jury and Stolzy 2018). In soils without 2:1 clays, the percent porosity (ϕ) will not vary with moisture content and therefore can be defined as equal to the saturated moisture content (θ_s). Porosity can also be calculated by one minus the bulk density (ρ_b) divided by the particle density (ρ_p).

$$\phi = \theta_s = \left[1 - \left(\frac{\rho_b}{\rho_p}\right)\right] \qquad [2]$$

Soil water content is the basic parameter that characterizes the hydrologic status and controls water transport in the vadose zone. It is usually defined by the amount of water removed by drying at 105°C and in this study all water was removed in this manner. The result of this determination will express the mass ratio of water (m_w) to the dry mineral component (m_{ds}) which is called the gravimetric moisture content (ω).

$$\omega = \frac{m_w}{m_{ds}} \qquad [3]$$

Water content has influences on physical properties and processes. When dealing with water transport, the water content in the soil is often represented volumetrically; this is called the volumetric moisture content (θ).

$$\theta = \frac{V_w}{V_s} = \omega \frac{\rho_b}{\rho_w} \qquad [4]$$

where (v_w) is the volume of water, (v_s) is the volume of the soil, (ρ_b) is the bulk density, (ρ_w) is the density of water, and (ω) is the gravimetric moisture content. The degree of saturation (S) is another way to represent the water content in the soil and is found by dividing the volumetric moisture content (θ) by either the porosity (ϕ) or by the saturated moisture content (θ_s), which are equivalent in non-swelling soils.

$$S = \frac{\theta}{\phi} = \frac{\theta}{\theta_s} \qquad [5]$$

The three mechanisms that bind water to the soil matrix are adhesion which binds water to the mineral surface by London and van der Waals forces, capillary action which binds water as the combination of adhesive and cohesive forces and controls its energy status by interfacial curvature and tension, and osmotic binding in diffuse double layers (Jury and Stolzy 2018). By

these matric forces, soil can retain water against evaporation and gravity. Understanding water movement in soil often requires the calculation of the evaporation rate. In this case the following equation was used to calculate evaporation rate (E) in cm/day

$$E = \frac{\Delta V_w}{\Delta t} \Big/ A \qquad [6]$$

where the (ΔV_w) is the change in volume of water, (Δt) is the time interval for ΔV_w, and (A) is the cross-sectional area of the evaporating surface. In this case, the HyProp was used and the cross-sectional area was equal to

$$A = \pi {r_c}^2 \qquad [7]$$

where (r_c) is the radius of the cylinder. The equivalent depth of the drying front (L_{DF}) is also calculated to determine the length of the capillary fringe at the time of transition between stage 1 and 2 of evaporation. The capillary fringe is not completely dried because moisture is left behind during the drying process. The amount of water left behind has to be taken into account. The drying front depth can be found by taking the volume of water lost (ΔV_w) during evaporation and dividing it by the cross-sectional area [eq.7] and multiplied by the difference between the total porosity (ϕ) and the volume of remaining water at the transition from stage 1 to stage 2 evaporation (V_{rw}).

$$L_{DF} = \frac{\Delta V_w}{A(\phi - V_{rw})} \qquad [8]$$

Three fundamental soil water equations effectively explain water dynamics in a porous media: Young-LaPlace, Darcy's law and Richards Equation (Hillel 1998). The British scientist Thomas Young (1773-1829), and Pierre-Simon Laplace (1749-1827), are credited with the

formation of the Young-Laplace equation (Kirkham 2014). The equation describes the capillary pressure difference that occurs across a curved interface between air and water. For a circular capillary tube, the pressure difference (ΔP) between the capillary water and the atmosphere is expressed by the following:

$$\Delta P = \frac{2\sigma}{r} = \frac{2\sigma cos\beta}{R} \qquad [9]$$

where (R) is the radius of the capillary tube, (σ) is the surface tension, and (r) is the radius of curvature of the interface. In a capillary tube, this interface between water and air creates a meniscus which has a contact angle (β) between liquid and tube. It was assumed that the liquid, in this case water, will wet the surface. As it is pulled through the tube, the meniscus will be concave with respect to the air phase and the contact angle is expected to be less than 90°. For simplifying purposes this equation was used with zero contact angle ($cos\beta = 1$), a common assumption made during drying. A relationship between water pressure and pore radii can be obtained using as a model of the geometry of a vertical capillary tube that balances the upward force due to surface tension by the weight of the water. Therefore, the capillary pressure (ψ in units of Pascal) or the capillary tension head (h in length units) is obtained from the height of the capillary rise (h) and is equal to

$$\psi = -\frac{2\sigma}{R} \quad \text{or} \quad h = \frac{2\sigma}{g(\rho_w)R} \qquad [10]$$

where (R) is the capillary radius, (g) is the acceleration of gravity, (σ) is the surface tension, and (ρ_w) is the density of water. This demonstrates that pores desaturate at tensions inversely proportional to their size. The smaller the radii of curvature of the meniscus created by a pore, the greater the capillary rise or capillary pressure required to drain that pore (Hillel 2012). Using

this equation and carefully selected assumption, the pore-size distribution has been used to create a simple form of the Soil Water Characteristic Curve - SWCC (Tuller and Or 2005). Using the concept of the Young-Laplace equation, in which pores will drain if their radii is equal to or greater than the corresponding applied capillary head. These particular conceptual models were used along with a representation of the pore geometry as a bundle of capillary tubes in order to form the SWCC (Tuller and Or 2004). The SWCC is the relationship between soil water tension (h) and the volumetric moisture content (θ) of the sample. The (h-θ) relationship therefore is a function of the pore size distribution. Using the same conceptual model of the soil as a collection of capillary tubes, the time it will take for pores of specific sizes and larger to desaturate can be calculated. In the experiments described later, where soil is allowed to drain to a controlled value of head, the desaturation time for pores corresponding to the applied head value is here called the *equilibration time*. Flow properties through these pores can be quantified using Darcy's law. By definition the velocity through a saturated cylindrical pore ($\bar{v}$) is equal to the specific discharge (q) which is given by Darcy's law [eq. 11a]. The value of the hydraulic conductivity (K) can be obtained from the Poiseuille Equation [eq.11b]. It then follows that the time for water to drain through the pore a distance (d) is given by Equation 11c.

$$\bar{v} = \frac{q}{f} = K\left(\frac{\Delta H}{d}\right) \qquad [11a]$$

$$K = \frac{k}{\mu} = \frac{R^2}{8\mu} \qquad [11b]$$

$$t = \frac{d}{\bar{v}} = \frac{d8\mu}{R^2}\left(\frac{d}{\Delta H}\right) = \frac{8\mu d^2}{\Delta H R^2} \qquad [11c]$$

Symbols are defined as, the viscosity of the fluid (μ), the average velocity ($\bar{v}$) within the saturated pore, distance (d) traveled over time (t), the Darcy flux or specific discharge (q), pore

radius (R), total head gradient applied (ΔH), the hydraulic conductivity (K) and the porosity that for a single saturated pore $f = 1$. Eq. 11c can be applied to the problem of a soil sample draining from saturation, where drainage is controlled by a hanging water column set at a head of h_c. The pressure head determines the size of the smallest pore to drain, pores smaller than that will stay saturated. For this case, the distance traveled by the water is the length of the soil sample, d = L, and the time (t) becomes the *equilibration time* (t_{eq}) for the experiment. At time of equilibration, $\Delta H = h_{bottom} - h_{top} = (h_c) - (h_c - L) = L$. The smallest pore draining has a radius of $R(h_c)$, which is given by Eq. 10. Substituting these concepts into Eq. 11c yields the *equilibration time* (t_{eq}) for capillary desaturation of the pore with radius $R(h_c)$ in terms of measurable parameters [eq. 12].

$$t_{eq} = \left(\frac{\rho_w g h_c}{2\sigma}\right)^2 8\mu L \qquad [12]$$

If water continues to drain after the equilibration time, then the excess water held in the pore can be associated with film flow, which is controlled by osmotic forces. During the stage of capillary drainage ($t < t_{eq}$), both films and capillary water are draining, and their relative contribution cannot be separated by this method; it is only after the capillary drainage stage ($t > t_{eq}$) during which film flow can be isolated. Film water speed depends on film thickness, with a film of thickness D draining at the same rate as a water in a pore whose radius is $R = D$. Therefore, films that drain after the equilibration period are likely to have thicknesses $D < R(t_{eq})$. Films impacted by biological material may exhibit slower speeds caused by increases in effective viscosity. Therefore, biofilms with thickness greater than $R(t_{eq})$ may be draining after the equilibration time. Although we know that the natural porous media is more complex than a capillary tube (Tuller and Or 2004), relating this simple approach can in fact be a useful technique when

examining adsorbed and biotic films. The hydraulic properties can also be found using additional equations and compared with the previous technique. In 1980, van Genuchten proposed a parametric model for the SWCC where he related the effective saturation (Θ) to the matric potential by incorporating the Mualem model into an equation that used observed data to define the parameters (Van Genuchten 1980). This parametric model is commonly used today. Key parameters can be obtained using RETC (pc-progress.com) computer software to analyze the soil water retention curve and hydraulic properties needed to generate a fitted (h-θ) curve to the measured data (Genuchten *et al.* 1991). Once the parameters for the soil are obtained, the effective saturation, Θ, can be calculated,

$$\Theta = \frac{\theta-\theta_r}{\theta_s-\theta_r} = \left[\frac{1}{1+(\propto h)^n}\right]^m \qquad (m=1-1/n) \qquad [13]$$

where m is given by the Mualem constraint. The residual volumetric moisture content is represented with θ_r, it can be measured experimentally from extremely dry soil or predicted by extrapolating low moisture contents by extending the moisture retention curve. The saturated volumetric moisture content is θ_s, the matric potential is h, α is associated with the inverse of the air entry pressure, and n is related to the steepness of the curve and dependent on the pore size distribution. Prior to the van Genuchten model, Mualem produced a model to predict the hydraulic conductivity in unsaturated media derived from prior knowledge of the SWCC (Mualem 1976). Using the effective saturation, the relative hydraulic conductivity, $K_r(\Theta)$ can then be obtained.

$$K_r(\Theta) = \Theta^{1/2}\left[1-(1-\Theta^{1/m})^m\right]^2 \qquad (m = 1-1/n) \qquad [14]$$

$$(0 < m < 1)$$

van Genuchten then expressed the relative hydraulic conductivity in terms of pressure head by substituting in [eq.13] into [eq. 14] which is seen in [eq.15] (Van Genuchten 1980).

$$K_r(h) = \frac{\{1-(\alpha h)^{n-1}[1+(\alpha h)^n]^{-m}\}^2}{[1+(\alpha h)^n]^{-m/2}} \qquad \text{(m = 1-1/n)} \qquad [15]$$

Calculating the relative hydraulic conductivity function is useful because in unsaturated soil $K_r(h)$ changes with h, during the drainage process.

A second method for quantifying K is to use the Darcy-Buckingham equation. Buckingham (1916) expanded the relationship that was formulated by French engineer Henry Philibert Gaspard Darcy (1803-1858) in 1856, which was developed to quantify flow through saturated sands, making it applicable to unsaturated media (Kirkham 2014). The equation is used to calculate the saturated and unsaturated hydraulic conductivity, *K*, of a porous media. The volume of water (*V*) flowing through the media over time is proportional to the pressure gradient ($\frac{\Delta H}{L}$) and the cross-sectional area (*A*), with the constant of proportionality the hydraulic conductivity (*K*)

$$\frac{V}{t} = Q = \mathrm{K(h)A}\frac{\Delta H}{L} \qquad [16]$$

The equation can be rearranged to calculate the hydraulic conductivity of the media (K).

$$K(h) = \frac{QL}{A\Delta H} \qquad [17]$$

The hydraulic conductivity is a media and fluid property that depends on the intrinsic permeability of the media, degree of saturation, as well as the density and viscosity of the fluid (Kirkham 2014).

1.3 Hypotheses and Conceptual Model

Biofilms

Bacteria are found in two different forms, either freely existing in the bulk soil solution, planktonic, or sessile where the bacteria are attached to the surface (Costerton and Lewandowski 1995). The sessile population growing on surfaces often reside within the confinement of a biofilm to increase chances of community survival (O'Toole *et al.* 2000).

The growth process and development of the biofilm is complex, often regulated by properties of the substratum, cells, and environmental factors (Donlan 2002). Water is necessary for nutrient accessibility thus becomes essential for microbial growth yet it also influences factors that impact formation such as the presence of cations, antimicrobial agents, regulation of temperature and pH (Stewart 2003). The unit itself is established in stages where the planktonic bacteria adhere to the soil particle, then aggregate together to form micro-colonies that excrete extracellular polymeric substances (EPS) to provide an environment ideal for protection against environmental stresses, the exchange of genetic material, as well as cell to cell communication by means of quorum sensing (Vu *et al.* 2009).

The components of EPS are comprised of polysaccharides, proteins, lipids, and nucleic acids which entangle together to make up the intracellular space in the biofilm matrix (Flemming and Wingender 2010). The complex mixture of biopolymers surrounding microbial cells create a heterogeneous structure that has a unique porosity and permeability contrary to the surrounding conduit (Stewart 1998). Adding further complexity, the rheology of the biofilm has been found to be viscoelastic, having the capacity to maintain a highly hydrated state (Billings *et al.* 2015b). Voids created by the intertwined components as well as the viscoelastic properties alter the hydrodynamics of the system via transport mechanisms (De Beer and Stoodley 1995). Stoodley

et al. observed liquid flow through water channels permeating within the biofilm and flowing through porous medium channels (Stoodley *et al.* 1994). Flow was detected to follow the path directed by the channels and at times went against the current of the bulk flow, suggesting nutrient transport via the channels (De Beer *et al.* 1994). In 2015, via fluorescence microscopy and nuclear magnetic resonance, fluid was observed being transported through channels confirming flow within biofilms (Billings *et al.* 2015b, 2015a).

During further stages of drying, properties of the biofilm may be altered as a result of stress factors causing changes in the behavior of the bacteria within the complex matrix (Roberson *et al.* 1993; Chenu 1995; Stewart and Franklin 2008). Stewart suggested at this point that water does not actually flow through the biofilm clusters but moves slowly around them instead (Stewart 2012). The rhizosphere processes are therefore impacted by the water status of the system; more water is retained within the biofilm by the elastic tension rather than being transported throughout the pore spaces.

It is noteworthy that the water dynamics could also be affected by the changes to the rhizosphere processes, which would also change the means by which the water can be extracted from the pores. It is important that we explored both ways in which water could be removed from the system, therefore evaporation and drainage were investigated to understand how biofilms were affecting the drying cycle.

Evaporation

I. Hypotheses:

    a. Microbial exudates increase water loss during evaporation.

b. Microbial exudates increase the depth of the capillary fringe.

c. Moisture content in the capillary fringe is greater with microbial exudates.

II. Hypothesized Mechanisms:

a. Biofilm may sustain a connected water phase against more negative matric tensions than an abiotic film, permitting deeper extraction of water.

b. Hydraulic conductivity supporting evaporation will drop off very rapidly in the abiotic soil.

c. The drying front moves down faster in the biotic soil to support the same potential evaporation as the abiotic soil, because more water is being left behind in the drying fringe, water that is held by EPS.

III. Expected Results:

a. The first stage of evaporation will be extended for the biotic soils.

b. Net loss of water will be greater in the biotic soil.

c. Moisture content within the drying fringe will be higher in the biotic soil at the end of first stage evaporation.

Gravitational Drainage

I. Hypothesis:

a. Microbial exudates change soil pore structure, affecting the SWCC.

b. Microbial exudates increase water retention during drainage.

d. Hydraulic conductivity of a biotic soil will be lower at low matric potentials.

II. Hypothesized Mechanisms:

a. Biofilm acts as a cementing agent, creating micro aggregates which in turn form larger pores thereby affecting drainage behavior.

b. Biofilms have the capacity to hold large quantities of water due to their viscoelastic properties and due to internal biofilm porosity created by their intertwined components.

c. Biofilms contain polysaccharides, proteins, lipids, and nucleic acids, entangling together to adsorb more moisture inside the pores created by the intertwined compounds. Water drains slower due to more overall moisture being held in these pore spaces and the decrease in permeability.

III. Expected Results:

a. The pore size distribution of the biotic soils will show greater relative abundance of large pores due to micro-aggregation.

b. In a drainage experiment under controlled pressure head the biotic soil will release more water than the abiotic sample.

c. During drainage the biotic sample will have a higher hydraulic conductivity at early time due to large pore spaces, followed by a decreased hydraulic conductivity compared to the abiotic sample.

1.4 Background

The influence of organic matter (OM) on water retention has been highly controversial, with some experiments showing no effects and other showing substantial differences (Rawls *et al.* 2003; Minasny and McBratney 2018). The bulk density of the soil is directly impacted by OM content. In fact, bulk density is often regarded as a better predictor of water retention parameters than OM content as it also takes into account management practices and land use (Zacharias and Wessolek 2007). Although it is well known that OM will increase the water holding capacity, the mechanisms by which this happens are still under investigation (Bauer and Black 1981; Díaz-Zorita and Grosso 2000; Rawls *et al.* 2003). In fact, research has found that OM content is only influential to water retention at certain matric potentials; others found that OM only influences water retention in certain soil textures, particularly with substantial effects in coarse textures (Calhoun *et al.* 1973; Hollis *et al.* 1977; Bauer and Black 1981). Rawls et al. (2003) found that coarse textured soils with high organic carbon content had on average higher water retention than samples with fine-textured soil with similar organic carbon content. The larger abundance of smaller pores in finer textured soils may mask the effect of the organic matter because its capillary conductivity is likely to be small. It is clear that the variable impacts of OM on water retention could be due to the textural class the experiments were performed on. When the media is composed of a coarser material, it does not have as many small capillaries so a greater impact on water retention may be observed.

Root and microbial exudates have been an area of recent investigation into the mechanisms of OM impacts. Mucilage or root exudates are mostly composed of polysaccharides but also contain lipids (Carminati *et al.* 2016). Microbial exudates or biofilms are also composed primarily of polysaccharides but have varying amounts of lipids, proteins, DNA and vitamins. The lipid portion of these exudates is thought to be responsible for reducing the surface tension

of soil water (Read *et al.* 2003) whereas the polysaccharides possess the capacity to adsorb water. This ability of polysaccharides to retain water far exceeds that of clays, with water holding capacities reaching more than 70 g of water per gram of polysaccharide (Or *et al.* 2007). The rheology of exudates, reduced surface tension and increased viscosity, allows for the persistence of long liquid filaments between particles at very negative water potentials (Carminati *et al.* 2017). These long liquid filaments provide a connected water phase so as the surrounding soil continues to dry, the moisture content remains higher where the exudates are present. Mucilage is found within rhizosphere soil at concentrations ranging from 0.01 to 1% by mass with the highest near the root tip (Bengough 2012). Previous research has found that EPS in soils constitute 0.1 to 1.5% of the soil organic matter (Cheshire 1979). Although both root and microbial exudates make up a small percentage of soil mass in the vadose zone, these exudates have the potential to drastically alter soil hydraulic properties, specifically water retention and hydraulic conductivity. The amount of biofilm and mucilage in the soil will depend on several factors, some of which include: the soil water content, exudation rate, access to substrate, temperature fluctuations, length of root systems and soil structure. In fact, previous research has found that water flow, substrate transport and biofilm growth are tightly coupled (Rosenzweig *et al.* 2014). Modeling of exudates has shown that hydraulic properties are affected but depend specifically on soil texture similar to the OM research. The spatial distribution of biofilms also impacts observed changes. High concentrations, typically seen in model exudates, such as xanthan, *Capsells sp*. seed, scleroglucan, polygalacturonic acid, and chia seed, often show exaggerated effects of preferential pore clogging, improved mechanical stability and increased water retention (Czarnes *et al.* 2000; Traore *et al.* 2000; Zhang *et al.* 2008; Barré and of Science 2009; Peng *et al.* 2011; Naveed *et al.* 2018). Biofilm growth can also occur within pore-spaces

which can then bind particles together and effect the pore size distribution split. Some numerical models account for exudates that uniformly grow/spread throughout the media and predict increasing influence on the hydraulic properties (Rosenzweig *et al.* 2014). Both numerical models and experiments using model exudate materials have given us a greater understanding of biofilm/mucilage dynamics through time yet there are few evaluations of natural biofilms occurring in agricultural soils.

1.5 Experimental Approach

The goal of this experiment was to partition the contribution to water retention provided by biotic and abiotic soil components. The following points were investigated.

(1) Biofilm effects on evaporation dynamics

(2) Biofilm effects on water retention during free drainage

(3) Biofilm contribution to osmotic water

(4) Microbial exudate's effect on the hydraulic conductivity of the media.

To address these points, three experiments were performed:

(1) "Simple evaporation method experiment" addresses point 1

(2) "Free drainage experiment" addresses points 2 and 4

(3) "Stepped retention experiment" addresses point 3

Chapter 2: Materials and Methods

2.1 Overview

Three experiments were preformed to quantify the role of biofilms on water dynamics: the HyProp machine was used to characterize soil water potential and conductivity during evaporation, the hanging water column with head control was used to quantify retention during controlled drainage, and the hanging water column was also used to quantify free drainage.

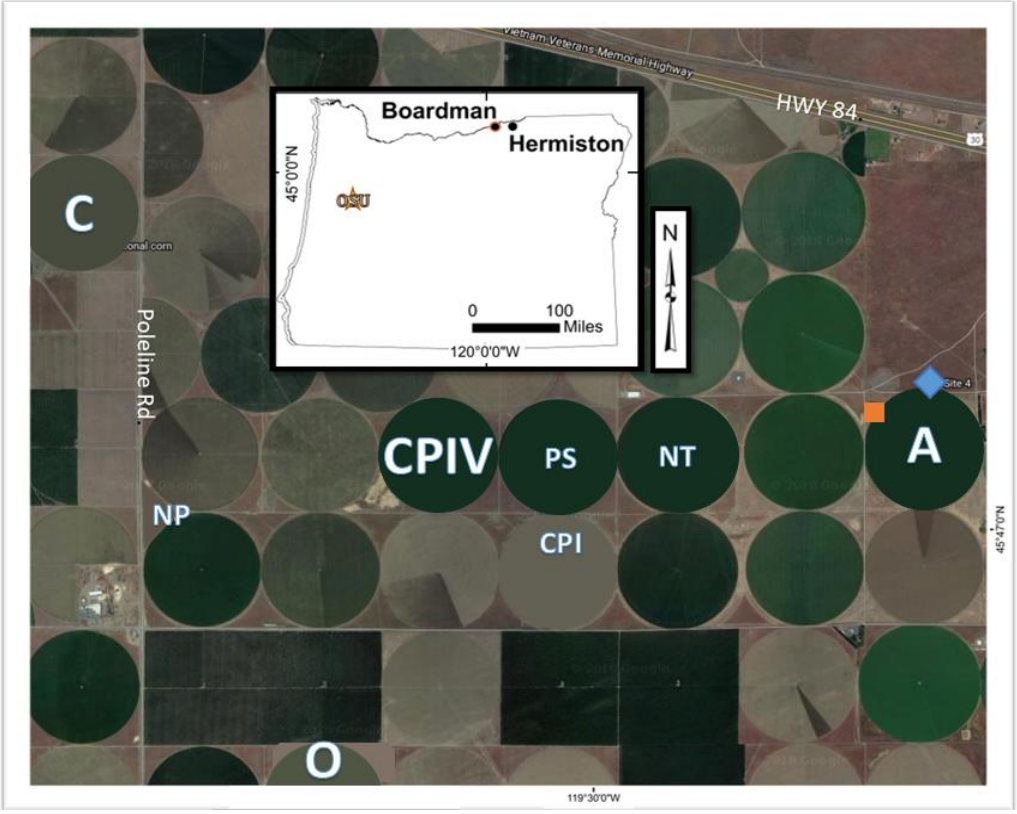

Figure 1. Map of field sites where Quincy soil was collected. All locations are in Morrow County, Oregon. The circle plot that was planted in alfalfa, marked with an A, will be the focus in this paper. Sample sites: indicated by the orange square marker is site 5 which is Alfalfa I, and the blue diamond marker is site 4 which stands for Alfalfa II. Circle Plot IV will also be investigated for a portion of this study which is indicated by the initials CPIV. All other labels correspond with table 1.

We collected soil in the Quincy soil series, a loamy sand soil classified as a *mixed, mesic Xeric Torripsamments*, from several agricultural fields located in Morrow County, Oregon. Soil samples were collected in March of 2016, December 2016 and July 2017 (Table 1). A subset of these samples are being used for this study.

Table 1. The following is a list of soil samples collected throughout this study. The bold indicates the sample location that are used in this study. Sample ID, description and date collected are indicated below.

Sample ID	Description
Alfalfa I	Site 4 (45.791815, -119.470425) Northern location on Holzapfel Ranch. Owned by Larry Carroll and located at the end of Desert Road in Irrigon, OR. One bucket collected on July 2, 2017 from 0-30 cm.
Alfalfa II	Site 5 (45.789954, -119.475652) Western location on Holzapfel Ranch. Owned by Larry Carroll and located at the end of Desert Road in Irrigon, OR. Two bags collected on July 2, 2017 from 0-30cm.
Circle Plot IV	CP4 (45.787558, -119.517631) Field site was planted in wheat and samples were collected March 4, 2016. Sample numbers 23, 24 and 25 were homogenized.

These locations were specifically chosen because they are high crop production areas in Oregon utilizing sustained intensified agricultural management practices. Understanding the fundamental soil processes of the area will potentially give insight to improve productivity in other semi-arid to arid regions with coarse textured soil. Sampling was first taken from circle plots that were originally chosen for the project. In March 2016, soil from Circle Plot IV was collected from a field that was in wheat crop rotation. In December 2016, samples were taken from the Native pit, No-till field site, Poplar field site and Conventional tillage field site. In May of 2017, new field sites were chosen to achieve long term project goals which were being limited by grower collaboration. Therefore, in the Summer of 2017, soil samples from the new field sites were collected. There are four current active sites for the Quincy Project under the control of two growers; one site each presently growing in Onion, Corn and two sites in Alfalfa (Figure 1). Soil samples were taken from all 4 site locations for future analysis. The 2 sites from the Alfalfa plot will be analyzed in this paper both of which are located in the same circle plot but were selected because of differences in soil texture. The Alfalfa circle plot is in a low tillage crop rotational

system which has a significant amount of manure applied before each rotation (wheat-alfalfa-grass / grass-corn-wheat) (Nolasco 2018). This plot belongs to the Holzapfel Ranch who is owned by Larry Carroll. The average amount of water applied to the field per year is around 32 inches (Nolasco 2018). In addition to the Alfalfa sites, soil samples from Circle Plot IV were also used for the HyProp experiment. The results will be discussed in this paper yet future sampling from CPIV location is no longer permitted.

2.2 Treatments to obtain an abiotic soil specimen

Soil hydraulic properties were investigated for the two Alfalfa field sites and Circle Plot IV. To understand the biotic component, it was necessary to establish an abiotic specimen for comparison. All soil samples were sieved through a 2 mm sieve with visible roots and rock fragments removed. Two treatments were selected to generate an ‘abiotic soil’. One treatment consisted of soaking the soil in ethanol. The rationale was that this would disrupt the biofilm components and kill the microbial community. The ethanol treatment was used on Circle Plot IV soil sample.

However, there are indications that this only dehydrates the biofilm, which can then be regenerated to some degree following rehydration. This ethanol treatment was completed on the soil collected from Circle Plot IV (CPIV). The CPIV soil was placed in a 15" x 10" Pyrex dish inside the fume hood. Ninety-five percent ethanol was poured on the soil until the sample was completely drenched with ethanol. The saturated soil solution was left to evaporate in the fume hood for twenty-four hours to remove all ethanol. The soil was then placed in the oven for twenty-four hours at 105 degrees Celsius. Sample was remoistened to approximate field moisture content by adding deionized water. This treatment for an abiotic sample did not give the necessary results therefore it was no longer pursued.

The second technique used to generate an abiotic sample, was using thirty percent hydrogen peroxide. This method was used for samples from the two Alfalfa sites. After sieving, the soil was soaked in hydrogen peroxide for a total of 48 hours. In order to prevent loss of sediments from rapid bubbling, the reaction was contained in a bath of cool water, slowly adding more hydrogen peroxide after bubbling had settled. Addition of hydrogen peroxide aliquots continued until no reaction occurred or bubbling had subsided, and then the soil continued to soak for the remaining twenty-four hours inside the fume hood to eliminate any remaining hydrogen peroxide through evaporation. The specimen was then placed in the oven at 105 degrees Celsius for twenty-four hours.

2.3 Soil treatment for biotic soil specimens

To protect soil biology, field soil samples (grab samples) were kept in a cool room at field moisture content until used for the experiment.

2.4 Simplified Evaporation Method (SEM)

The simplified evaporation method (SEM) was chosen as the method to determine the soil hydraulic properties of the biotic and abiotic samples because it has been well-established and commonly used among researchers to investigate evaporation, water retention curve and hydraulic conductivity. The procedure used the HyProp device (METER Group Inc., 2015).

Analyzing results from this methods depends on assumptions that can be violated during the evaporation process, such as spatial linearity in pressure head and water fluxes (Peters *et al.* 2015). Because past research highlighted concerns, with the validity of this method for some textures, specifically sandy soils, certain measures were taken to ensure the computer-generated data was correct. Particularly in coarse textured medias, the pressure difference between the lower and upper tensiometers becomes non-linear as the soil continues to dry. When calculating

a combined tension, the arithmetic mean of these tensiometers would not be sufficient during the later stage of evaporation. Peters et al. (2015) found that combining the geometric mean with the arithmetic mean by a weighing parameter to control the shift between the two as the soil dries is the best way to account for the non-linearity.

The following equations from Peters et al. (2015) were used to calculate the mixed tension between the lower and upper tensiometers. Three methods for calculating the tension are used: the arithmetic mean [eq.18], the geometric mean [eq.19], and the weighted average [eq.20]. The arithmetic mean ($\bar{h}_{ari}$) is calculated by

$$\bar{h}_{ari} = 0.25(h_{1,i-1} + h_{1,i} + h_{3,i-1} + h_{3,i}) \quad [18]$$

where the symbols are top tension at time one ($h_{1,i-1}$), top tension at time two ($h_{1,i}$), the bottom tension at time one ($h_{3,i-1}$) and bottom tension at time two ($h_{3,i}$). The geometric mean is calculated by

$$\bar{h}_{geo} = \frac{\sqrt{(h_{1,i-1}+h_{1,i})\cdot(h_{3,i-1}+h_{3,i})}}{2} \quad [19]$$

The mixed tension accommodates for the fact that over some tension range the arithmetic mean is considered exact, while over drier tension ranges the geometric mean is considered more accurate. The mixed tension ($\bar{h}_{mix}$) uses the weighted average (W_{avg}) to control the tension range over which one or the other averaging methods dominates. The weighted average is equal to the inverse of the tension gradient.

$$W_{avg} = \frac{1}{\nabla h} \quad [20]$$

The mixed tension ($\bar{h}_{mix}$) is found by combining Equations 18, 19, 20.

$$\bar{h}_{mix} = W_{avg}\bar{h}_{ari} + (1 - W_{avg})\bar{h}_{geo} \quad [21]$$

Using Equation 21, for the soil moisture tension calculations the evaporation method proves to yield reliable results.

Estimates of hydraulic conductivity during evaporation can also be obtained by simply inverting Darcy's equation and using the above equation for mixed tension [eq. 21]. To calculate the hydraulic conductivity between two time points using the HyProp it is assumed that the flow of water content between the two tensiometers is the same throughout the cross-sectional area (A), therefore it can be calculated from the volume of water loss (ΔV_w) at the center of the column determined by weight changes. The following equation is used:

$$K(\bar{h}_{mix}) = -\frac{{}^{1}/_{2}\left({}^{\Delta V_w}/_{\Delta t A}\right)}{\left({}^{\Delta h}/_{\Delta z}\right)+1} \qquad [22]$$

where (Δh) is the difference between tensions of the top and bottom tensiometer, (Δz) is the distance between the top and bottom tensiometer (Figure 2) and (Δt) is the time interval between both points. The above equation is the theoretical basis behind the HyProp conductivity data evaluation which is provided with the HyProp-Fit software (Pertassek *et al.* 2011). The simplified evaporation method (SEM) was completed with the Hydraulic Property Analyzer (HyProp machine) to achieve two goals. First, it was used in conjunction with the Dewpoint Potentiometer (WP4C, METER Group, Inc.) to determine the soil water characteristic curve. To find an analytical expression for the soil water characteristic curve, RETC program (Genuchten *et al.* 1991) was used to generate van Genuchten parameters [eq.8] for the measured data with the mixed tension calculations from the HyProp machine. Because tension range of the HyProp Device is limited, a different laboratory method needed to be used to obtain values that would help pin down the residual moisture content and more accurately control the RETC fit. Values for tensions greater than 800 hPa, data was obtained using a Dewpoint Potentiometer (WP4C,

METER Group Inc., 2015) in collaboration with Stephanie Nolasco for both abiotic and biotic samples.

The Dewpoint Potentiometer (WP4C) uses the chilled mirror dew point method for accuracy and speed of measurements. The sample is placed in a chamber where the vapor pressure in the atmosphere trapped above the sample equilibrates with the water energy of the sample yielding a relative humidity value of the air (ERH) that is equal to the water activity (Aw) of the sample. As the temperature of the chamber is forced to decrease, a sensor detects the first point in which condensation occurs on the mirror inside the device and the dew-point temperature is measured. To determine the water activity the dew-point and temperature are used, shown in the following equation

$$ERH\% = Aw \cdot (100) \qquad [23]$$

The measurement range for the Dewpoint Potentiometer is around 0-1 MPa to 49 MPa. This allowed for a better estimate of the residual moisture content in the biotic and abiotic samples. The measured data from the WP4C was combined with the subsampled data collected with the HyProp and input into RETC software for the regression analysis. This software uses the collected data points to estimate the van Genuchten fitting parameters by a nonlinear least squares parameter optimization method (Genuchten *et al.* 1991).

Secondly, the HyProp was used to explore evaporation dynamics in abiotic and biotic soil samples. The schematic illustration of the HyProp is shown in (Figure 2). The device uses transient measurements of the soil specimen's mass, which is measured with the UMS HyProp analytical balance (±0.001 g). Tensiometer shafts installed within the soil at two depths transduce the matric potentials of the soil specimen through the porous ceramic tip to a water

filled shaft which is connected to high-accuracy pressure transducers within the sensor unit (Figure 2). Transducers measure tensions to an accuracy of ±0.15 kPa. For the pressure to be transduced, air must be eliminated from the water in the system prior to data collection. The HyProp Refill Unit by METER Group, Inc. was used to degas the water in the system (Figure 3).

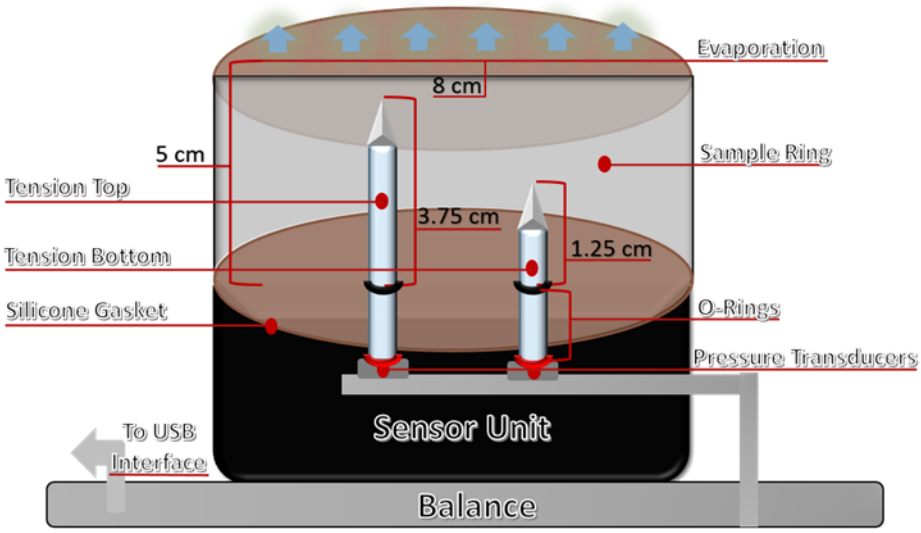

Figure 2. Schematic illustration of Hydraulic Property Analyzer containing a top tensiometer with the height of 3.75 cm and a bottom tensiometer with a height of 1.25 cm. Each tensiometer is connected to the pressure transducers in the sensor unit. The diameter of the soil specimen is 8 cm and the vertical offset of the tensiometers allows for measurements in pressure gradients.

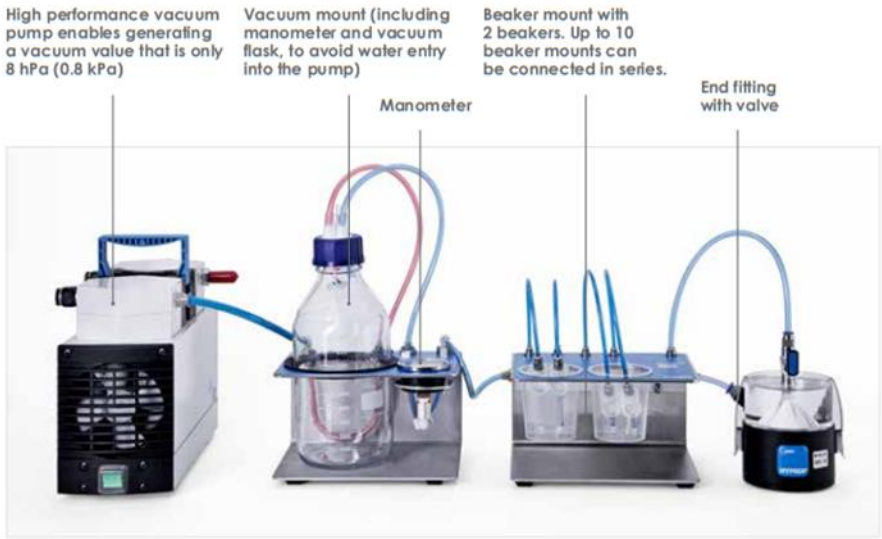

Figure 3. HyProp Refill Unit was used for degassing the water in the tensiometer shafts and the pressure unit. The containers with the tension shafts and the holes of the sensor unit were filled with de-aired, deionized water. The sensor unit and tensiometers were connected to the Refill Unit, turning on for 5 minutes and off for 55 minutes. Totaling for a minimum of 24 hours to ensure device is completely degassed. (Image from HYPROP Manual, METER Group, Inc. 2015)

Once the system is degassed, the experiment is initiated by inserting the tensiometers into the soil and uncovering the sample. The combined instrumentation tracks changes in moisture content and tension, occurring as a result of evaporation over time from the surface of the soil specimen. The UMS HyProp balance is connected via USB interface to a laptop computer where the HyProp datalogging software is running (Figure 6). Data is collected through the measurement wizard at approximately 60 second intervals.

2.5 Preparation Details for HyProp

Biotic soil specimens for the HyProp experiments were prepared at field water contents. Each sample was sieved through a 2 mm sieve removing all rock fragments and visible roots (Figure 4, C).

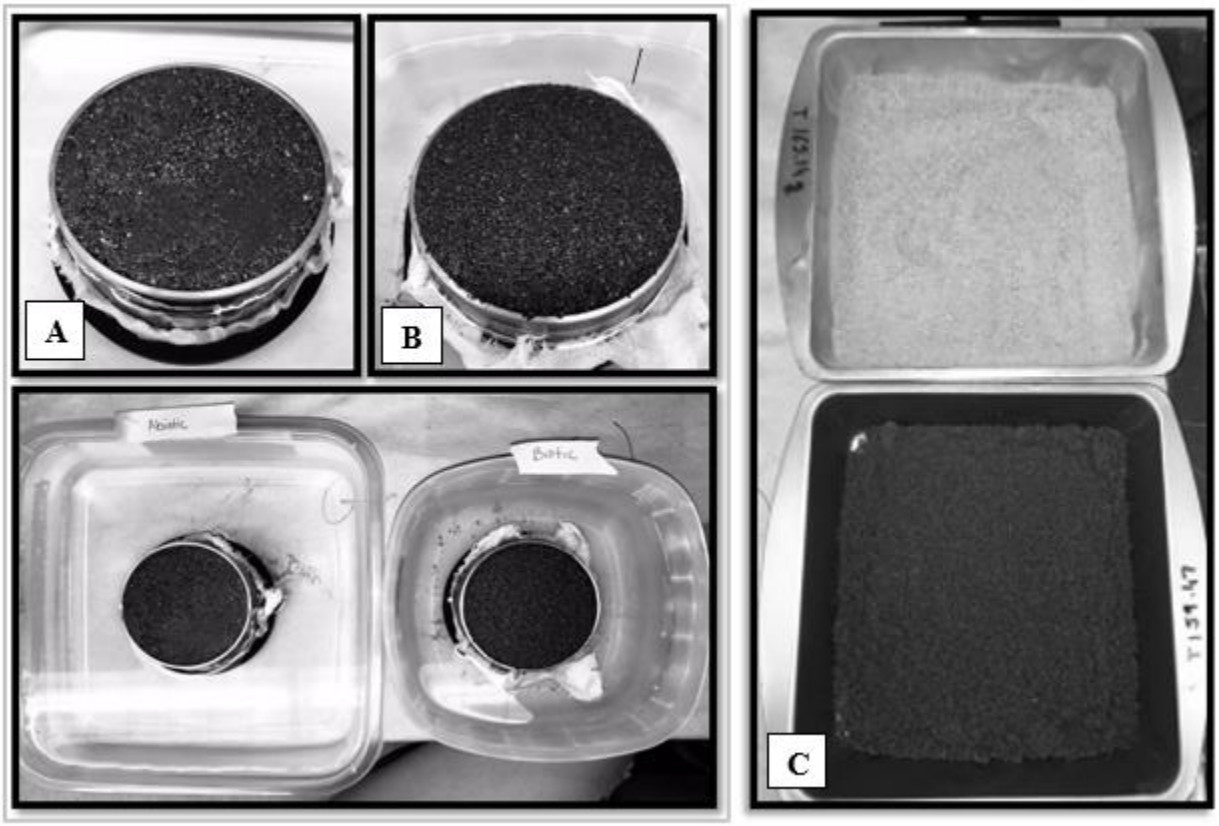

Figure 4. Abiotic (A) and Biotic (B) soil specimens soaking in 1 cm of water during saturation preparation for HyProp. Soil has been packed inside sample ring to approximate bulk density and placed on cheese cloth then

saturation plate. Image (C) shows both soil specimens in the fine earth fraction, top container abiotic treatment and bottom container biotic prior to packing.

The cylinders were packed to field bulk densities, which required prior knowledge of the initial moisture values of the soil sample. A sub sample of the soil was taken to calculate the field moisture content prior to preparation. Once the approximate moisture content was calculated, the approximate mass needed to fill the sample ring was calculated to achieve the field bulk density within the sample ring of volume 250 cm^3. The plastic cap was then placed on the sample ring on top of the mass balance, and the weight was then tared. Soil was packed uniformly inside the sample ring to the approximate bulk density. The top was gently scrapped with a knife to ensure a flat, uniform soil surface. The cap was placed on the cutting edge of the sample ring and placed upside down on the table. The other plastic cap was removed and replaced with cheese cloth. The sample was then placed upside down on the saturation plate and the other plastic cap (from the cutting edge) was removed. Specimen was then placed in 1- cm of water to fully saturate for twenty-four hours (Figure 4. A, B). Once the specimen is saturated, the soil can be prepared for the insertion of the tensiometers (Figure 5). First the tensiometers were connected to the sensor unit to monitor the pressure while entering the sample ring. The sensor unit was carefully detached as well as the tensiometers from the Refill Unit ensuring that the meniscus is built up on top of each tension shaft. The sensor unit was connected to the USB adaptor to the laptop interface where the HYPROP View Software was running. After clicking on the “Refilling” icon, the silicon gasket was placed on top of the sensor unit. A silicone cap filled with deionized water was placed on the ceramic tips while gently screwing in each tension shaft into the sensor unit. Once the red O-Ring in the sensor unit begins to seal the tension shaft to the pressure transducer, pressure increases rapidly but never exceed 2000 hPa and was monitored via the wizard on the screen. The zero-point potential was then checked by removing the silicone cap,

then placing a water drop on each ceramic tip after both shafts were completely screwed into the sensor unit, screen then indicated zero potential. To ensure that the tensiometers were reading correctly, the speed of the reading was checked by uncapping the silicone cap and waving a paper to create air flow on each ceramic tip.

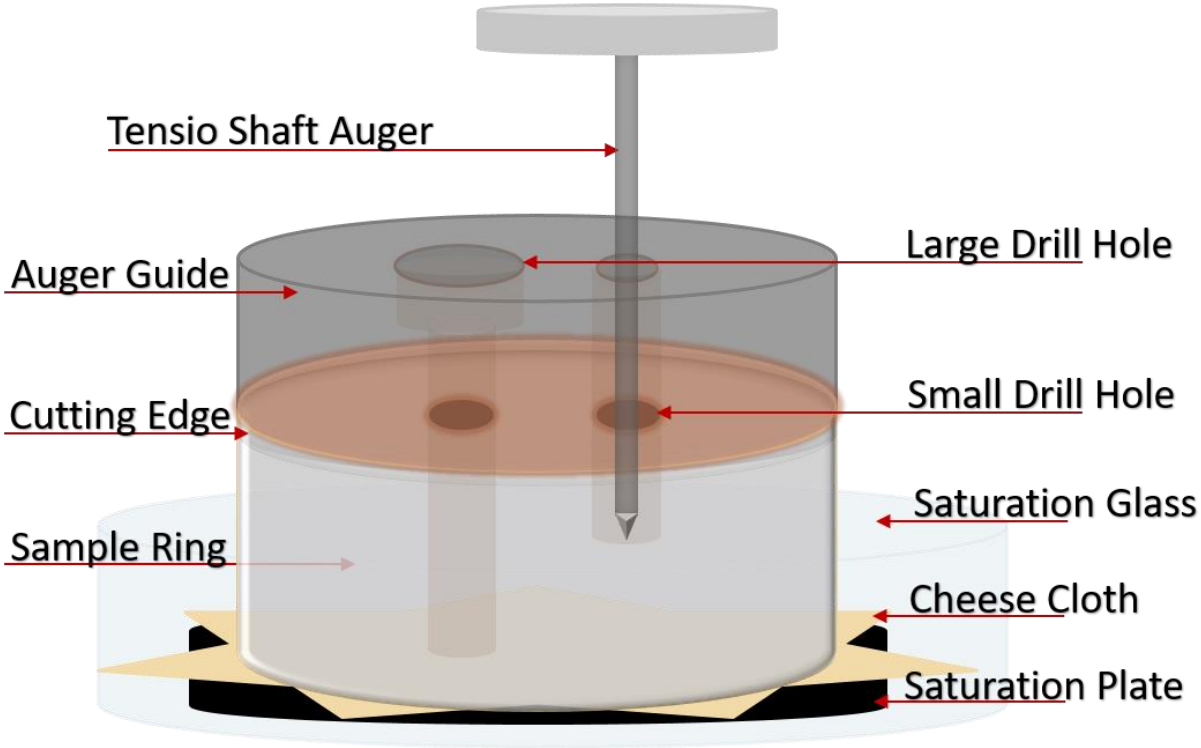

Figure 5. Schematic illustration of the soil specimen during HyProp preparation. Prior to saturation, the sample ring (with soil specimen) must be placed on top of the saturation plate with cheese cloth in between and completely saturated for at least twenty-four hours. After specimen is fully saturated, the auger guide is placed on top of the sample ring's cutting edge. Using the tension shaft auger, soil is removed from the small drill hole to a depth of 1.25 cm below the surface and the large drill hole which is 3.75 cm below the soil surface.

The tubing was recapped immediately and refilled each with deionized water. These steps were repeated to prepare the next two sensor units. The program was in multi-balance mode, which allows one senor unit per balance (Figure 7). Once the soil was removed with the auger, degassed water was used to fill the holes to prevent any air from being pushed into the specimen upon insertion of tensiometers. The sensor unit with tension shafts attached, was now carefully flipped upside down and inserted into the designated holes (Seen in Figure 6). After flipping the

specimen over again, the saturation plate and cheese cloth was removed to reveal the soil surface where evaporation will occur.

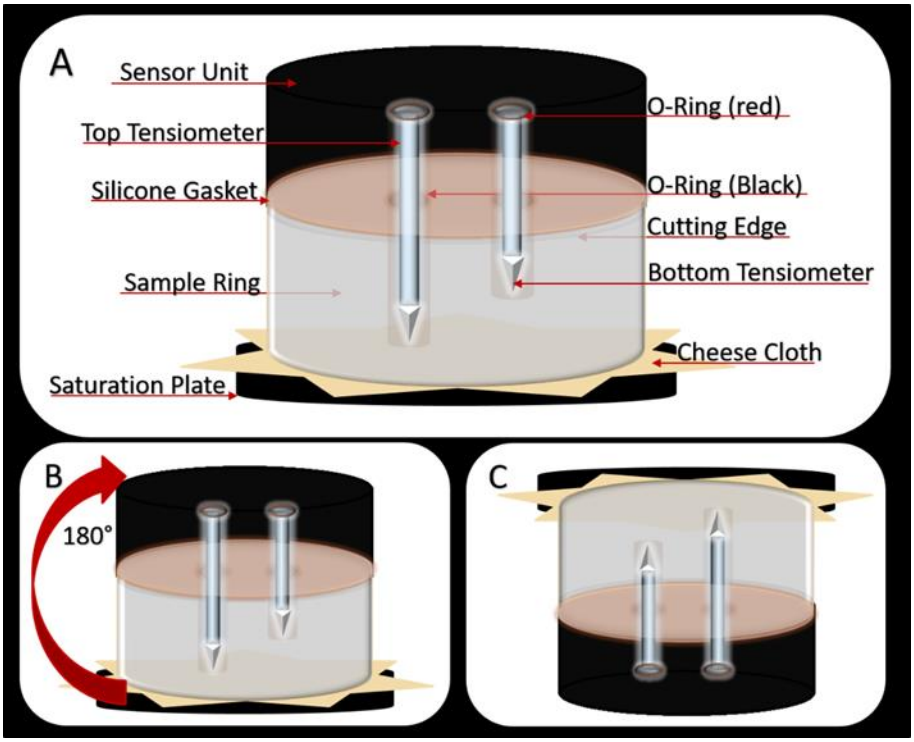

Figure 6. Schematic illustration of sensor unit with both top and bottom tensiometers carefully inserted into the soil specimen. Tensiometers are attached into the pressure transducer through designated holes created by an auger. The silicone gasket is placed in between the sensor unit and bottom of soil to prevent any dirt from entering the pressure transducer. The red O-Rings inside the sensor unit are for sealing while the black O-Rings placed on the tension shafts are used for dirt protection. After inserting the tensiometers into the sample ring, the whole assembly is turned 180° and the saturation plate with cheese cloth is removed to uncover the evaporation surface of the soil specimen.

Finally, the clips are connected from the sides of sensor unit onto the sample ring. The specimen was then placed on the Hyprop balance connecting a cable to the sensor unit, the magnet clamp to the balance and the other end of the cable into the Hyprop balance. The USB cable was plugged into the Hyprop balance and into the laptop (Figure 7). After the three specimens are prepped and connected to the designated balance, the devices showed up via the device tree. In the Hyprop software, each sample was named according to field site location and treatment type. Then the data was collected on the three samples starting at the same time from the Hyprop software. Cores were allowed to evaporate for approximately two weeks depending on each soil

specimen. Then the device was disconnected from Hyprop balance after data collection was finished.

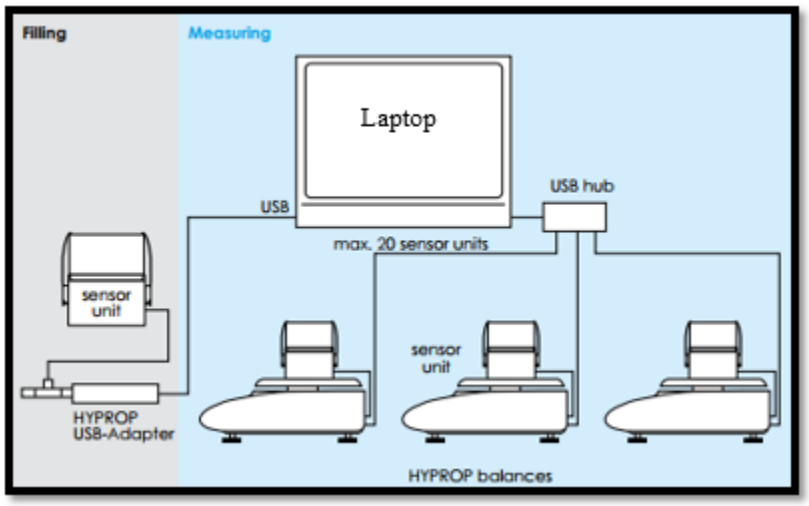

Figure 7. Schematic illustration in the Hyprop Manual depicting connections of the sensor units via USB adapter to laptop for "Refilling" wizard. The above image also shows the multi-balance mode, seen in the measuring light blue area, where one sensor unit is measured on its own individual Hyprop balance connected through a USB port to the laptop (Edited image from HYPROP Manual, METER Group, Inc. 2015).

Once data collection was completed, the soil was removed from the sample ring and either oven dried immediately at 105°C for 24 hours for measurement of the dry soil weight, or it was used on another experiment run and then oven drying was performed at the end of all runs, to avoid impacting the biological component. The value of the dry soil mass was entered into the HyProp-Fit software to accurately evaluate the data collected by system's program. If the dry weight of the sample is not obtained immediately after data collection, the HyProp-Fit software will estimate this value by assuming the initial water content entered is the saturated value therefore, it is not necessary to immediately oven dry the sample. Since all samples were coarse textured and saturated for twenty-four hours, the initial value of the water content was usually equal to porosity even after entering in the dry weight. The error for the estimation of the initial water content can change with texture and in practice the initial water content is rarely saturated thus

the dry weight should be used for the calculation of water contents. The first two runs were oven dried immediately to obtain the exact dry weight, yet the final run was not dried until all experimental testing was done with the hanging water column (Table 5).

2.6 Preparation Details for the Hanging-Water-Column

The soil samples used for the last run on the HyProp were removed from the HyProp sample rings and stored in the cooler until further analysis with the hanging-water-column apparatus. The same cores were used for evaporation and drainage experiments to eliminate subsample variability as well as variation between treatments, in turn allowing the data from each experiment to be comparable.

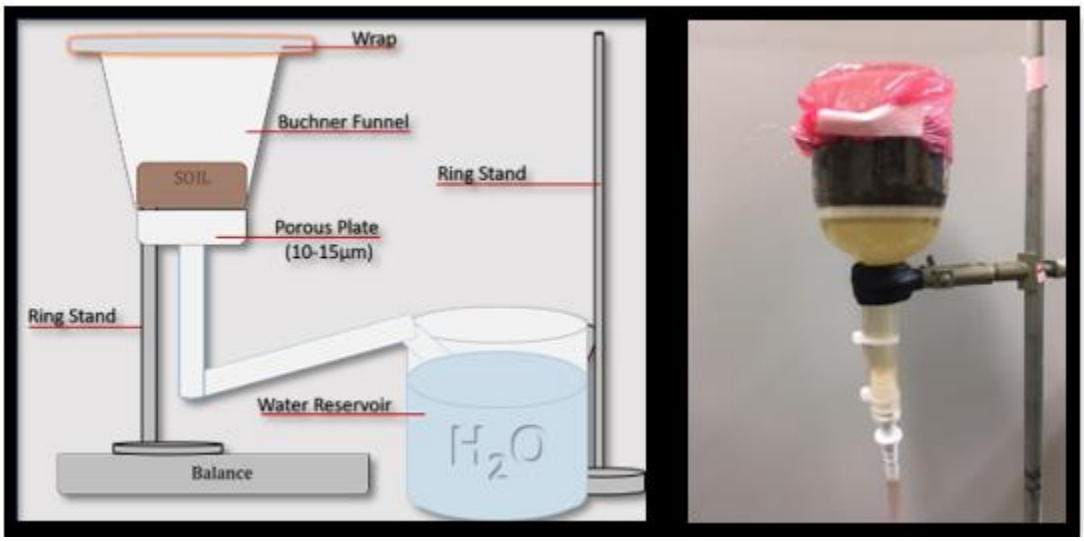

Figure 8. The left is a schematic illustration of the hanging-water-column. The right image is a photograph of the actual experiment with the soil specimen in the Buchner funnel with the plastic wrap around the top.

Water retention curves are usually measured by using either a pressure plate, where pressure is applied above the sample or by tension funnel, where tension is applied by a hanging-water-column. The water retention curve can be measured on one sample over the entire low-tension range (<200 cm) using the tension funnel. The maximum tension for our experiment was constrained by the bubbling pressure of the funnel's ceramic plate, which was about 90 cm.

Because the HyProp tests the same range, the two data sets can be compared. Although the tension range is similar to the HyProp, the hanging-water-column will be investigating drainage properties instead of evaporation. The tension funnel allows a fully saturated soil to slowly drain by gravitational forces. The following procedures give a precise method of measuring a water retention curve for low tension (0- 60 cm) using the hanging-water-column method. The amount of water released is determined by weighing. The initial moisture content of the soil is determined at the end of the experiment after drying in the oven at 105°C for 24 hours, from which also the moisture content at each capillary head can be calculated.

Three separate hanging-water-columns were set up to run concurrently, to investigate the drainage properties of Alfalfa II – abiotic, Alfalfa II – biotic, and Alfalfa I – biotic. Each hanging-water-column uses a Buchner Funnel that has a ceramic plate of 10 – 15 micron pores. The funnel is attached to sterile tubing that is filled with deaired water. All remaining air was eliminated from the system prior to use. The tubing extends to a water reservoir which could be moved to different heights during the experiment. The funnel was attached to a stand that was placed on a mass balance connected to a data logger. To calculate the mass of the water lost (ΔM_w) during the experiment, the equipment mass (M_E) was measured and the HyProp estimated dry mass of each soil specimen was used initially to calculate the mass of the water (M_w) retained (moisture content of the sample); final values were recalculated after the soil was oven dried. Each sample from the Hyprop, was taken from the cooler and sieved through a 2 mm sieve to restore the soils original form. The specimens were then carefully placed in the Buchner Funnels. The height (L) of each sample was measured with the diameter (d) of the funnel to calculate the volume of soil for each specimen. The water reservoir was then moved upward to 1 cm above the porous plate to allow the soil specimens to saturate via capillarity. The accuracy is

slightly limited by the fact that the amount of water released by the soil at each tension head is determined volumetrically. To eliminate water loss due to evaporation, a plastic film with tape was placed over the tension funnel. The samples were then saturated and allowed to desaturate for 24 hours at 60 cm of tension. This permits capillary rearrangement of soil particles prior to running the experiments. As will be discussed, in hindsight it may be best to run the wetting and drying cycles twice to complete the rearrangement of soil particles and development of the soil's hierarchical drainage structure.

Table 2. Table of symbols and measurements taken initially and during each hanging-water-column experiment.

Initial Measurements	
M_E	Mass of Equipment
M_{DS}	Mass of Dry Soil
M_{E+DS}	Mass of Equipment + Dry Soil
V_{DS}	Volume of Dry Soil
L	Height of Soil Cylinder
d	Diameter of Tension Funnel
A	Cross-sectional Area
Measurements During Experiment	
M_{E+DS+W}	Mass of Equipment + Soil + Water
h	Capillary Head
Δt	Total time allowed for drainage
M_w	Mass of Water

2.7 Static Stepwise Retention

The hanging water column method was used to quantify drainage under controlled tension. Three samples were tested concurrently: Alfalfa I – biotic (Port VII), Alfalfa II – biotic (Port IV), and Alfalfa II – abiotic (Port I). To determine how long it would take for the soil to equilibrate during the stepwise retention experiment, we decided to use a simple calculation which involves a few assumptions. Using the capillary bundle theory, the pore space is assumed to be a

collection of capillary tubes. We can then use [eq.10] to find each pore radii associated with the capillary pressure applied. First assumption is that only pores of equal or larger radii will drain. The *equilibration time,* or total time for pores to drain, is then calculated using Equation 12. It was found that pores draining at tensions below 50 cm head will drain in less than three hours. From that, two experiment times were selected. An experiment lasting three hours would drain all capillary water and an experiment lasting much longer, i.e., twelve-hours, may allow also for films held by osmotic forces to also drain. The time increments of three-hours and twelve-hours were used as hold times for each tension adjustment. First, the experiment consisted of holding the soil specimens at a tension for a 3-hour drainage period, then lowering the water table to the next tension value without re-saturating the soil, and holding that tension for 3-hrs, and so on. This stepwise experiment was completed twice for the following series of controlled heads: 1cm, 10cm, 20cm, 25cm, 30cm, 35cm, 40cm, 60 cm. The data collected was compared to two other stepwise retention experiments which were performed identically except the time allowed for drainage was increased to 12-hour increments. The first 3-hour test was run after one wetting and drying cycle was completed with all three samples on January 29, 2018. Because the order of the experiments may be relevant in the interpretation of results, the following is summarized:

Table 3. Dates for the Stepwise Retention experiment, with the associated data port labels, that were run during each event. (raw data is labeled by port number). The hold time indicates the length of time allowed for the soil to drain between tension level reset. For each event, three ports were used that correspond with the following sample ID: Port 1 – Alfalfa II – abiotic, Port IV- Alfalfa II – biotic, Port VII – Alfalfa I – biotic.

Event #:	1			2			3			4		
Date:	2/3/2018			2/7 -2/11			2/13-2/16			2/17/2018		
Hold Time:	3 Hour			12 Hour			12 Hour			3 Hour		
Port:	I	IV	VII	I	IV	VII	I	IV	VII	I	IV	VII
Sample ID:	A-IIa	A-IIb	A-Ib	A-IIa	A-IIb	A-Ib	A-IIa	A-IIb	A-Ib	A-IIa	A-IIb	A-Ib

Throughout the experiments, the abiotic system was carefully watched to ensure it was free of contamination. If the tubing or any equipment at any time during the experiments appeared to develop growth indicating potential biological contamination, then the equipment and soil sample needed to be sterilized again. The sterilization procedure involved exchanging tubing for sterile tubing, new de-aired water introduced, and soil rinsed with 95% ethanol, poured directly onto the soil and allowed to drain through the funnel after it is detached from the contaminated tubing. This was repeated three times to ensure that the soil returned to its abiotic status. The use of hydrogen peroxide at this time would involve removing the soil from the funnel which would disturb the pore size distribution and cause error from mass loss. To ensure the results would continue to be comparable across experiment runs, it was decided that ethanol would be the best choice as it would allow the soil to remain in the funnel yet still reduce biotic growth. After rinsing with ethanol, the new sterile tubing system was re-saturated and connected to the tension funnel again.

2.8 Dynamic Drainage

The hanging water column set up was used, but this time the water reservoir was placed at sixty centimeters and the soil was allowed to drain for seventy-two hours. The drainage experiment was performed three times, with the same three soil samples, Alfalfa I – biotic, Alfalfa II – biotic, and Alfalfa II – abiotic, running concurrently.

Procedure

1. Saturate sample by placing water reservoir 1 cm above the top of the soil surface.

2. Soil surface appears glistened when saturation has been reached.

3. Clamp tube tightly on each column prior to moving water reservoir to 60 cm.

4. Check program on laptop to ensure that mass of equipment plus soil and water is being recorded.

5. Move each water reservoir so that the water table is at 60 cm. Once the ring stands are secured, unclip each clamp holding the tubing below the tension funnel.

6. Set timer for three hours for placement of the plastic wrap around the top of the funnel and allow system to drain for the remaining designated time.

A problem arose during event #2. An air bubble formed beneath the ceramic plate of the tension funnel. The other two columns, Alfalfa I - biotic and Alfalfa II - biotic, continued to run for the 72 hours. After deairing the abiotic system, all three columns experienced a wetting and drying cycle to test the equipment. After ensuring that everything was in fact working correctly, all three samples were saturated again, and two more experiments were run. For those runs, the soil was covered with plastic wrap after the first three-hours of drainage to eliminate the influence of evaporation. The wrap plus tape was added to the mass of the equipment and this new weight was taken into consideration when calculating the mass of water loss over time. The following table shows the dates of the dynamic drainage experiments with the asterisk on event two to indicate when the air entered the abiotic equipment.

Table 4. Dates of the dynamic drainage experiments with the same soil used in the Stepwise experiment, indicated by Port number. Each event corresponds to the run number. The tension was set to 60 cm and allowed to drain for the associated hold time. The sample ID indicates the crop (A – alfalfa), followed by the site location (I or II) and treatment type (abiotic or biotic).

Event #:	1			2*			** Equipment Check	3			4			5		
Date:	3-Feb			26-Feb				2-Mar			6-Mar			13-Mar		
Hold Time:	36 Hours			72 Hours				72 Hour			72 Hours			72 Hour		
Port:	I	IV	VII	I*	IV	VII		I	IV	VII	I	IV	VII	I	IV	VII
Sample ID:	A-IIa	A-IIb	A-Ib	A-IIa	A-IIb	A-Ib		A-IIa	A-IIb	A-Ib	A-IIa	A-IIb	A-Ib	A-IIa	A-IIb	A-Ib

*Alfalfa – IIa (Port I) is missing data because of an equipment malfunction, allowing an air bubble to form below the ceramic plate.

** Equipment retested by re-saturating and draining samples once. No data was collected during this retest run.

Chapter 3: Results

Results are organized as follows: First, section 3.1 discusses all the physical properties of the samples tested; these are summarized in Table 5 as well as Table 6. Sections 3.2 and 3.3 present results from HyProp experiments providing two types of information: Evaporation data (Section 3.2) and Moisture Retention data (Section 3.3). Sections 3.4 – 3.6 discusses the results of drainage experiments. Section 3.4 presents the drainage-based moisture retention curves comparing results from experiments that stepped through different tension levels every three hours to results where the tension steps were taken every twelve hours. Section 3.5 discusses the proportion of water that is being held by films found by comparing the time increments of the three-hour period which is associated with capillarity and the twelve-hour period which has both capillary and film flow. Section 3.6 has the results of the hydraulic conductivity during drainage and Section 3.7 discusses the results from the dynamic drainage experiment, free drainage set to 60 cm.

3.1 Soil Physical Properties

Each sample has a dry mass (taken after sample was dried at 105°C for 24-hrs), initial moisture content, porosity, and bulk density values (Table 5). This table is shown first because the order and timeline in which these experiments took place are important for the discussion as well as the analysis of the results.

Table 5. Combined information from all of the data collected from the HyProp experiments. Includes the samples name, treatment type, the physical properties, starting and ending date/time of each sample as well as the total run time in days.

HyProp Sample Information											
Sample Name:	Treatment Type:	Sample ID:	Dry Mass (g)	ρ (g/cm^3)	Φ	Initial θ	Start		End		Total
							Date	Time	Date	Time	Time
CPIV	Biotic	QH -1	417.54	1.68	0.37	0.3716	29-11-16	10:51:10 AM	07-12-16	5:01:20 PM	9 Days
CPIV**	Ethanol	QH - 2	445.1	1.81	0.32	0.385	17-02-17	10:35:49 AM	27-02-17	10:58:24 AM	10 Days
Alfalfa II	Abiotic	AQSite5	440.66	1.77	0.33	0.3135	07-08-17	10:33:06 AM	17-08-17	5:43:32 PM	10 Days
Alfalfa II	Biotic	BQSite5	391.35	1.57	0.41	0.44542	07-08-17	10:35:01 AM	22-08-17	11:24:55 AM	15 Days
Alfalfa II	Abiotic	Site5AQ	383.3*	1.54	0.42	0.419	04-12-17	1:38:35 PM	17-12-17	3:02:24 PM	13 Days
Alfalfa II	Biotic	Site5BQ	320.8*	1.29	0.51	0.514	04-12-17	1:38:38 PM	17-12-17	3:02:27 PM	13 Days
Alfalfa I	Biotic	Site4BQ	265.2*	1.07	0.6	0.59799	04-12-17	1:38:39 PM	17-12-17	3:02:29 PM	13 Days
Alfalfa II	Abiotic	QA-S5II	386.53	1.55	0.42	0.35522	18-12-17	6:34:02 PM	31-12-17	8:13:16 PM	13 Days
Alfalfa II	Biotic	QB-S5II	344.64	1.38	0.48	0.500	18-12-17	6:33:55 PM	31-12-17	8:11:52 PM	13 Days
Alfalfa I	Biotic	QB-S4II	362.37	1.46	0.45	0.44787	18-12-17	6:33:53 PM	31-12-17	8:11:50 PM	13 Days

** indicates a volume correction.
* indicates that this is the estimated weight used from HyProp software.

The next information is on the field physical properties. The impact of the texture difference between the two samples on field behavior is explored in Nolasco, 2018. Here the textural classes of Alfalfa II and Alfalfa I biotic and abiotic treatments were evaluated (Table 6). The slight difference in the proportions of sand, silt and clay seems negligible when comparing the abiotic treatments yet the biotic soil is more affected. Abiotically the soil texture is very similar yet minor differences in clay content does impact the potential for micro-aggregation in the presence of OM. With organic matter, the proportion of larger particles increases, and smaller particles decrease.

Table 6. Percentage of sand, silt and clay as well as the corresponding textural class for both sites in the Alfalfa field. Data for biotic sample shows micro-aggregates rather than primary particles distributed into these textural class sizes. Abiotic sample was (treated with hydrogen peroxide). Both sites fall in the same textural class of Loamy Sand yet have slight differences in proportions of sand, silt and clay (Nolasco 2018).

Treatment:	Alfalfa I			Alfalfa II			Textural Class
	Sand	Silt	Clay	Sand	Silt	Clay	
Abiotic	75.59	21.71	2.69	78.67	16.1	5.23	Loamy Sand
Biotic	79.66	20.34	0	83.97	15.84	0.19	Loamy Sand

3.2 Evaporation Data

The HyProp run (29th of November 2016) used soil from Circle Plot IV (Fig. 9 and 10). Circle Plot IV has a history of conventional tillage with no additional OM, inorganic fertilizer application and fumigation. This treatment was considered biotic at natural abundance, meaning that the soil is in its natural, unaltered state other than being collected as a disturbed soil, then being sieved and having visible roots removed. The soil had been kept in a frozen state or in a cooler below 40F until experiments were performed to protect microbial population. In all of these HyProp data, stage one evaporation (S-1) is indicated by a constant evaporation rate, followed by a decreasing or falling rate which marks the beginning of stage two (S-2). Transition from Stage one (S-1) evaporation occurs after 3.6 days and at a tension of 450 cm (Figure 9). The depth of the drying front reached to 2.8 cm when the transition occurred with an evaporation rate during S-1 of 0.25 cm/day (Figure 10). Because of the much lower evaporation rate following transition to S-2, the drying front only reached 1 cm further for the remaining six days (Figure 10).

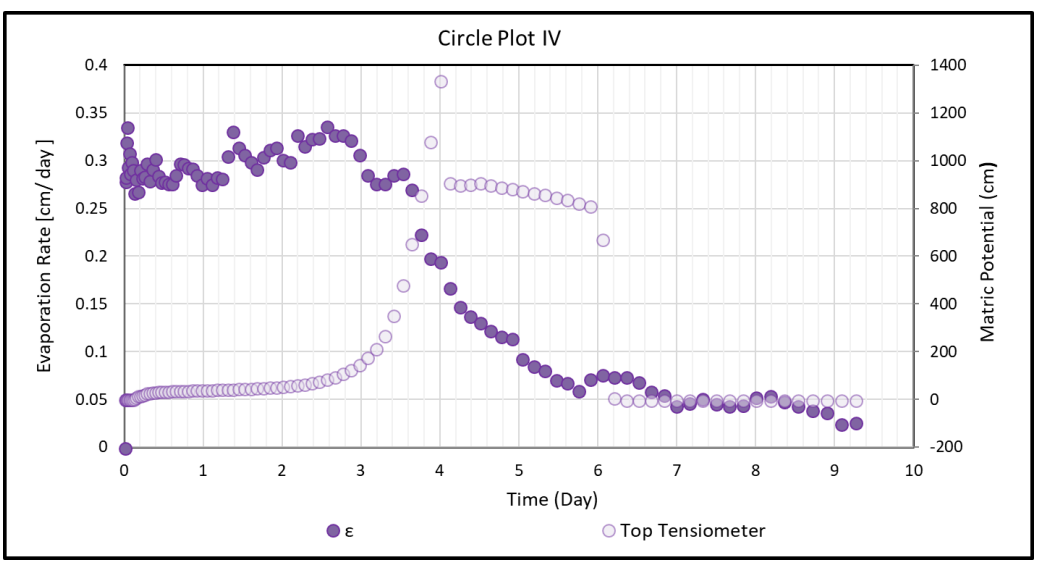

Figure 9. Evaporation Rate shown in cm per day for the biotic treatment in Circle Plot IV. The secondary axis includes Matric Potential from the top tensiometer.

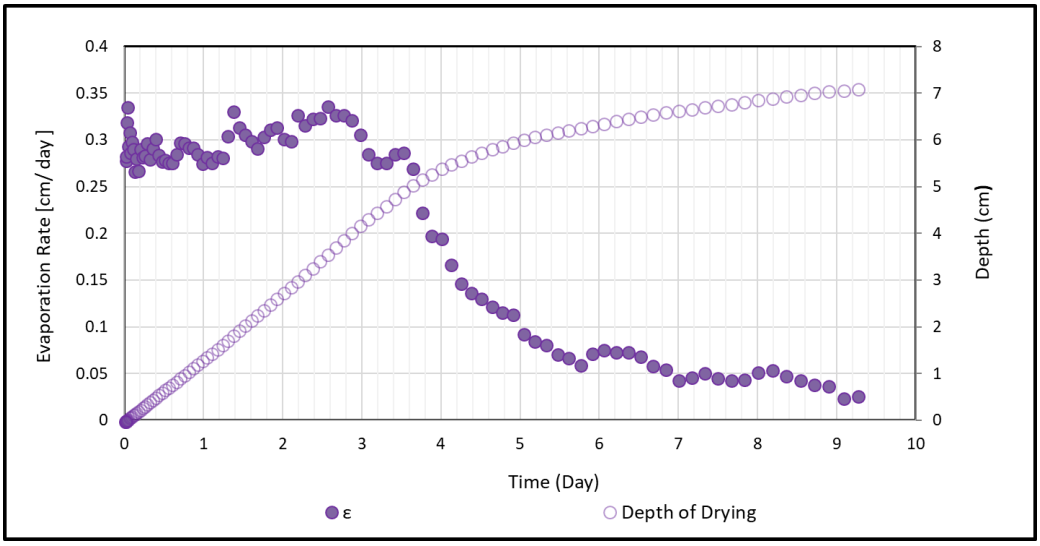

Figure 10. Purple always will signify Circle Plot IV. The secondary axis has the depth of the drying front and the primary axis is showing the evaporation rate for the biotic treatment.

Run 2: Circle Plot IV – abiotic

The second sample run on the HyProp was also from Circle Plot IV, but it was treated with Ethanol to reduce the influence of biology on water movement. This sample was considered to be "abiotic." It was run after the biotic for ten days beginning on the 17th of February 2017. The results from this abiotic sample show a transition from S-1 to S-2 after only 2 days and at a tension of 248.74 cm – more rapidly and at a lower tension than the "biotic" sample (Figure 11). The drying front depth at time of transition was also lower (2.8 cm) (Figure 10). However, there are a number of important considerations associated with laboratory conditions. S-1 evaporation was higher, this creates ambiguity in interpretation since difference S-1 evaporation rate will affect duration of S-1. Also, higher evaporation rates may force transition to S-2 at lower values of tension, therefore there is ambiguity as to whether the differences in evaporation behavior between the biotic and abiotic samples was due to atmospheric conditions or the physics inside of the soil associated with soil biology. The differences between the treatments made it evident

that the samples needed to be run at the same time to ensure that the potential evaporation rate was identical for both samples, which would allow comparable evaporation results.

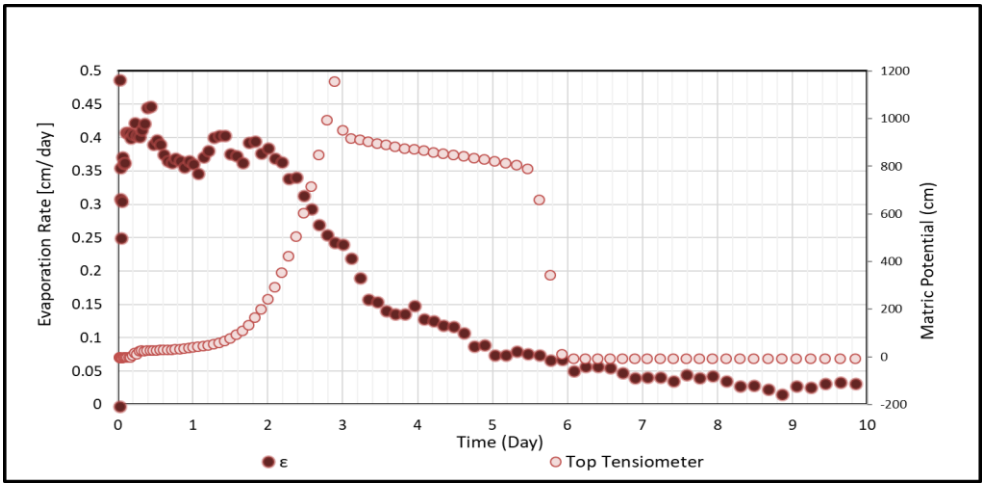

Figure 11. Ethanol treated Circle Plot IV soil sample. The left-hand y-axis shows the evaporation rate and the right-hand y-axis shows matric potential.

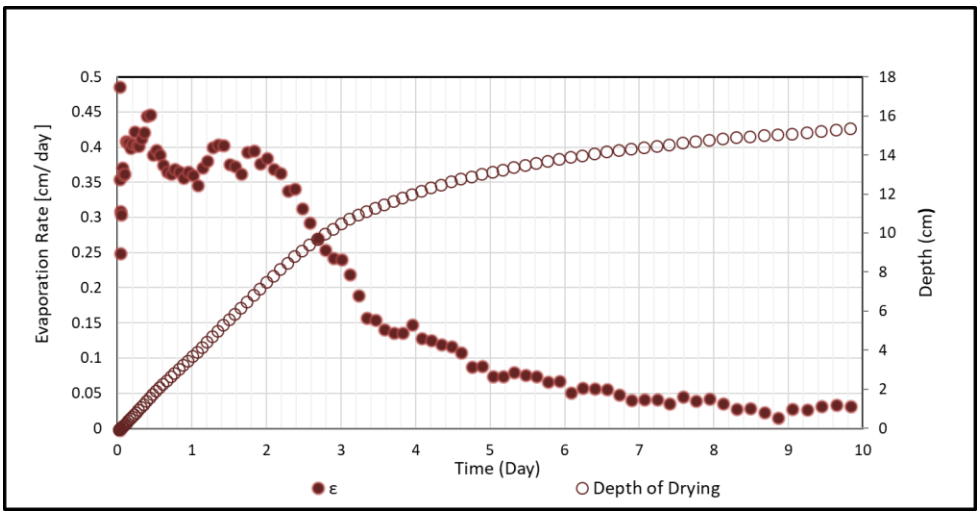

Figure 12. Evaporation rate and the depth of the drying front for the Ethanol treated Circle Plot IV soil sample. Depth of drying front is on the right-hand axis.

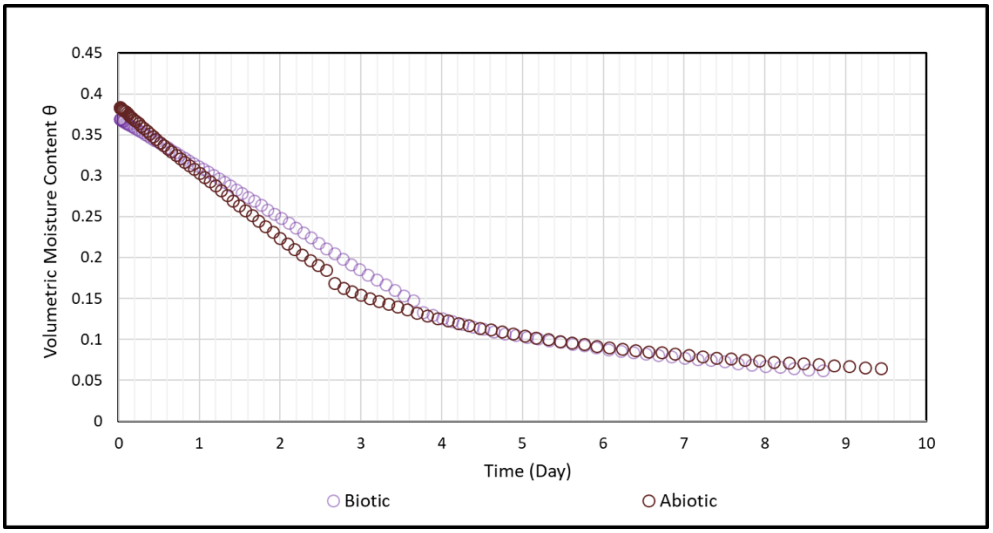

Figure 13. Volumetric moisture content of evaporating soil sample from Circle Plot IV. Comparison of both abiotic and biotic soil treatments. The abiotic sample loses moisture more rapidly initially. Potential evaporation rates for biotic and abiotic samples were 3.0-3.5 and 3.5-4.0 cm/day, respectively.

Run 3: Alfalfa II Plot samples, biotic and abiotic treatments

In the summer of 2017 soil samples were collected at a new site (Figure 1) with difference management history and crop. These samples are called Alfalfa II. From this point on all *abiotic* treatments consist of soil treated with hydrogen peroxide, and pairs of *biotic* and *abiotic* samples are run concurrently. There was a significant amount of noise seen in these measurements (specifically due to variation in temperature and/or vibration caused by construction) during the beginning stages of evaporation. Vibration in the laboratory may be the reason for both samples to have transitions from S-1 to S-2 at the same time. But, there is an important difference in their behavior, the biotic is transitioning to S-2 at a higher mixed tension [eq. 21] (Figure 14). In the abiotic sample the tensiometers have a greater gradient at the transition of S-1 to S-2. The tensiometers in the biotic sample increase almost identically, with the less steep gradient in the biotic sample as expected. The biotic tension decreases much less rapidly. Water is being delivered to the evaporation surface at a much lower tension for the abiotic than the biotic. Is this effect due to the change in pore structure between the abiotic and

biotic or because soil biology is increasing the osmotic potential of the film and this is expressed as capillary energy?

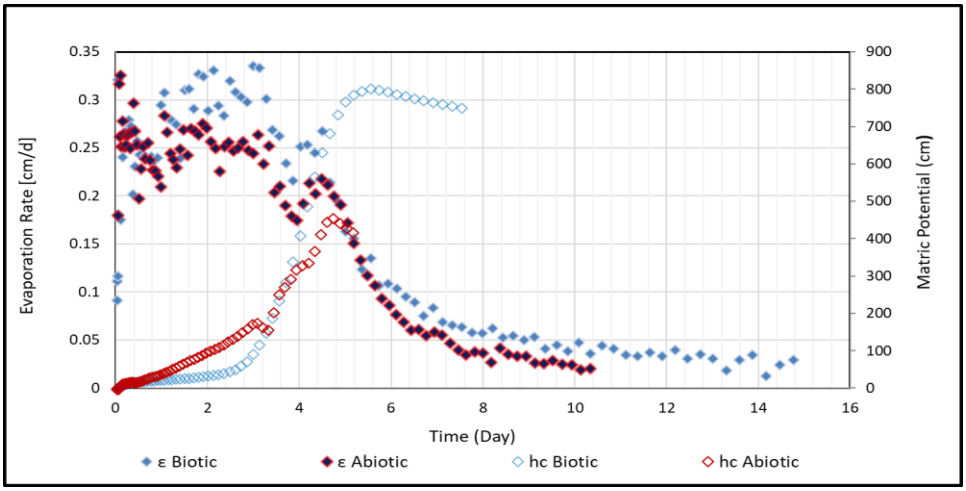

Figure 14. Evaporation rate from Alfalfa II soil sample comparing – abiotic (red diamond markers) vs biotic (blue diamond markers), from HyProp data. The abiotic treatment was completed with hydrogen peroxide. The left-hand y-axis shows the evaporation rate and the right-hand y-axis shows the mixed tension [eq.21].

If the hydraulic conductivity is calculated by the flux divided by the gradient, then in Figure 15 the abiotic sample has a larger gradient compared to the biotic sample because the difference between the top and bottom tensiometers is vastly different. In the biotic sample the difference between the two tensiometers is minimal, increasing the conductivity.

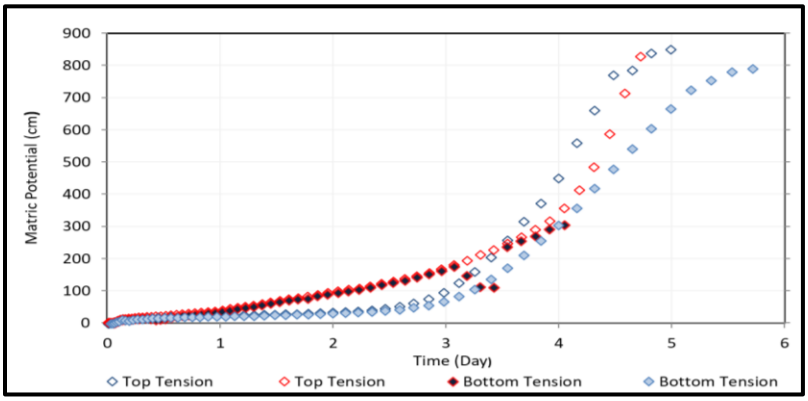

Figure 15. Tension of top and bottom tensiometers for the biotic and abiotic Alfalfa II soil samples. The abiotic is in red with top tension open diamond and bottom solid diamond marker. The biotic has a top tension with an open blue diamond and a bottom tension with a blue filled diamond marker.

One of the challenges in interpreting the data from biotic and abiotic is that the biotic soil has a larger porosity and therefore initial moisture content than the abiotic soil (Figure 17). To highlight this moisture content difference, volumetric moisture content is graphed in Figure 17 and as degree of saturation in Figure 16.

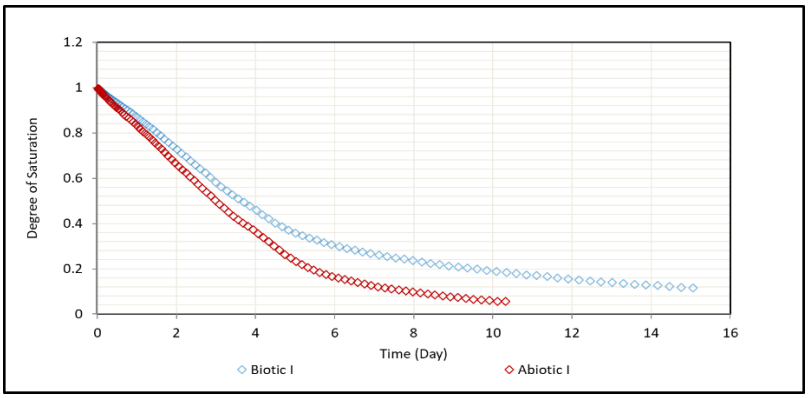

Figure 16. Alfalfa II – biotic and abiotic treatments for the first run on with the HyProp. The y-axis shows the degree of saturation [eq. 5] calculated by the division of the saturated volumetric moisture content.

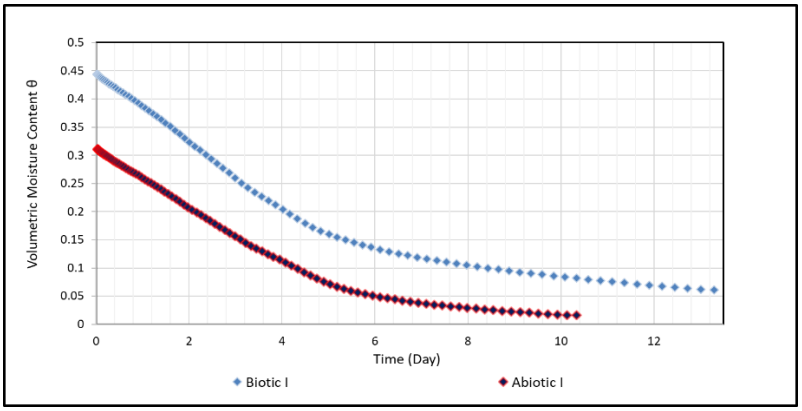

Figure 17. Primary axis shows volumetric moisture content of biotic and abiotic soil from Alfalfa II lost over time. Biotic soil is represented by blue diamond markers and the abiotic soil is represented with red outlined diamond markers.

The Alfalfa II biotic soil has a larger porosity than the abiotic soil (Figure 17) and during the experiment (Figure 16) the biotic soil was more saturated than the abiotic soil despite the biotic

soil extracting water from deeper depths (Figure 18).

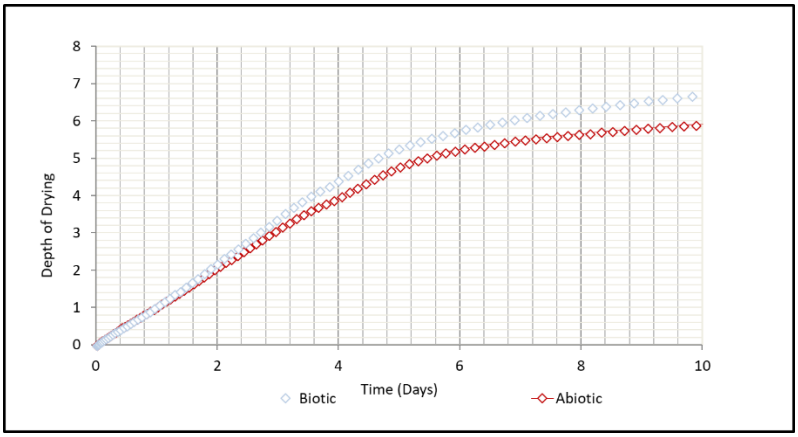

Figure 18. The estimated depth of the drying front [eq.8] is on the y-axis and the time in days is on the x-axis.

Run 4: Alfalfa II and Alfalfa I samples, biotic and abiotic treatments

The next HyProp run was performed with three samples, two from Alfalfa II with - *abiotic* and *biotic* treatments and one sample from the Alfalfa I site that was left - *biotic*. To facilitate discussion, hereto, Alfalfa I biotic and Alfalfa II biotic are termed A-Ib and A-IIb, and Alfalfa II abiotic is termed A-IIa. These samples were started on the 17th of December 2017 and ran for a total of thirteen days. There was a significant reduction in noise for these samples (relative to the previous experiment) as the construction in the building was finished. The evaporation rate is more distinct than the previous runs. A-I has a slightly different texture than A-II (Table 5). Running samples from these two locations at the same time is expected to show a comparison for abiotic verse biotic yet also a comparison in texture. The evaporation rate from all three samples over time is shown in Figure 19.

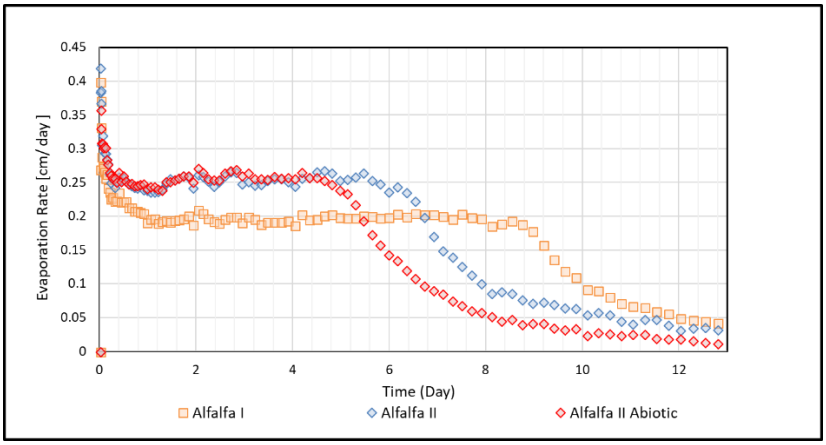

Figure 19. Evaporation rate of three soil samples. The orange square markers indicate the evaporation rate for Alfalfa I. The blue diamond markers indicate the evaporation rate for Alfalfa II biotic sample. The red outlined diamond markers indicate the Alfalfa II abiotic sample.

It is clear from Figure 19 that the A-IIb and A-IIa samples can be readily compared because their S-1 evaporation rates are identical. However, the A-1b sample exhibited a much lower S-1 evaporation rate, lower than the room's potential evaporation rate. The reason is unknown, but from visual observations it is suspected that a biotic crust formed suppressing the evaporation rate; the longer duration of S-1 could be simply because of the lower rate of S-1. It is well known that the lower the S-1 rate, the longer the duration.

Leaving A-Ib out of the discussion temporarily, the differences between A-IIb and A-IIa are extensive. A-IIa has a shorter duration of S-1 (5 days) than A-IIb (6.5 days) (Figure 19). The biotic samples have a larger porosity thus beginning with a higher initial volumetric moisture content (Figure 20). All three samples begin at saturation and during the evaporative process the abiotic soil has a steeper slope compared to the biotic treatments (Figure 20). At the end of S-1 the saturation was 27%, 33% and 38% for A-IIa, A-IIb and A-Ib, respectively.

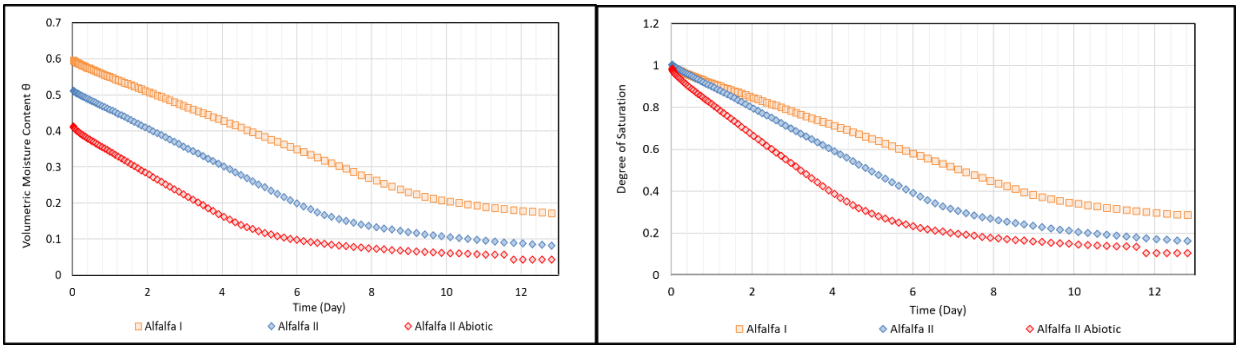

Figure 20. The graph on the left displays volumetric moisture content during evaporation process for three samples: A-Ib in orange squares, A-IIb in blue diamonds, A-IIa in red diamonds. All three samples were running simultaneously on the HyProp from saturation. The degree of saturation over time is displayed in the graph on the right.

This could facilitate a longer duration of S-1 for the biotic sample. A deeper investigation of the data indicates that the transition from S-1 to S-2 occurred when the effective drying depth reached 5 cm depth for A-IIb, 4 cm for A-IIa and 5 cm for A-Ib (Figure 21).

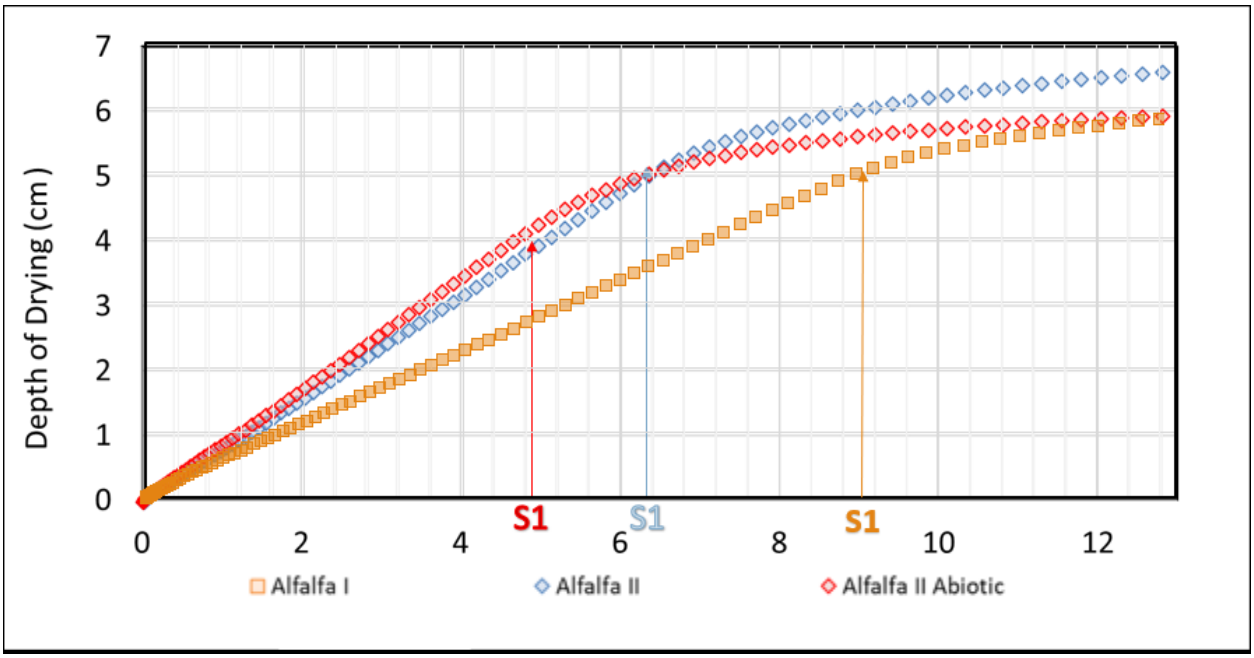

Figure 21. Depth of drying on x-axis over time during the evaporation process. A-Ib is represented by the orange squares, A-IIb is shown with the blue diamonds, and A-IIa is the red diamond markers. S1 marker for each sample indicates there the transition occurs.

However, A-IIb reaches a much greater tension at transition than A-IIa. This can be interpreted in 2 ways: (1) The hydraulic conductivity of the abiotic and biotic films is the same (K = E at transition), but the biotic film tension is a composite of capillary and osmotic potential (Figure 22). (2) While the effective drying depth is similar, if more water is left in films above the drying front in the biotic sample, then the actual drying front is much lower, and the biotic sample is sustaining longer films. The data at this point is not able to distinguish between these two possibilities. The data in Figure 22 uses the matric potential for only the top tensiometers, which was thought to better represent the tension value of films above the drying front. The location of the ceramic tip of the top tensiometer is 1.25 cm (Figure 2) below the upper soil surface and thus above the drying front at the time of transition between S-1 and S-2. Note that the transition takes place at a higher matric potential for both biotic treatments compared to the abiotic.

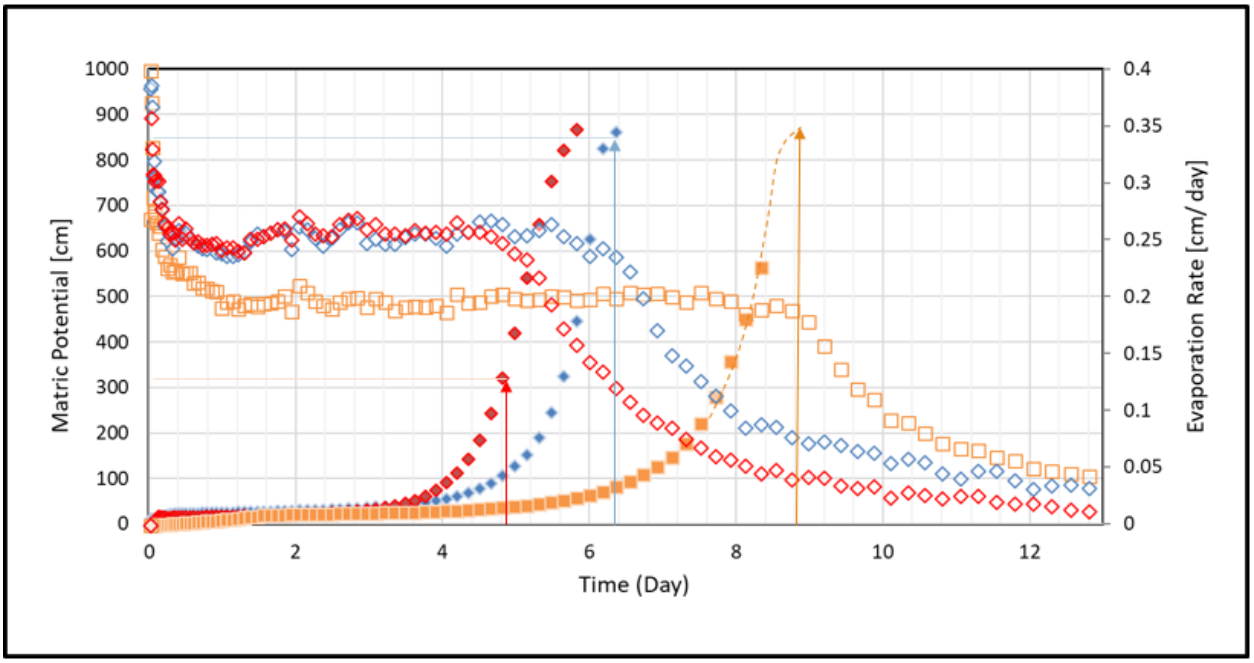

Figure 22. Matric potential of each soil sample during the evaporation process. The open markers are plotted on the secondary axis which represents the evaporation rate. The filled in markers are plotted on the primary axis which is matric potential. Note the matric potential data is only from the top tensiometer from all of the samples. The blue diamonds are for A-IIb, the red diamonds are A-IIa, and the orange squares are A-Ib.

The biotic films are able to support water transport up to the location of the top tensiometer and to the surface by sustaining films at higher matric potentials (Figure 22). The top tension was used to form a moisture characteristic curve to approximate the moisture content at the top tensiometer during the transition from S1-S2 (Figure 23). It was found that the volumetric moisture content for A-IIb was 18.47% and for A-IIa it was 12.46%, respectively (Figure 23).

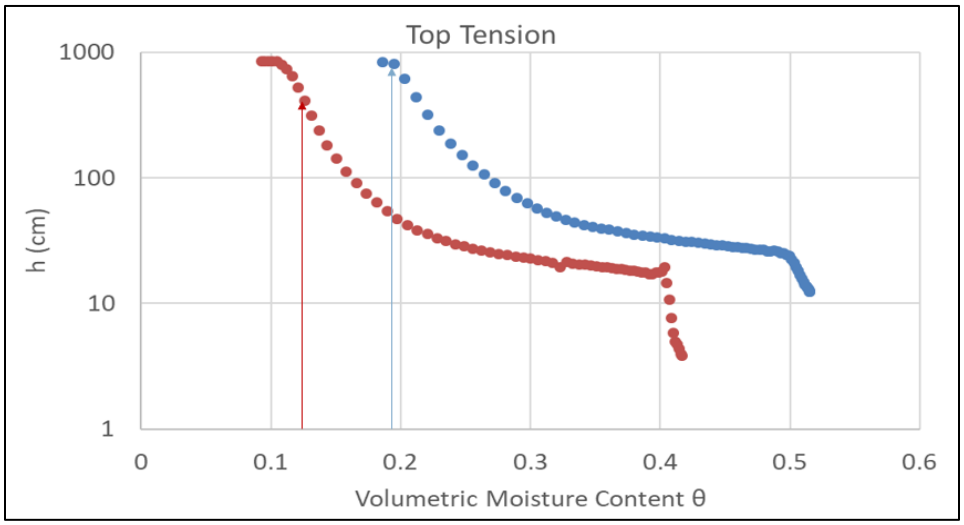

Figure 23. Data for top tensiometers of A-IIb blue dots and A-IIa red dots were used to form the h(θ) relationship. Tension is shown on the y-axis in cm and volumetric moisture content is on the x-axis.

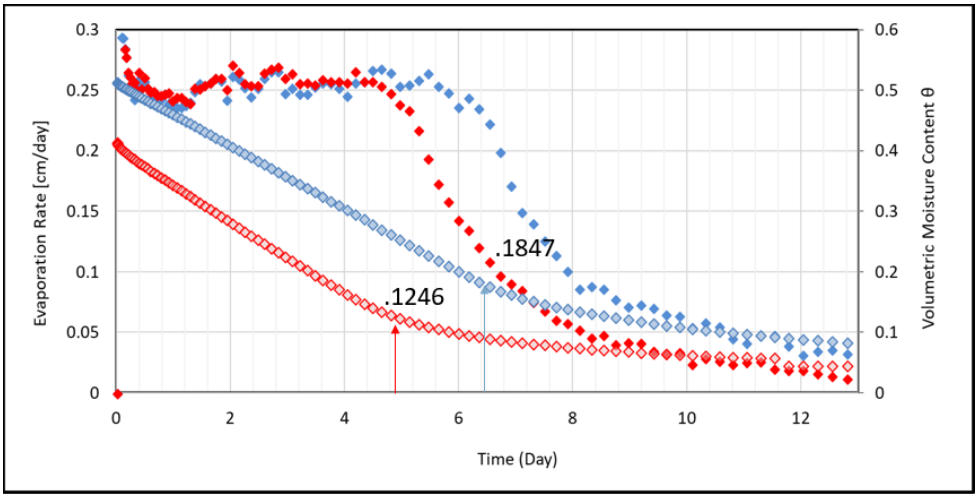

Figure 24. Volumetric moisture content at the time of transition from S1 to S2 for A-IIb blue diamond markers and A-IIa red diamonds.

The volumetric moisture content during S1-S2 transition for the biotic soil is 6% higher than the abiotic (Figure 24) yet the biotic has a 1 cm deeper effective drying depth (Figure 21). This could possibly indicate that water is being held inside biofilms while water is extracted from deeper depths. When the effective drying depth is graphed against the evaporation rate, it is clear that the S-1 transitions to S-2 for the biotic when the effective drying front is 1 cm deeper (Figure 25). This confirms that the biotic soil is extracting water from deeper depths. The mixed tension (Figure 26) shows that the abiotic has a larger gradient in tension between the bottom and top tensiometer at the point of transition between S-1 and S-2. The mixed tension for the biotic soil reaches a higher overall tension compared with the results from the abiotic soil. Both the bottom and top tensiometer in the biotic treatment reached similar tensions.

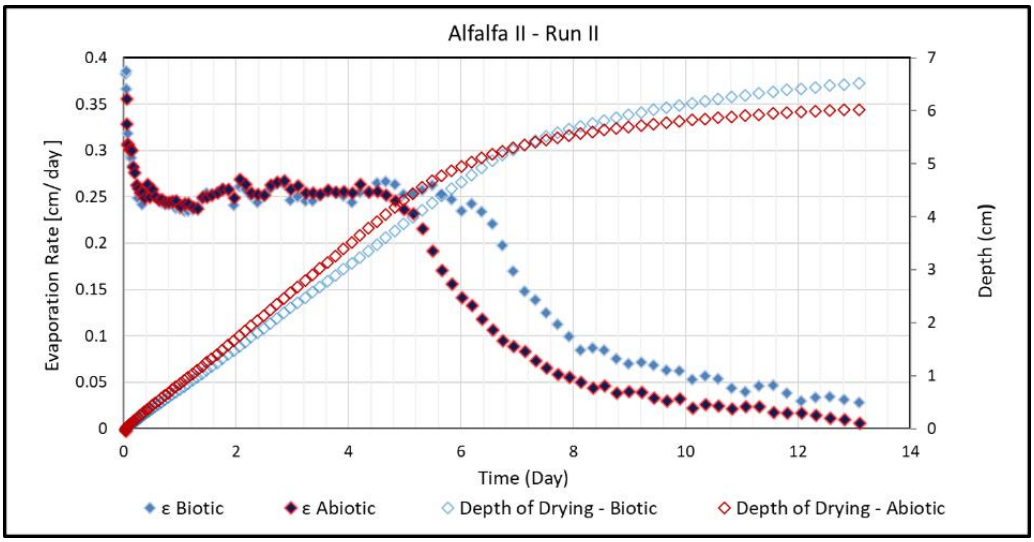

Figure 25. Evaporation on the primary y-axis for the Alfalfa II data and depth of the drying front on the secondary y-axis in cm.

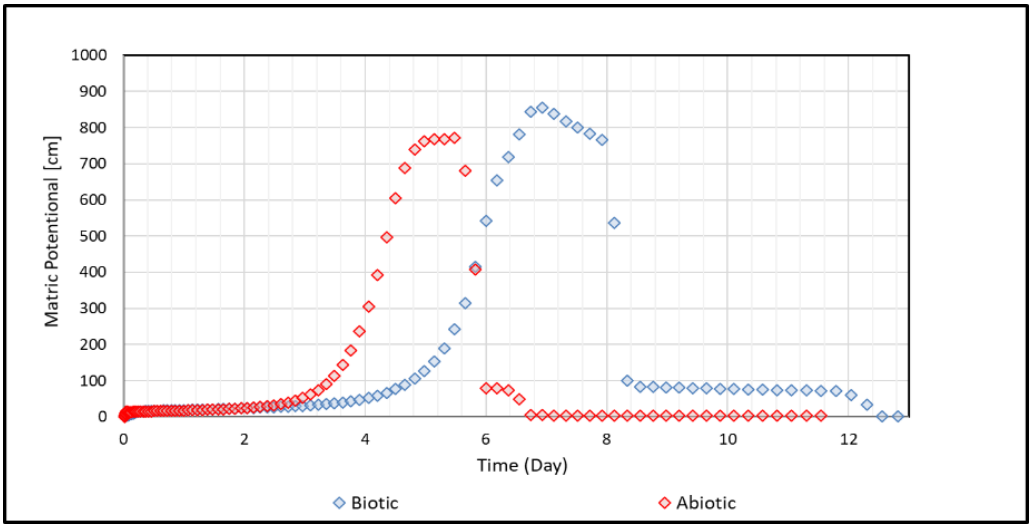

Figure 26. The mixed tension for the Abiotic and Biotic treatments for Alfalfa II was calculated using equation 21.

Run 5: Alfalfa II Plot samples, biotic and abiotic treatments

The same samples used for the HyProp Run 4 were used for Run 5. For this next run, the idea was to re-saturate the samples and immediately rerun them on the HyProp. In order to complete this task, the holes that were originally augured out needed to be refilled. At this point all holes in the samples were filled with silica sand to be re-augured out after saturation. During the previous measurement, both biotic samples had issues with the bottom tensiometer and it was suggested that the bulk density might be too low causing little connection around the ceramic tip of tensiometer causing it to reach air entry more rapidly than usual. The sample ring for A-Ib and A-IIb had a lower bulk density than expected compared with the field bulk densities thus the soil surface was roughened, and twenty grams of soil was added to increase the bulk density for Alfalfa II – biotic and about sixty grams was added to Alfalfa I – biotic. This also reduced the need for a volume correction at the end of the HyProp experiment as the volume of the cylinder for these samples were not completely full. All three samples were then saturated for about fifteen hours and the experiment started on the 18th of December 2017. The runs provided excellent data so that all three samples could be compared (Figure 27).

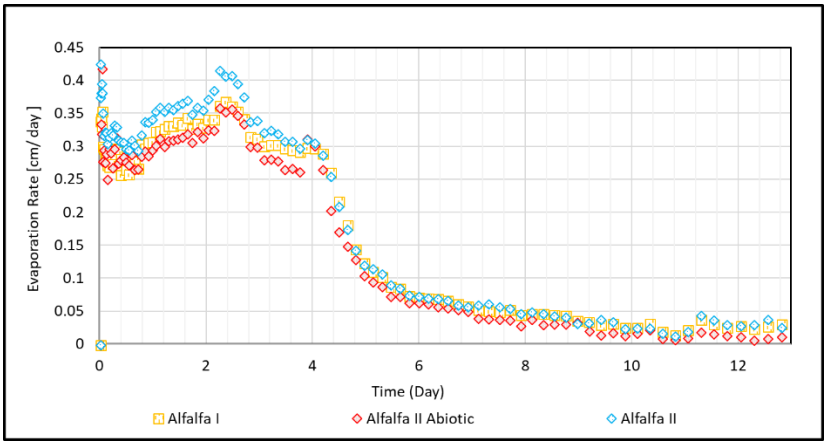

Figure 27. The evaporation rate for all three samples, two biotic and one abiotic. All three samples transition from S-1 to S-2 at the same time. The soil used in these samples had already been saturated and evaporated for thirteen days, then re-saturated for fifteen hours and placed on the HyProp machine for evaporation.

It is rather interesting that during Run 5 all three samples transitioned to S-2 at the same time (Figure 27). Note that this run also has a higher potential evaporation in the room and it was not constant compared to the other runs. The results appear rather similar to Run 3 where the abiotic and biotic transitioned to S-2 at the same time but at different matric potentials (Figure 14). During Run 3, it was known that there was construction activity in the building (fans and vibration) that potentially affected the room's potential evaporation rate, but during this Run it is unknown if there was anything in particular that would have affected this. Run 5 did have an addition of soil to both biotic samples, and this addition may have potentially caused a capillary barrier that may have encouraged films to break earlier. Especially since the addition of soil may not have led to biotic films reaching to the evaporation surface. The effective depth of the drying front is calculated using [eq. 8] (Figure 28). The transition from S1 to S2 evaporation occurs at 18.08% volumetric moisture content for A-IIb, 9.73% for A-IIa, and 17.86 % for A-Ib. Due to the manner in which the effective depth of the drying was calculated [eq.8], despite all the samples having the same evaporation rate and transitioning from S1-S2 at the same time, the effective depth of drying is greater for the biotic treatments compared to the abiotic treatment

(Figure 28). This could either be because the biotic treatments have a higher initial volumetric moisture content, the abiotic sample started with 20% less saturation, or because water is being left behind in biofilms in the biotic treatments. The biotic treatment from Alfalfa I and Alfalfa II had a higher volumetric moisture content at the time of transition from S1-S2 (Figure 29). Alfalfa II has the highest initial volumetric moisture content followed by Alfalfa I, indicating a higher porosity for the biotic treatments. Figure 29 shows that the abiotic treatment began with the lowest initial volumetric moisture content. Due to time constraints, these samples were only saturated for a little over a half of a day when usually the samples are saturated for 24 hours. This caused A-IIa to only saturate to 80% water filled pore space (Figure 30).

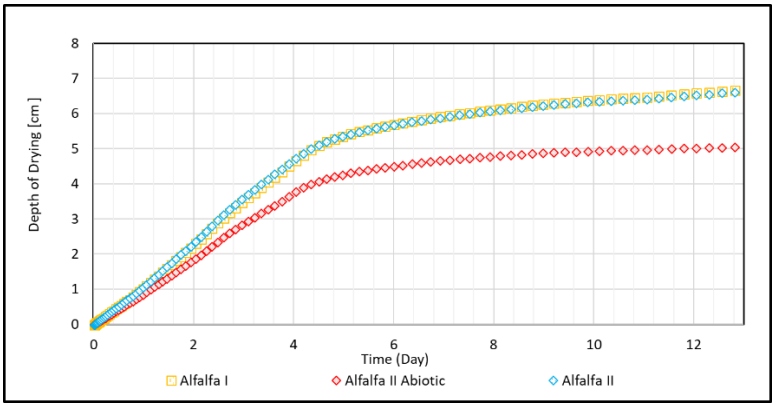

Figure 28. Estimated depth of drying front during the evaporation process for three soil samples.

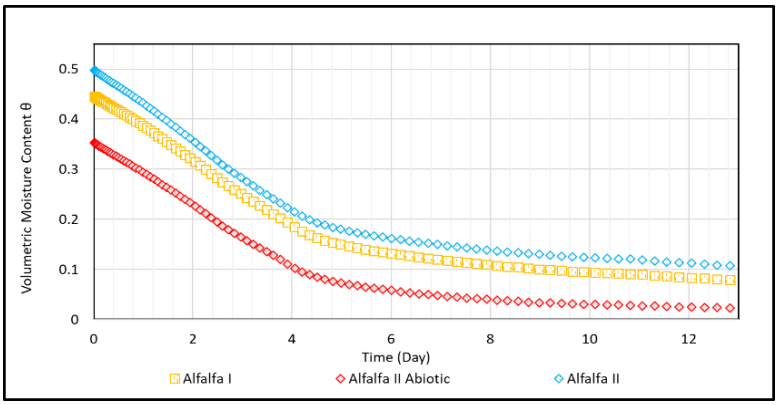

Figure 29. Volumetric moisture content during the evaporation process for three soil samples.

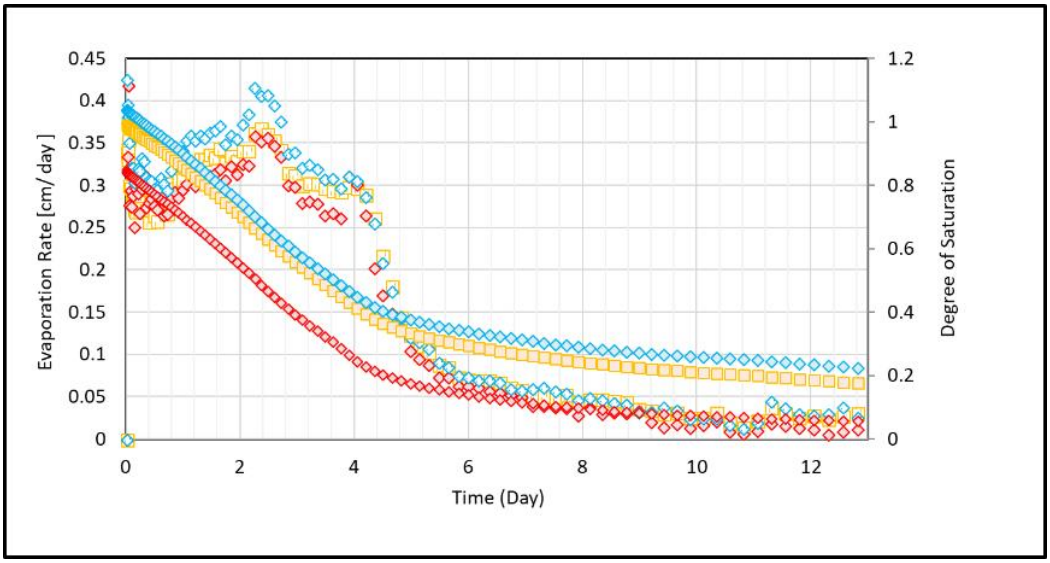

Figure 30. Superposition of the evaporation rate and degree of saturation data during the evaporation process for three soil samples. The abiotic sample begins at twenty percent less saturated than the other two samples. The two biotic samples transition to stage two evaporation at about forty percent saturation and the abiotic sample transitioned at twenty.

3.3 Moisture Retention Curve obtained from HyProp Data

After all the data was collected from the HyProp runs, the top and bottom tensions were used to calculate mixed tensions [eq.21] for generating a moisture release curve graph. An analytical expression to the experimentally obtained moisture release curve was obtained by inputting the mixed tension and the volumetric moisture content values into RETC software (Figures 32-40). Table 7 shows all the van Genuchten values for the fitted curves to each soil sample.

Table 7. Displays every run from the HyProp and the associated parameters found using RETC software.

RUN #:	1	2	3		4			5		
Sample:	CPIV - B	CPIV - A	AII - A	AII - B	AII - A	AII - B	AI - B	AII - A	AII - B	AI - B
α	0.02	0.03	0.03	0.05	0.04	0.03	0.02	0.04	0.04	0.04
N	3.32	1.52	1.78	1.54	3.18	2.96	1.83	2.85	2.13	1.69
M	0.70	0.34	0.44	0.35	0.69	0.66	0.45	0.65	0.05	0.41
θ_r	0.14	0.09	0.06	0.13	0.16	0.21	0.08	0.19	0.40	0.06
θ_s	0.37	0.39	0.33	0.45	0.43	0.52	0.45	0.46	0.53	0.45

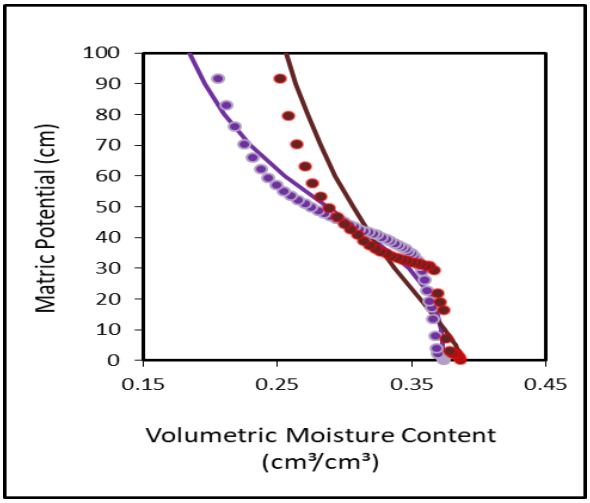

Figure 31. Runs 1 and 2. Moisture release curve obtained from HyProp data for Circle Plot IV. Biotic (purple) and ethanol-based abiotic soil samples (red). The two samples were not run concurrently on the HyProp. Collected data is represented with symbols, and the RETC fitted van Genuchten curve is a continuous line. Van Genuchten parameter values are summarized in Table 7.

Both samples have a similar saturated moisture contents yet as matric potential increases the samples release water differently (Figure 31). The saturated moisture content for the biotic sample is higher than the abiotic sample (Figure 32). The shape of the moisture release curve is similar yet shifted over because of the saturated moisture content in the biotic sample. As the matric potential increases the biotic sample is always at a higher moisture content compared to the abiotic sample.

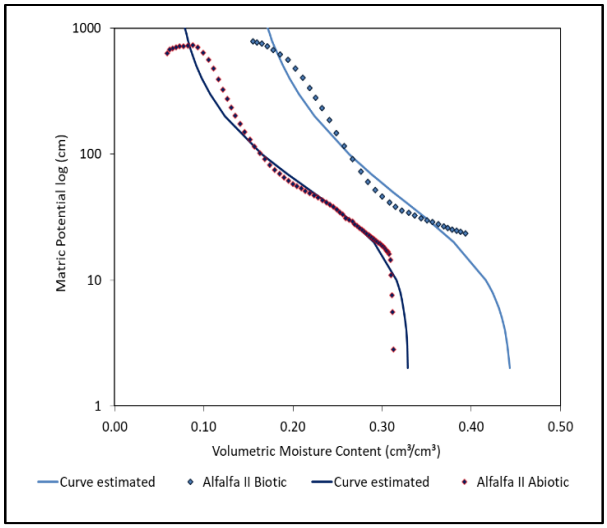

Figure 32. Run 3. Moisture release curve created from the data collected from Run 3 with the HyProp. Alfalfa II abiotic (red) and Alfalfa II biotic (blue) measured data shown with markers and lines represent the estimated curve with the parameters in Table 7.

The h-θ relationship with volumetric moisture content and log base 10 of the matric potential shows that once again the biotic sample has a larger saturated moisture content which indicates a higher porosity than the abiotic sample (Figure 33). The shapes of the curves are similar to each other indicating that the particle size distribution is similar, but arrangement of the particles may be different.

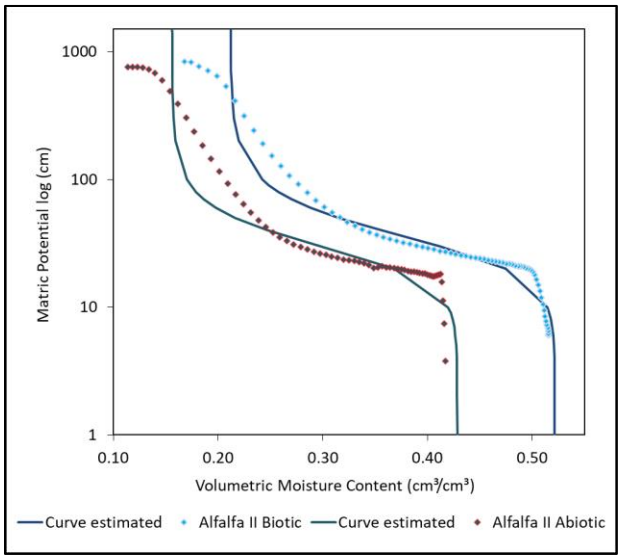

Figure 33. Run 4 of Alfalfa II biotic and abiotic with the HyProp. The moisture release curve is shown above created with the measured data gathered from the HyProp and an estimated curve created by the van Genuchten parameters.

During Runs 4 and 5 it shows that Alfalfa II biotic may have a higher saturated moisture content than Alfalfa I biotic (Figure 34). One of the curves of Alfalfa II biotic follows rather closely to Alfalfa I biotic and would appear to have the same saturated moisture content. The shapes of the moisture release curve are different supporting the fact that these two samples differ in texture (Figure 34). Figure 35 combines all the data from Runs 4 and 5 for A-IIa, A-IIb and A-Ib. The estimated curve is created by the parameters found in Table 7.

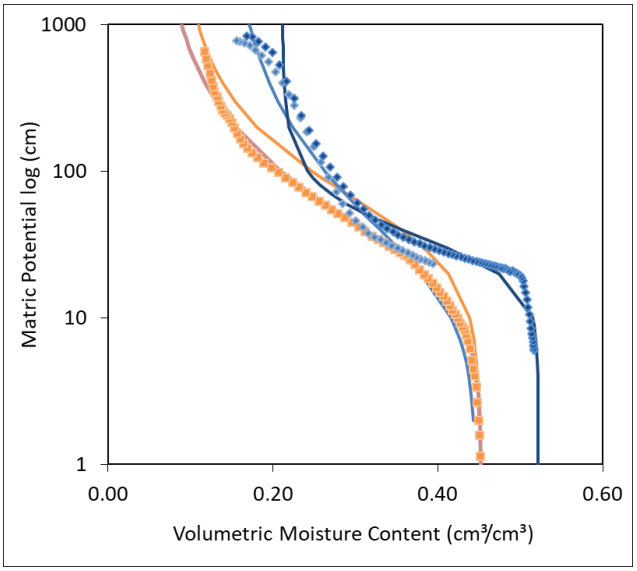

Figure 34.Runs 4 and 5 for Alfalfa I biotic and Alfalfa II biotic measured data from the HyProp. The estimated curves are created using the parameters from Table 7.

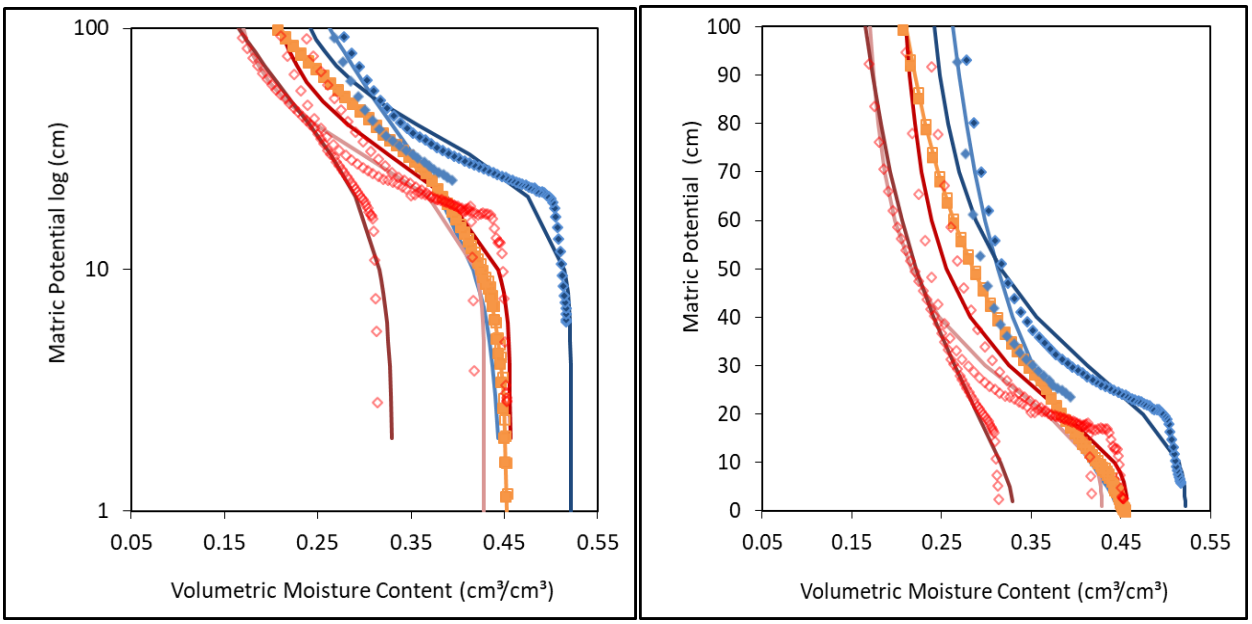

Figure 35. The moisture release curve for Runs 4 and 5 for Alfalfa II biotic (solid blue diamond) and abiotic (red open diamond) and Alfalfa I biotic (solid orange square). The figure on the left has the y-axis showing log base 10 of matric potential and the figure on the right does shows matric potential in centimeters.

Combined data for Runs 4 and 5 for Alfalfa II abiotic and biotic treatments is displayed in Figure 36. The red open diamond markers indicate A-IIa measured data from the HyProp while the solid red lines represent the estimated curve generated using the van Genuchten equation. The solid

blue diamonds represent the measured data from A-IIb with the solid blue lines showing the estimated curve. The abiotic measured data is represented well with the estimated curve, yet the biotic treatments measured data is not as well represented with the estimated curve (Figure 36).

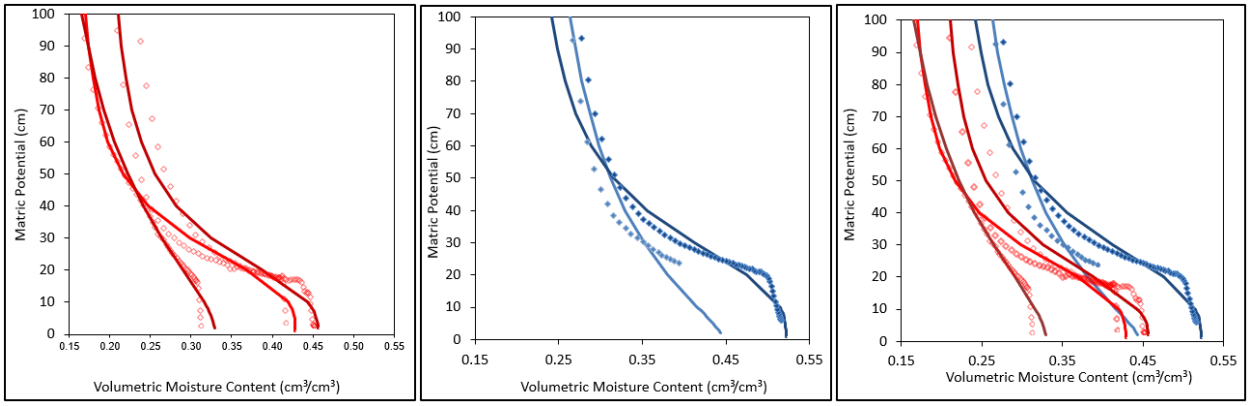

Figure 36. Moisture release curves for Run 4 and 5 for abiotic and biotic Alfalfa II. The first graph on the left shows A-IIa measured data (red open diamond markers) graphed with the estimated fitted curve. The middle figure shows A-IIb (solid blue diamond markers) HyProp measured data combined with the fitted curve. The final graph on the right combines both the abiotic and biotic data. The solid lines are estimated curves using the van Genuchten equation with the parameters generated by RETC software (Table 7).

The HyProp software fits a van Genuchten curve based on a small range of tensions, and therefore does not provide a realistic value of the residual moisture content. To obtain a moisture retention curve that represented a broader range of tensions, data from the WP4C potentiometer was obtained. The combined data set was then inputted into RETC software to generate a fitted curve. The mixed tensions values [eq.21] and volumetric moisture contents from the HyProp results for Alfalfa II biotic and abiotic, and Alfalfa I biotic was combined with data from the WP4C to create a soil characteristic curve for each sample. The solid lines on figure 37 represent the curve generated by the van Genuchten equation using the parameters generated from the RETC software (Table 8) differing from the previous parameters generated in Table 7 because the WP4C data was added to the HyProp measured data. All markers represent data collected with the HyProp and WP4C. The saturated moisture content in the biotic is higher compared to

the abiotic (Alfalfa II). At the residual moisture content, the biotic soil continues to lose moisture, whereas the abiotic soil is fitted with a straighter, more vertical, portion of the curve. It is unclear if this is a reasonable fit. The abiotic appears to have reached a residual value of ~5% at very low matric potentials (~800 cm) and the van Genuchten formulation is not able to capture this, creating a false high residual value. The red dashed line is suggested as a more representative fit and has been conceptually drawn (Figure 37).

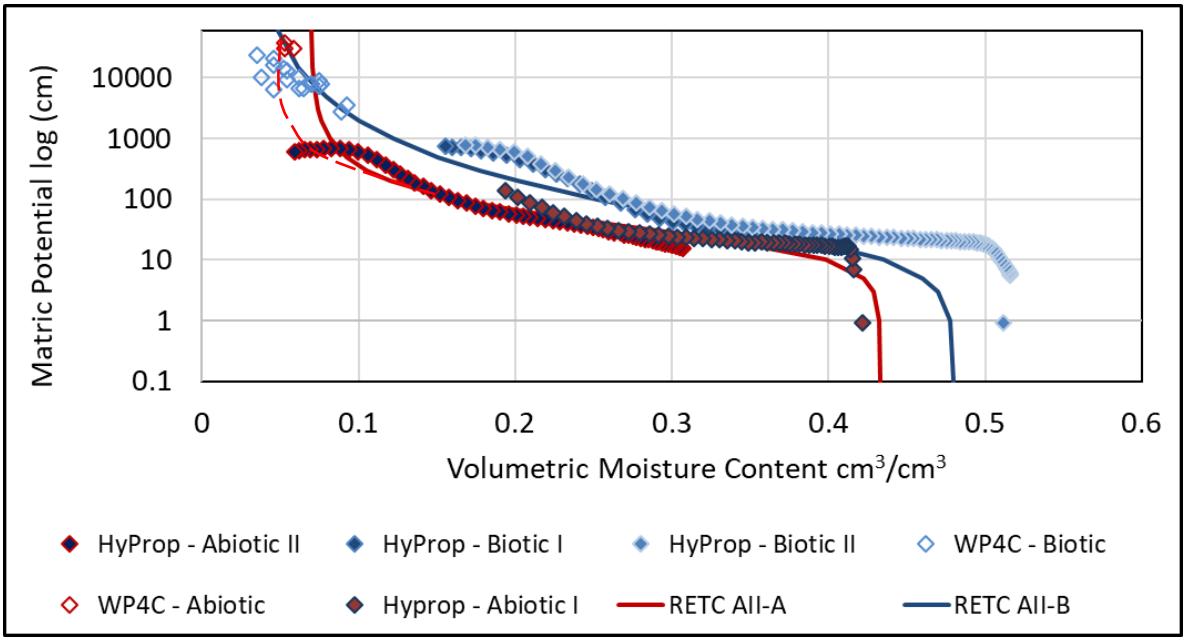

Figure 37. Comparison of biotic and abiotic conditions. Combined measured data from both runs on the HyProp for Alfalfa II biotic and abiotic as well as measured data from the WP4C. The above data was used to form the moisture release curve and estimate van Genuchten parameters using the software RETC (Genuchten *et al.* 1991; Nolasco 2018) The abiotic soil is represented by the red solid line and the biotic is the blue line.

The shape of the moisture release curves between the two textures (Figure 38) are similar indicating a similar trend in the pore size distribution, but Alfalfa II is retaining more moisture than Alfalfa I at all matric potentials. The higher retention for Alfalfa II could either be attributed by the higher clay content or a greater distribution of smaller micro-aggregates. Interestingly,

while A-Ib exhibits a fairly smooth function, A-IIb exhibits two plateaus, one at ~20 cm and one at ~900 cm. These two plateaus could indicate a bimodal distribution of pore sizes (Figure 38).

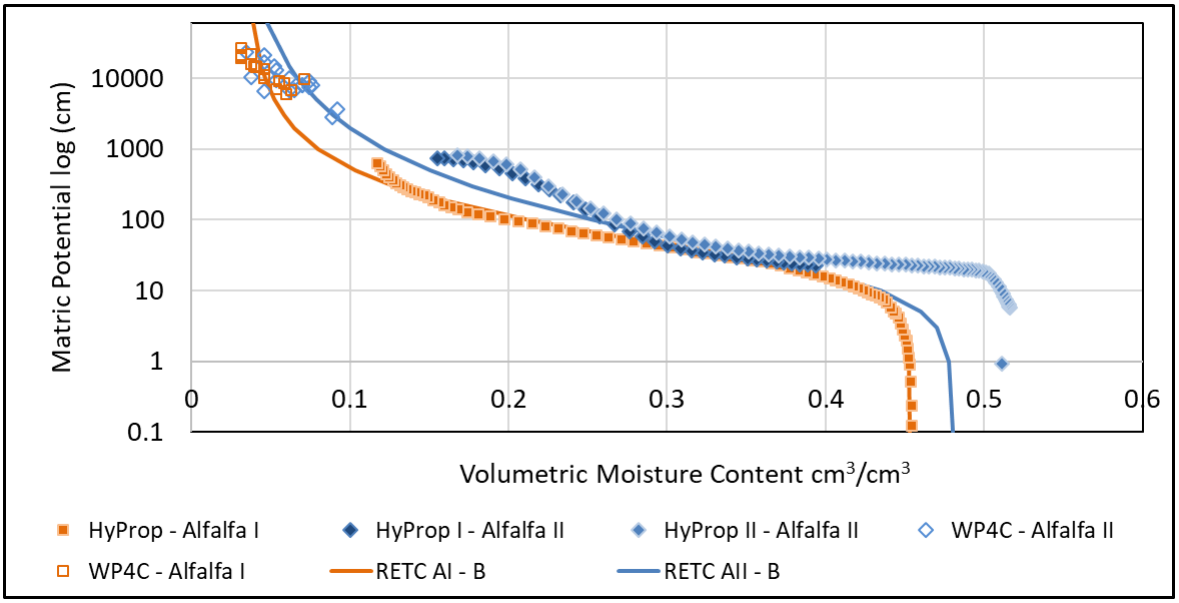

Figure 38. Comparison of two textures. Moisture release curve created using measured data from biotic treatments of Alfalfa I and Alfalfa II with the HyProp and WP4C to create the h-θ relationship. This data was inputted into RETC to generate parameters (Table 8). Alfalfa II is represented with the blue diamond markers and has a higher saturated moisture content. Alfalfa I is represented by the orange square markers, open markers are associated with the WP4C and filled are for the HyProp.

	AI	AII	AII A
α	0.03805	0.05667	0.04635
N	1.61579	1.39214	1.88386
θ_r	0.03582	0.02962	0.06958
θ_s	0.45324	0.48	0.43276
M	0.381108	0.281681	0.469175

Table 8. Van Genuchten parameters generated with RETC software using combined HyProp and WP4 data. AI stands for Alfalfa I, AII is Alfalfa II biotic, and AII A is for Alfalfa II abiotic. The parameters used in the equation are listed on the left column of the table. The residual moisture content value for Alfalfa II abiotic is higher than the biotic values and the saturated moisture content is highest in biotic Alfalfa II. The saturated moisture contents are also highest in the biotic samples than the abiotic. The air entry value of Alfalfa II biotic is the lowest, then the abiotic Alfalfa II followed by Alfalfa I.

There is a different potential explanation for the plateau of the A-IIb data at ~800 cm. 800 cm is approximately the tension where the tensiometers break contact with the soil. In a biotic soil, it is possible that biofilm has developed around the tensiometer's ceramic cup. In that case, the tensiometer system may have already broken contact with the soil water but is being kept moist by the attached biofilm. Therefore, the soil may be drying and increasing in tension, but the

tensiometer is reading only the tension of its surrounding biofilm. If that is the case, the plateau is a representation of this phenomena.

3.4 Analysis of the capillary gradient and hydraulic conductivity of evaporation

The following is an investigation of the difference in tension reading between the top and bottom tensiometer, for A-IIa and A-IIb. This comparison was investigated to examine the hydraulic gradient to give a prediction of the conductivity of each sample. The results were also used to calculate the mixed tension [eq.21] that was used to formulate the moisture release curves. The arithmetic and geometric mean were examined to find which was better to use when the gradient was greater. Data for A-IIb, A-IIa are analyzed in Figures 39 and 40, respectively. Figure 41 combines the top and bottom tensions from Run 3 Alfalfa II biotic and abiotic treatments. The largest separation between tensiometer readings occurs when the soil is at the lowest volumetric moisture content, just before soil water disconnects form the tensiometer.

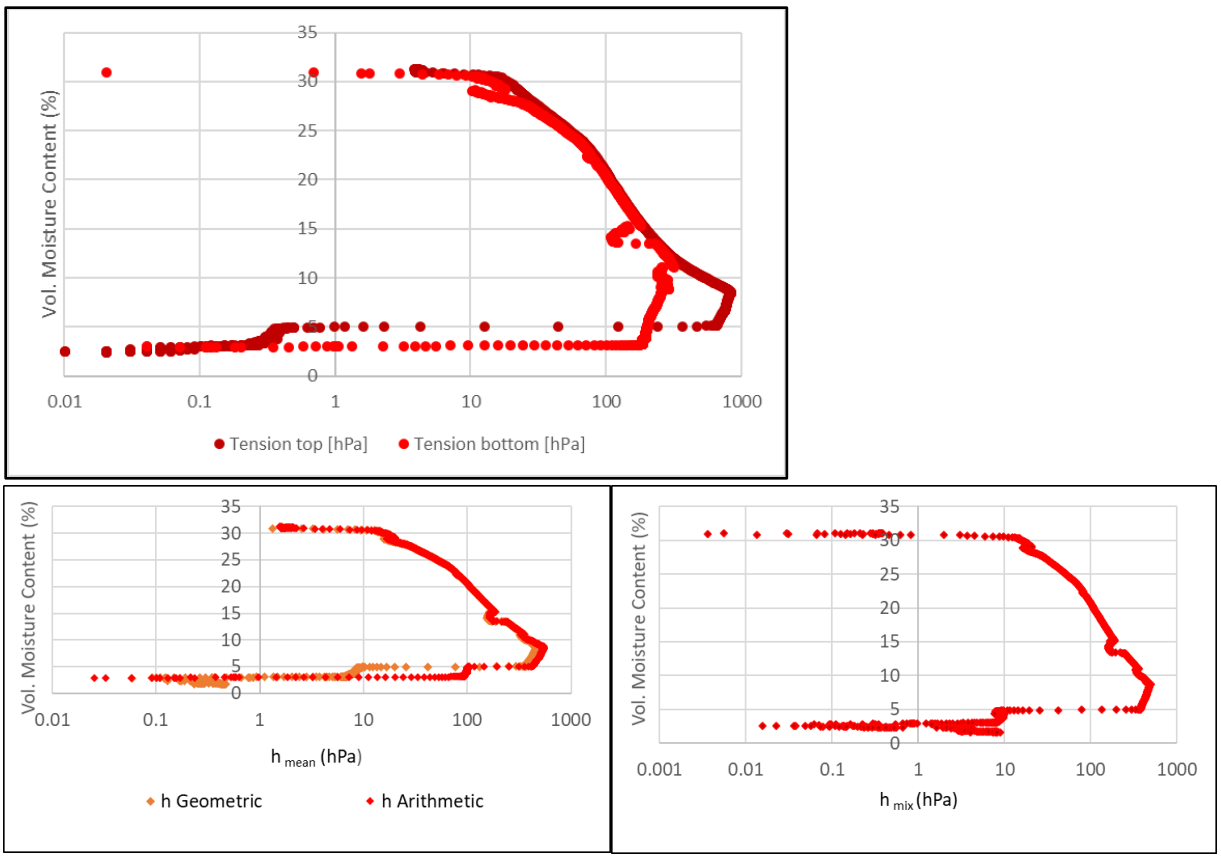

Figure 39. Abiotic Alfalfa II (A-IIa) Run 3 on the HyProp. Three graphs show the pathway of the process behind combining data from both tensiometers into a mixed tension. Volumetric moisture content is on the y-axis and matric potential is on the x-axis. Top figure shows raw data. Bottom left figure shows the geometric mean compared to the arithmetic mean for the tensions and the bottom right displays the mixed tension calculated using the weighted mean [eq.21].

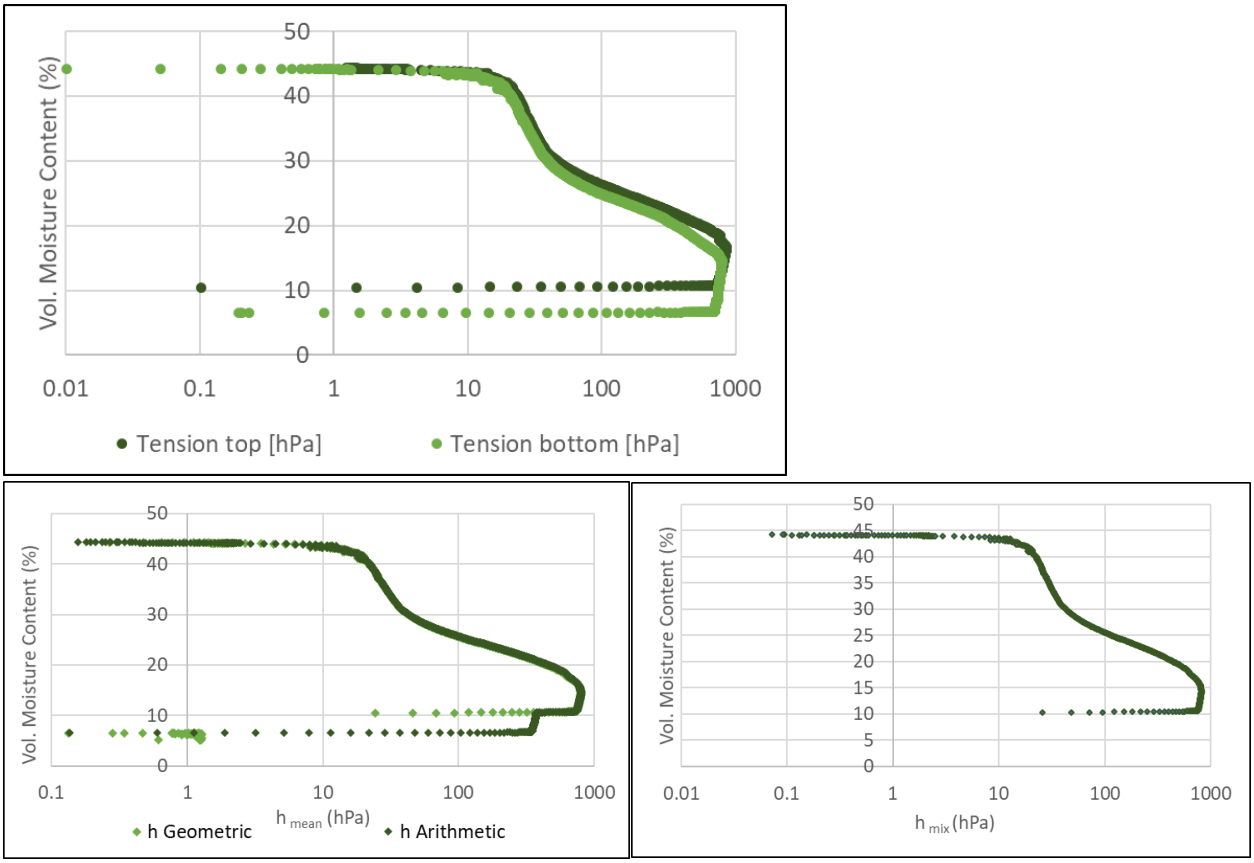

Figure 40. Biotic Alfalfa II (A-IIb) Run 3 on the HyProp. Top figure shows raw data of both bottom and top tensiometers. Bottom left figure shows the geometric mean compared to the arithmetic mean for the tensions and the bottom right displays the mixed tension calculated using the weighted mean [eq.21].

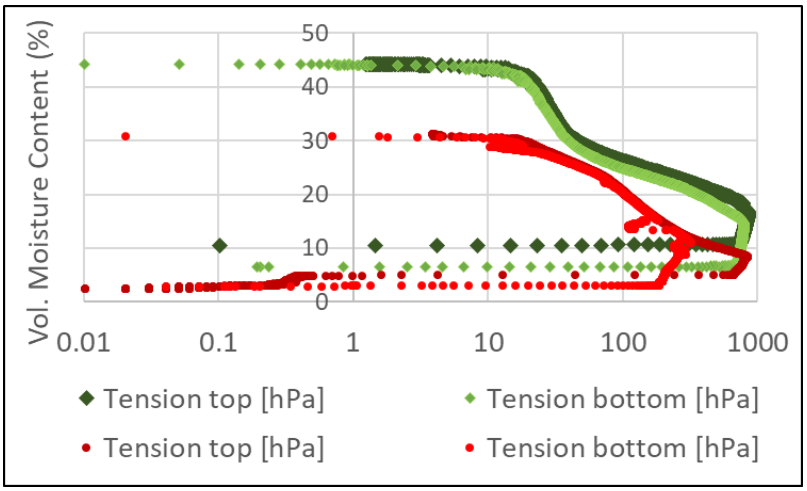

Figure 41. Run 3 Alfalfa II biotic (A-IIb) is shown in diamond green markers and has an overall higher tension during the entire experiment. Alfalfa II abiotic (A-IIa) is shown with the red circle markers and has a larger gradient between the two tensiometers. As the soil continues to dry the gradient between tensiometers becomes more evident.

	Silt	Silt Loam	Loam	Sandy loam	Loamy sand
Ks	0.25	0.45	1.04	4.42	14.59
α	0.016	0.02	0.036	0.075	0.124
N	1.37	1.41	1.56	1.89	2.29
θ_r	0.034	0.067	0.078	0.065	0.057
θ_s	0.46	0.45	0.43	0.41	0.41
M	0.27	0.29	0.36	0.47	0.56

Table 9. Van Genuchten parameters obtained from Carsel and Parish (1988). The parameters will be used to compare with the soil samples from this study. The following textural classes will be used for comparison: Silt, Silt Loam, Loam, Sandy Loam, Loamy Sandy.

Parameters that were generated using RETC will be compared with other textural classes from the Carsel and Parris paper (Carsel and Research 1988). The saturated hydraulic conductivity is listed with the van Genuchten parameters in order to use the equation which relates hydraulic conductivity to matric potential to formulate a figure representing this relationship (Table 9). The soil water characteristic curve will be generated to investigate which textural class the abiotic and biotic sample best matches. After matching the closest related textural class, then the hydraulic conductivity will be compared using the parameters generated from RETC. In Figure 42, it appears that the shape of the abiotic curve resembles more closely to that of the Sandy Loam textural class and the biotic resembles the Loam (Carsel and Parrish 1988).

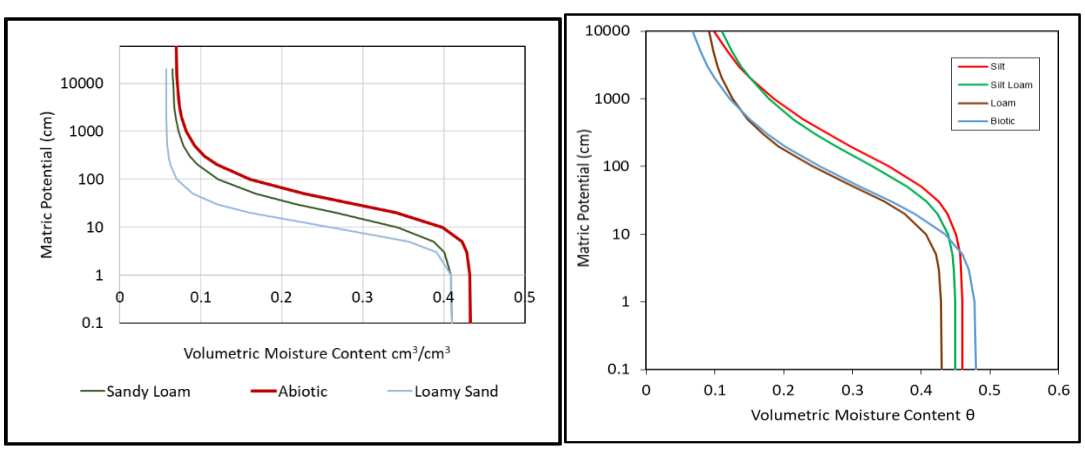

Figure 42. SWCC of Alfalfa II abiotic (left dark red) and biotic (right bright blue). All curves were produced using parameters generated with RETC software (Table 9).

The biotic sample from Alfalfa II has a larger hydraulic conductivity at every matric potential compared to Alfalfa I and abiotic Alfalfa II has a larger hydraulic conductivity than Alfalfa II biotic at lower matric potentials (Figure 43).

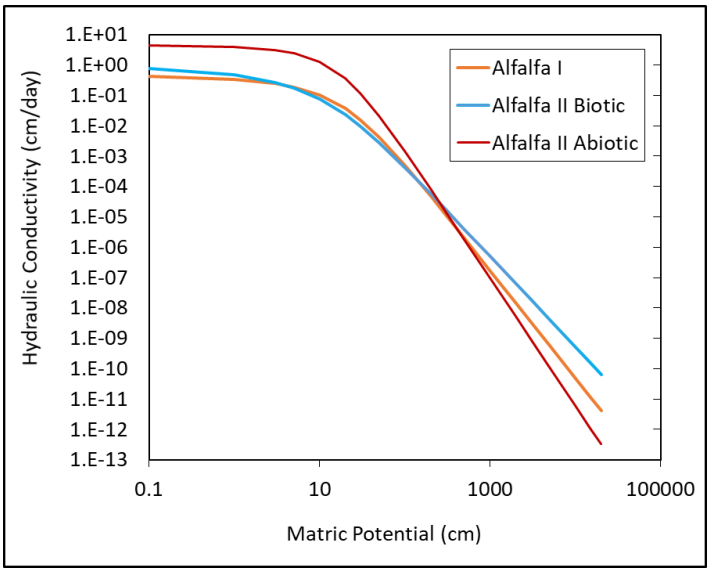

Figure 43. Hydraulic conductivity on the y-axis and matric potential on the x-axis for both biotic samples from Alfalfa II and Alfalfa I compared to abiotic Alfalfa II. Curves generated using the parameters from RETC into the van Genuchten equation [eq.14].

Alfalfa I has a similar shape to the biotic of Alfalfa II yet the dryer the soil becomes, the lower the hydraulic conductivity (Figure 44). The abiotic has the largest variable change with moisture content due to large pore size.

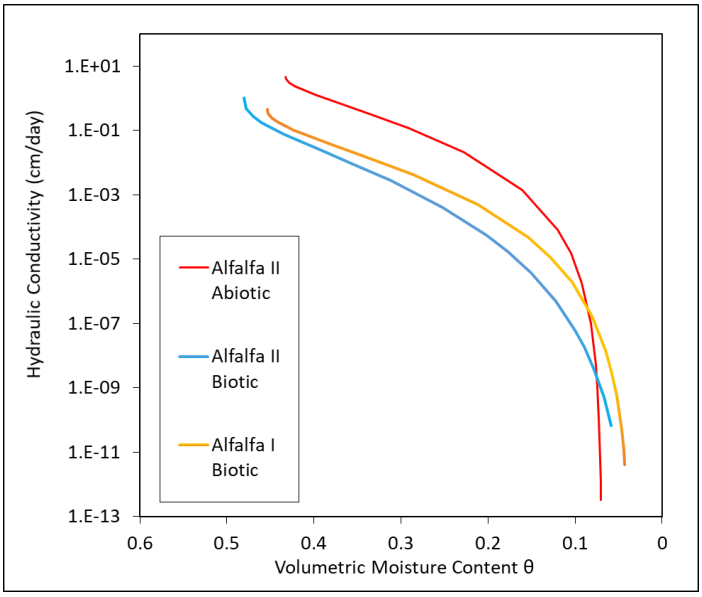

Figure 44. Volumetric moisture content on the x-axis verse hydraulic conductivity on the y-axis. All three samples in the study Alfalfa II abiotic, Alfalfa II biotic and Alfalfa I biotic are shown with estimated curves using the parameters generated from RETC.

3.5 Drainage Experiment: Static Stepwise

The hanging-water-column method was used to evaluate the difference in moisture retention at tension increments with either 3-hr or 12-hr equilibration times. This section used an experiment which is commonly applied to obtain moisture retention curves. The moisture retention curves for A-IIb, A-IIa and A-Ib were evaluated to achieve two goals. (1) The moisture retention properties of the soil under drainage can be compared to the data obtained by the HyProp under evaporation, and this comparison may yield information on the properties of biofilms. (2) Comparison of the moisture retention curves for the 3-hr and 12-hr equilibration times may shed light on the properties of films of different thickness. The moisture release curves will be evaluated for all three samples up to 60 cm of tension (maximum tension is determined by pore size of ceramic filter). Under common practice, the soil can drain until ‘it equilibrates’ under a specific applied tension. After it ‘equilibrates’ the tension is increased, and the soil is allowed to drain again. The time needed for ‘equilibration’ has never really been specified and different authors use different amounts of time. This experiment used the same protocol to tease out the proportion of drainage water that comes from filled capillaries versus

the proportion of water that comes from films in air-filled capillaries. It was determined prior, that 3 hours would be sufficient for all the capillary water to drain, therefore a longer time interval would also allow for film water to drain. This is not to say that some film water may be draining during the 3-hr interval. Therefore, two time intervals for drainage were investigated, 3-hrs and 12-hrs. Each experimental run shown in Table 10 and Figure 45 are called 'Events'. An Event tests concurrently three soil treatments, Alfalfa II abiotic (A-IIa) on Port I, Alfalfa II biotic (A-IIb) on Port IV, and Alfalfa I biotic (A-Ib) on Port VII (Table 10). At each controlled head there is a certain mass of water lost (Table 10).

Table 10. Mass of water lost at each tension during the events for the static stepwise hanging-water-column experiments. Port I is the abiotic Alfalfa II, Port IV is the biotic Alfalfa II, and Port VII is the biotic from Alfalfa I. The sum of the total water lost during the experiment is at the bottom row of the table.

Event #:		1			2			3			4		
Date:		3-Feb			2/7 -2/11			2/13-2/16			17-Feb		
Hold Time:		3 Hour			12 Hour			12 Hour			3 Hour		
Port:		I	IV	VII	I	IV	VII	I	IV	VII	I	IV	VII
ΔM_w		Volume of Water Lost (cm^3)											
Height (cm)	1	0	0	0	0	0	0	0	0	0	0	0	0
	10	1.58	10.45	3.71	1.53	10.03	18.21	4.19	25.55	11.44	2.47	31.08	25.08
	20	0.76	6.11	15.02	1.61	5.06	14.58	1.58	8.05	15.95	1.47	6.04	15.23
	25	0.82	1.85	8.97	5.92	6.71	7.28	6.63	5.19	8.29	6.49	5.46	8.47
	30	1.77	14.65	7.82	4.74	7.85	6.42	5.51	5.17	6.33	5.56	6.34	6.11
	35	14.93	9.42	6	4.51	6.82	5.36	3.98	5.23	4.52	3.35	5.22	5.06
	40	5.63	5.85	4.86	3.51	5.9	5.17	3.16	4.29	4.03	2.79	4.4	3.63
	60	11.03	15.99	15.62	7.86	11.02	11.37	6.49	10.22	11.72	5.97	9.99	10.47
$\sum M_w$		36.52	64.32	62	29.68	53.39	68.39	31.54	63.7	62.28	28.1	68.53	74.05

Figure 45 represents Alfalfa II abiotic and biotic calculated hydraulic conductivities from the 3-hr static stepwise experiments. During drainage the hydraulic conductivity begins with a lag then increases rapidly followed by a decrease while drainage from the pore continues (Figure 45). Both the abiotic and biotic have tensions where the hydraulic conductivity begins with a lag during drainage yet the biotic always has a larger lag comparatively. Figure 45 also displays the hydraulic conductivity during the early stages of evaporation, represented with the solid diamond

markers. Here the hydraulic conductivity is rather constant for A-IIb and drops off rather slowly. The abiotic treatment, on the other hand, has a hydraulic conductivity supporting the evaporation rate which drops off rapidly. This causes the abiotic treatment to transition to S-2 evaporation prior to the biotic sample, also seen in Run 4 (Figure 19).

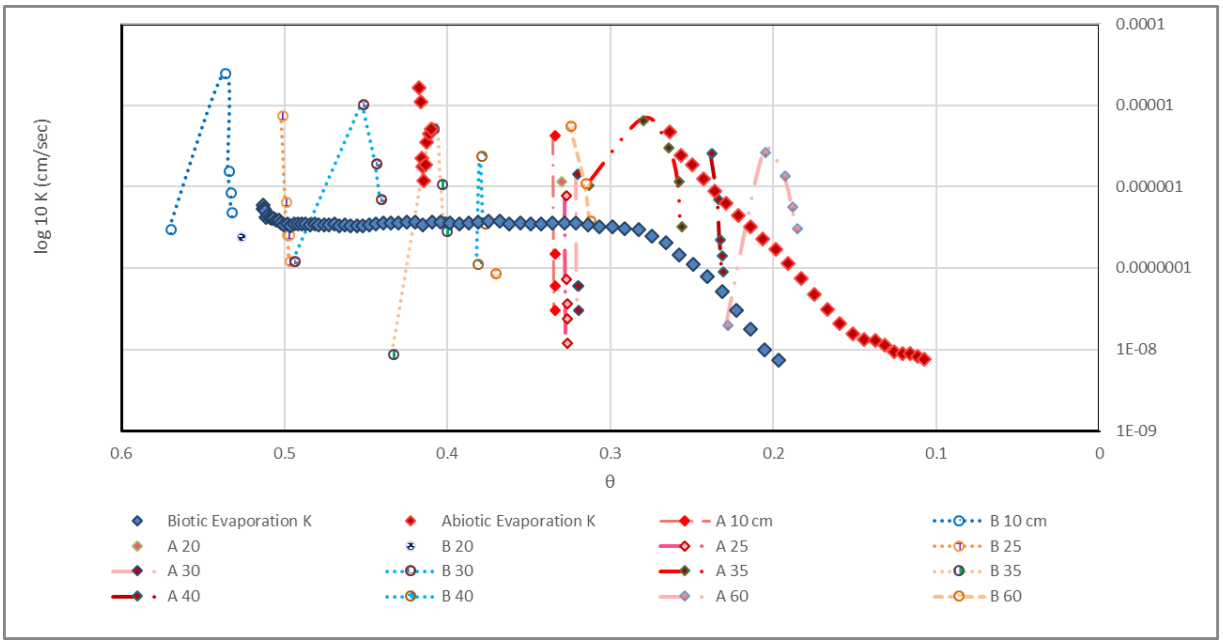

Figure 45. Hydraulic conductivity from the HyProp is compared with the hydraulic conductivities calculated from each controlled head during the hanging-water-column experiment. The legend indicates A for abiotic (A-IIa) and B for biotic (A-IIb) Alfalfa II and the number stands for the tension value.

Figure 46 displays all 4 Events for the static stepwise retention experiments with each treatment. The measurements shown in Figure 46 were taken at the end of each equilibration period. Events 1 and 2 represent the first 3-hr and 12-hr runs, respectively. A significant difference is seen in the moisture retention for the two biotic treatments. Event 1 shows very different results thus it was decided that this Event would be ignored in the discussion of the results due to the fact that there needed to be another wetting and drying cycle prior to data collection. This error with the system had corrected itself by Event 2, thus the data in Event 1 should not be considered. The differences seen in Events 1 and 2 for the biotic treatments are not seen between Events 3 and 4

particularly because of this reason. Therefore, it is interpreted that between Events 1 and 2, the wetting and drying cycles were still re-arranging particles in the media and the drainage pore structure had no stabilized. The stabilization of the pore structure occurred after Event 1, thus Event 2 data was evaluated.

Similar to the HyProp results, the biotic soils are showing a larger initial saturated moisture content relative to the abiotic soil. Focusing on Events 3 and 4 (Figure 46), it is clear that the biotic soils lost most of their ‘excess’ moisture during the first controlled tension of 10 cm, achieving the same moisture content as each other (A-Ib) and (A-IIb), while the abiotic soil (A-IIa) maintained a similar moisture content between the controlled tensions. While for all higher tensions the biotic soils remain wetter than the abiotic soil, the slope of the curves are similar up to a tension of 50 cm. B*y* the time a tension of 60 cm is reached, the abiotic curve becomes steeper, indicating the existence of smaller pores that hold water, whereas the biotic soil does not appear to have these smaller capillary pores.

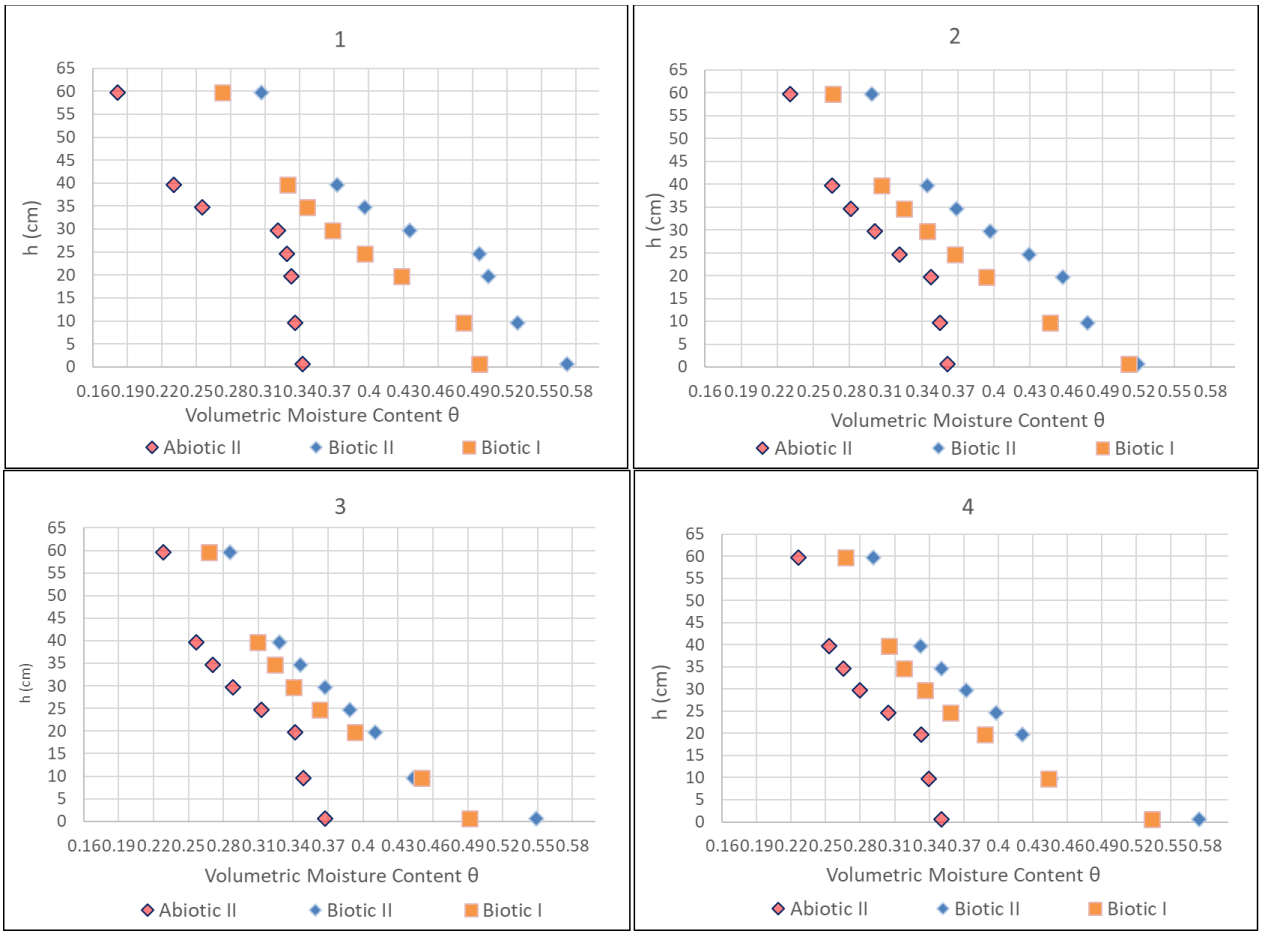

Figure 46. (Events 1 – 4) Static Stepwise retention experiment each displaying Alfalfa II, abiotic and biotic, and Alfalfa I, biotic. Volumetric moisture content is on the x-axis and the controlled head is on the y-axis.

When comparing data from the 3-hr and 12-hr equilibration times (Figure 47), it is clear that there is little significant difference in the moisture retained. If there is additional water leaving as thin films after the equilibration time, the amount of water is considered low. Note that data from Event 1 is ignored in our analysis because it was considered unreliable. However, for completeness it is included in the figures as a dashed line. There is a small difference in the biotic Alfalfa II (A-IIb) between the 12-hr Event 2 and the later runs. The difference indicates either the possible formation of a greater number of larger pores or improved drainage connection between these larger pores. This is seen in the lower retention held at 20 cm tension. The other two soil treatments do not show this evolution.

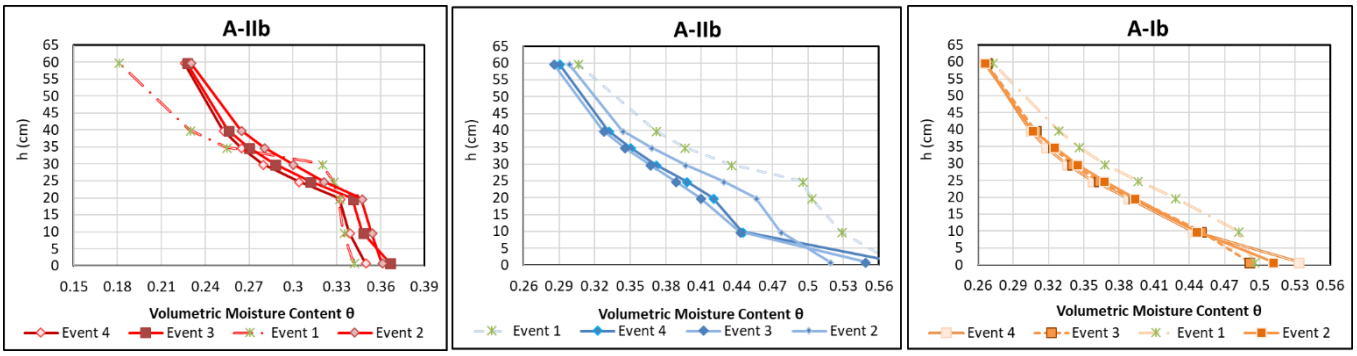

Figure 47. Moisture release curves for static stepwise experiment. Comparison of 3-hr and 12-hr equilibration times for each of the 3 soil treatments separately, A-IIa, A-IIb and A-Ib. Dashed line represents Event 1.

Table 11. shows the data in terms of saturation at each tension to account for the difference in soil porosity. If the soil is over 100% saturated, then it indicates that there was ponding that occurred on the soil surface. Alfalfa II biotic treatment appeared to have ponding during the first 3-hr, first 12-hr, and the last 3-hr controlled head experiments. The other two treatments did not have an issue with ponding comparatively, both treatments were either at saturation when the experiment began or a little below. Due to the fact that there were these differences at the first controlled step, these data points were eliminated from the results to appropriately compare between treatments (Table 11). The biotic treatments ended with a higher saturated moisture content at the end of the first 3-hr experiment. The abiotic treatment had the lowest degree of saturation at the end of the first 3-hr experiment but then the degree of saturation increased after the structure stabilized for the other three events. Until the structure is stabilized, the particle arrangement can change over time with multiple wetting and drying cycles thus changing where the moisture is retained (Figure 48). After eliminating Event 1 for all treatments, the 3-hr time increment was compared to the 12-hr for each treatment of A-Ib, A-IIb, and A-IIa (Figure 49 and 50). Graphing the data in terms of saturation makes the similarities between 3-hr and 12-hr runs (for the same soil) even more evident (Figure 49 and 50). However, when comparing across soil treatments, there is a significant difference (Figure 48).

Table 11. Final saturation of soil at the end of each equilibration period, during the static stepwise hanging-water-column experiments. The hold time for which the soil was allowed to drain at each tension is indicated on the third row of the table heading.

Event #:		1			2			3			4		
Date:		3-Feb			2/7 -2/11			2/13-2/16			17-Feb		
Hold Time:		3 Hour			12 Hour			12 Hour			3 Hour		
Port:		I	IV	VII	I	IV	VII	I	IV	VII	I	IV	VII
S		Degree of Saturation											
	10	1.00	1.00	1.00	1.00	1.00	1.00	1.00	1.00	1.00	1.00	1.00	1.00
	20	0.99	0.95	0.89	0.98	0.96	0.88	0.98	0.92	0.87	0.98	0.94	0.88
	25	0.98	0.94	0.82	0.91	0.90	0.82	0.90	0.88	0.81	0.90	0.89	0.81
	30	0.96	0.82	0.76	0.85	0.83	0.77	0.83	0.83	0.76	0.82	0.83	0.76
	35	0.76	0.75	0.72	0.79	0.77	0.73	0.78	0.78	0.72	0.78	0.79	0.72
	40	0.68	0.70	0.68	0.75	0.72	0.69	0.74	0.74	0.69	0.74	0.74	0.69
	60	0.54	0.58	0.56	0.65	0.62	0.59	0.65	0.64	0.59	0.67	0.65	0.60

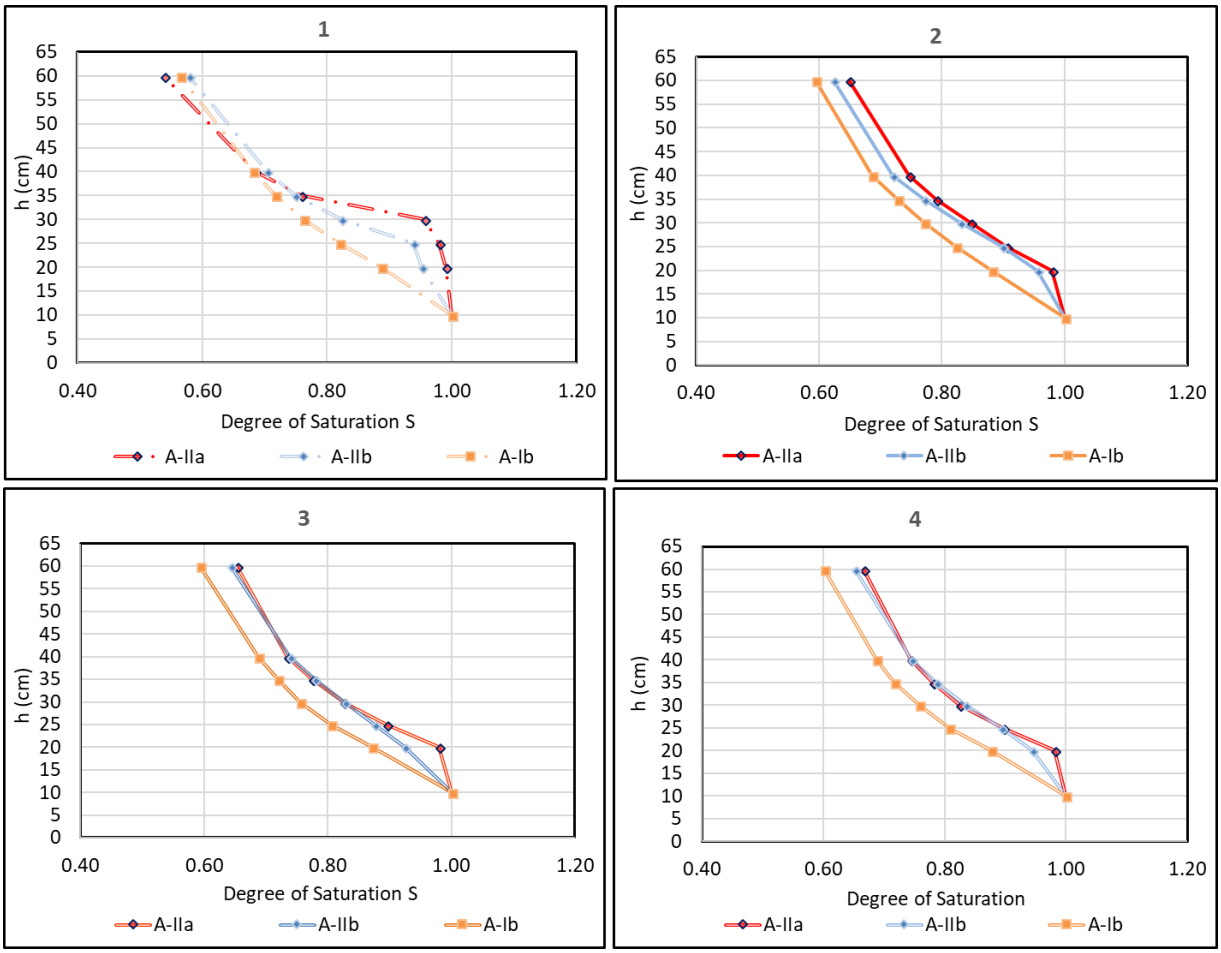

Figure 48. (Events 1-4) Moisture retention curve in terms of saturation for all three samples during each of the events. Event 1 is shown with dotted line because it does not follow the pattern of the other 3 events.

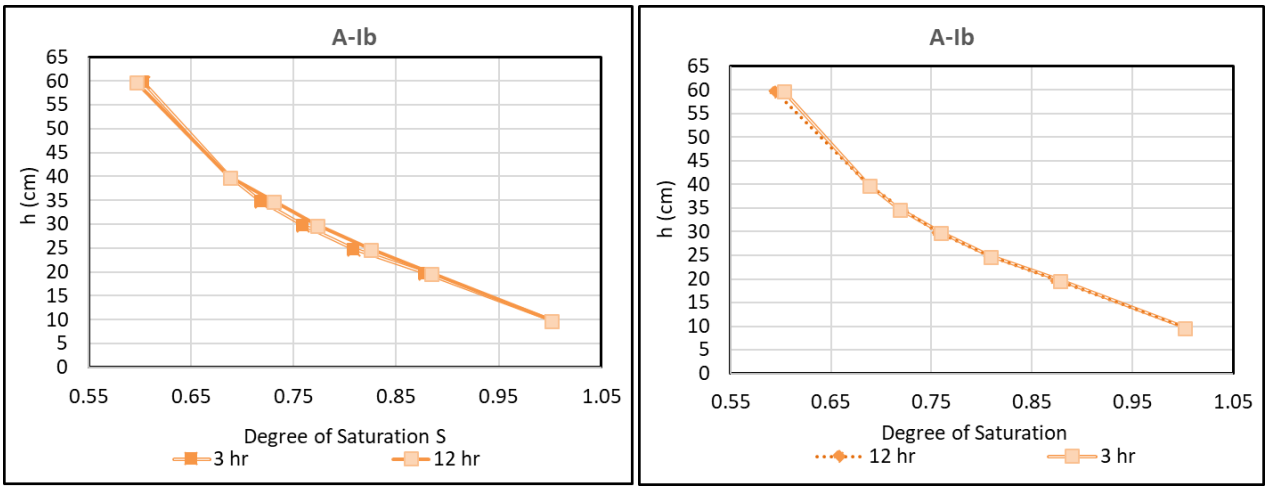

Figure 49. Moisture retention curve in terms of saturation for Alfalfa I biotic (A-Ib). Comparison of data from 3-hr (Event 4) and 12-hr (Events 2 and 3) equilibration times.

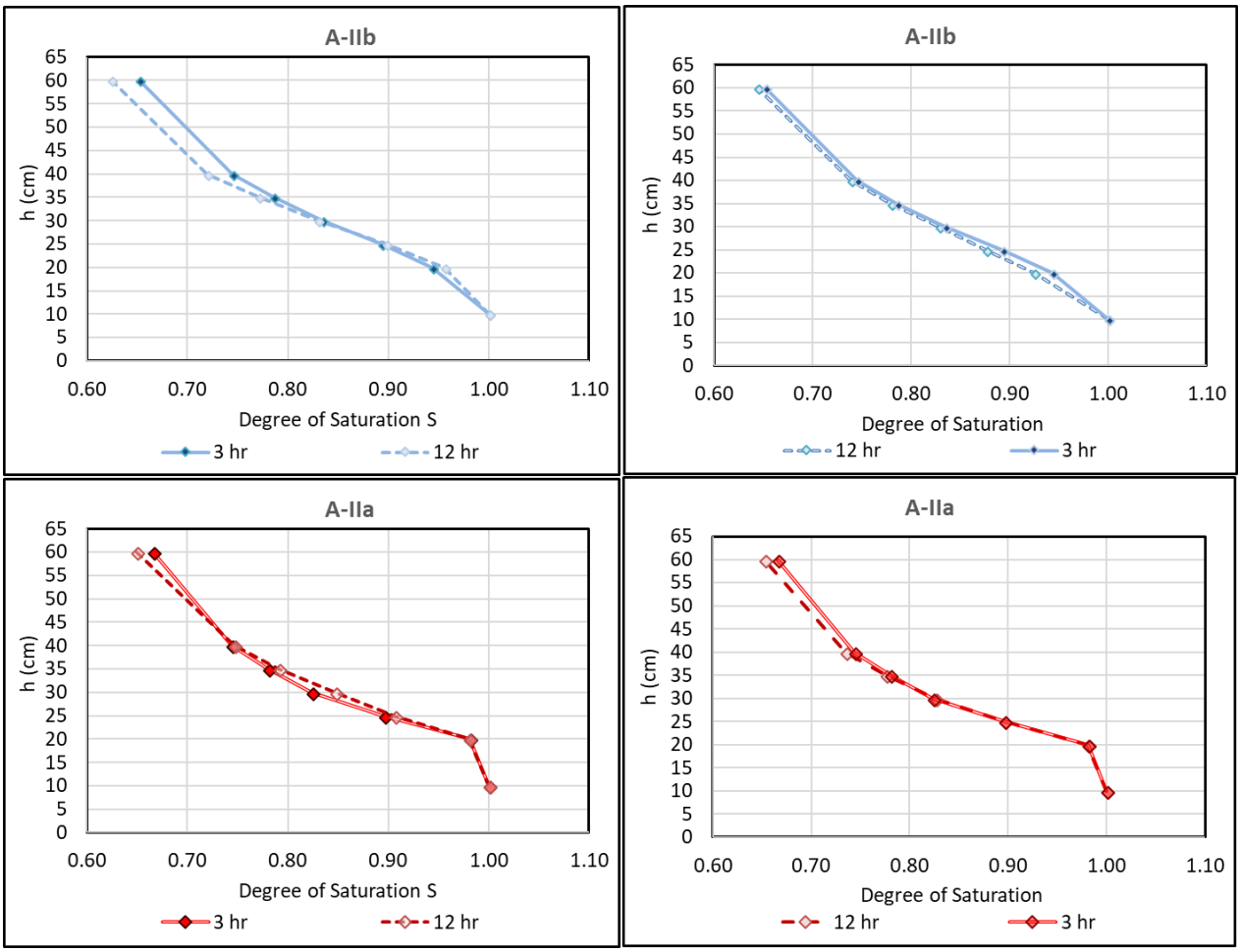

Figure 50. Moisture retention curve in terms of saturation for Alfalfa II abiotic (bottom red) and biotic (top blue). The 3-hr data is taken from Event 4 which is compared to the 12-hr data (Events 2 and 3).

3.6 Proportion of water held in films

The data collected with the hanging-water-column method is used here to identify the proportion of water that is drained from films after capillary drainage (Table 12). The saturation at the 3-hr equilibration time indicates water that remains after water has been drained by from capillary tubes of radius, R, larger than associated with the applied tension, i.e., $R > R(h_{c\ applied})$. During this time water held in films also drains. All films whose thickness, $D > R(h_{c\ applied})$ will also drain during this time because the hydraulic conductivity is the same [Note that as a simplification at this stage we are ignoring the reduction in hydraulic conductivity caused by biofilm rheology]. Once capillary equilibration at 3-hrs is reached, no more capillary water can drain (assuming a simple capillary bundle model), therefore and any water that does drain must be from thinner films, i.e., $D < R(h_{c\ applied})$ which have lower hydraulic conductivities and drainage rates. Therefore, the difference between the saturation values at 3-hr and 12-hr equilibration times quantify the water draining from these thinning films. Draining water may also include water from small capillaries that are would not otherwise drain because their capillary tension is greater but happen to be connected to films and therefore may slowly leak and drain via these thinning films. To calculate the proportion of this additional water draining purely as thin films, the following equation was used:

$$\%\ water\ in\ film = \frac{\theta_{3hour} - \theta_{12hour}}{\theta_{3hour}} \qquad [24]$$

Results are shown in Table 12, which shows the amount of water drained by thinning films and other capillary water that continued to drain via films, following capillary equilibration at 3-hrs, as a proportion to the total degree of saturated water held by both films and capillarity (i.e., saturation at 3-hrs). This proportion of total saturation held in films is represented by the solid

dark blue bar (Figure 51). There was an inconsistency with the first head values due to ponding, therefore this value was eliminated in the results (Table 12), beginning with the tension value of 10 cm instead.

Table 12. The proportion of total saturation that is held in films under the conditions corresponding from [eq. 24].

Event #:		#4 - #2			#4 -#3			#4 - #2			#4 -#3		
Hold Time:		3 hour - 12 hour			3 hour - 12 hour			3 hour - 12 hour			3 hour - 12 hour		
Port:		I	IV	VII	I	IV	VII	I	IV	VII	I	IV	VII
S		Proportion of total saturation held in films						Films hold what % of remaining water					
Height (cm)	10	0.00	0.00	0.00	0.00	0.00	0.00	0.00	0.00	0.00	0.00	0.00	0.00
	20	0.00	-0.01	-0.01	0.00	0.02	0.00	0.00	-0.01	-0.01	0.00	0.02	0.00
	25	-0.01	0.00	-0.02	0.00	0.02	0.00	-0.01	-0.01	-0.02	0.00	0.02	0.00
	30	-0.02	0.00	-0.01	0.00	0.01	0.00	-0.03	0.01	-0.02	0.00	0.01	0.00
	35	-0.01	0.01	-0.01	0.00	0.01	0.00	-0.01	0.02	-0.02	0.01	0.01	0.00
	40	0.00	0.03	0.00	0.01	0.01	0.00	0.00	0.03	0.00	0.01	0.01	0.00
	60	0.02	0.03	0.01	0.01	0.01	0.01	0.03	0.04	0.01	0.02	0.01	0.01

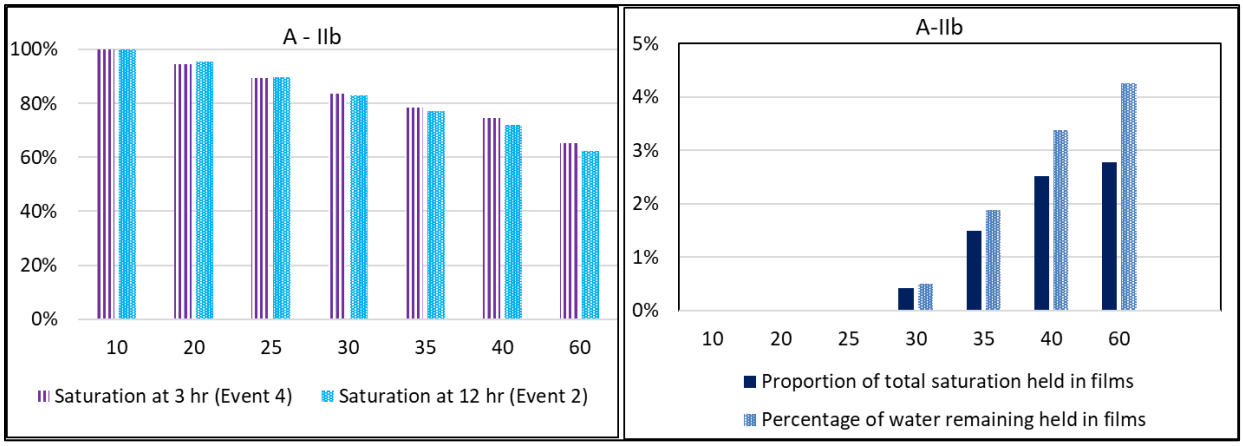

Figure 51. (Events 4 and 2) Alfalfa II biotic (A-IIb) soil moisture drained by thinning films, post 3-hr equilibration time. Saturation held in capillary water and in films that continued to drain after 3-hrs of capillary drainage. The stripped bars indicate the saturation at the 3-hr hold time (Event 4). The dotted bars indicate the 12-hr hold time (Event 2). The percentage of remaining water that is held by films is shown on the right represented with light blue bars found using [eq.24].

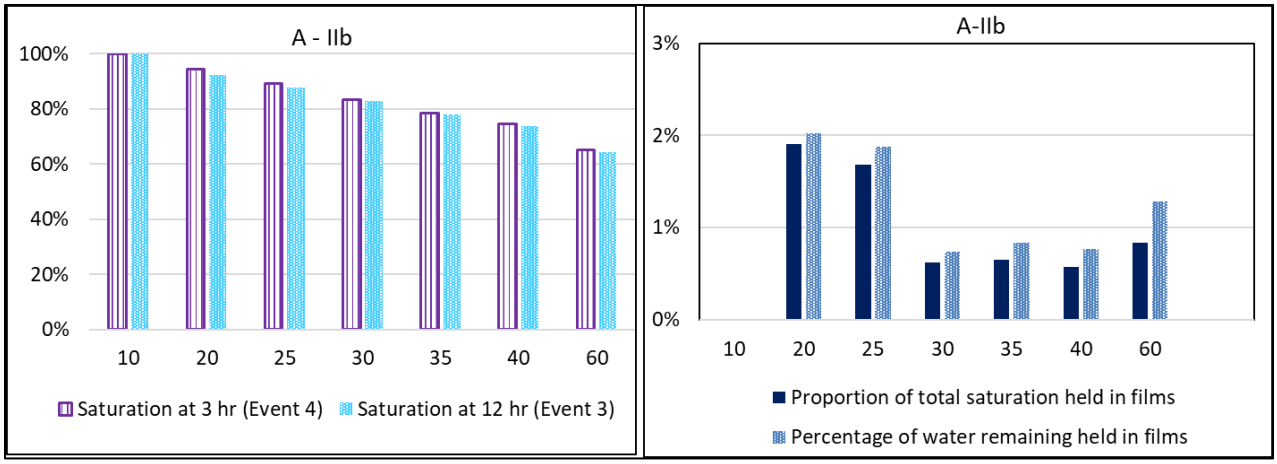

Figure 52. (Events 4 and 3) Alfalfa II biotic (A-IIb) saturation held in capillary water and films that continued to drain after 3 hours of capillary drainage. The saturation that is held by capillary and films is indicated by the stripped bars. The dotted blue bars indicate the hold time for the 12-hr increment which represents water drained from films. The proportion of total saturation held by films is indicated with the solid dark blue bar. The percentage of remaining water that is held by films [eq.24] is shown on the right figure in light blue.

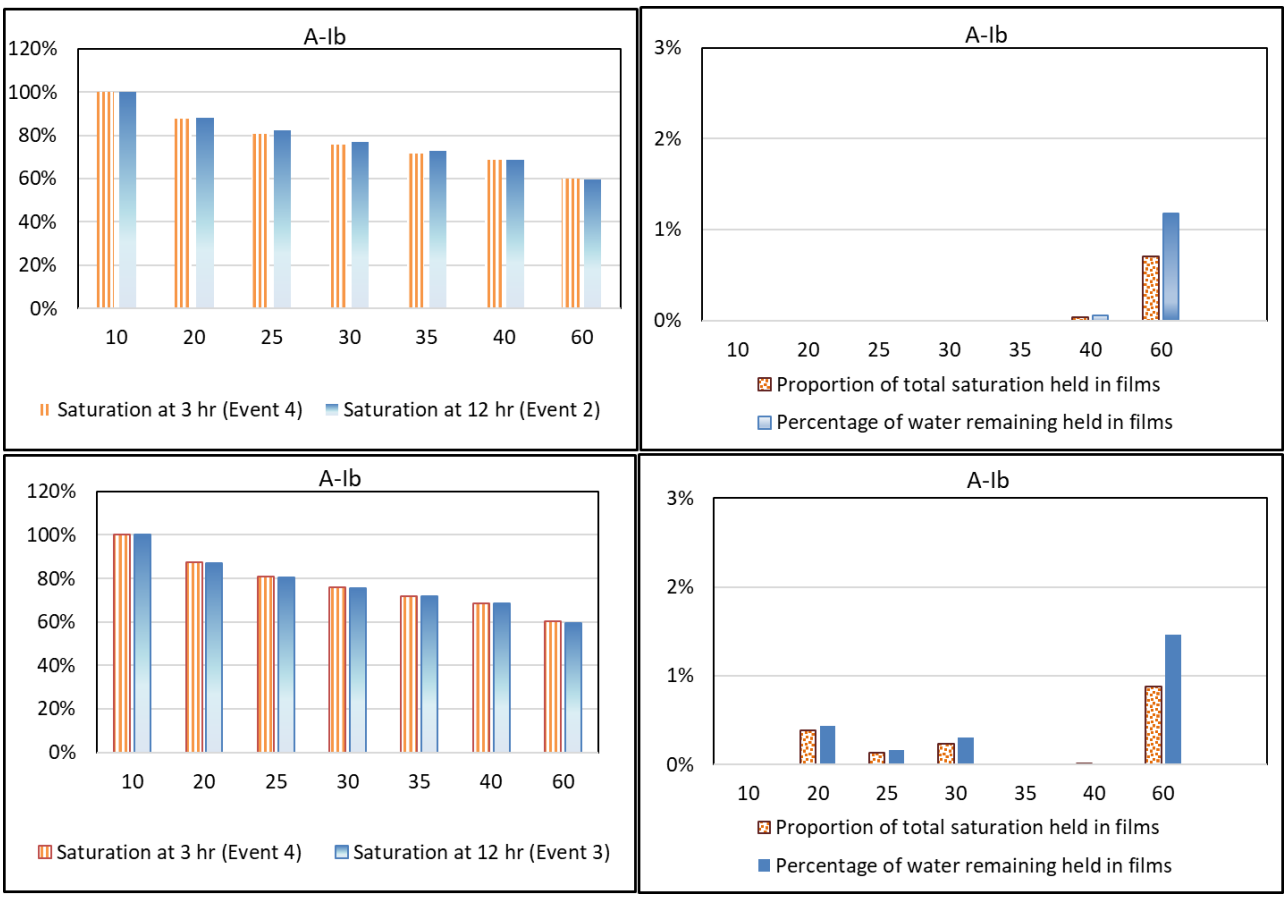

Figure 53. Alfalfa I biotic (A-Ib) soil moisture drained by thinning films, post 3-hr equilibration time. Data from comparison of Events 4 and 2 shown in the top two figures; Events 4 and 3 are compared in the bottom two figures. Event 4 is the 3-hr data and Events 2 and 3 are the 12-hr runs, respectively. Left figures show saturation at the end of

3-hr and 12-hr times for different applied tensions relative to the saturation at the tension at 10 cm. The difference between the 3-hr and the 12-hr saturations [eq.24] is interpreted as the water drained by thinning films.

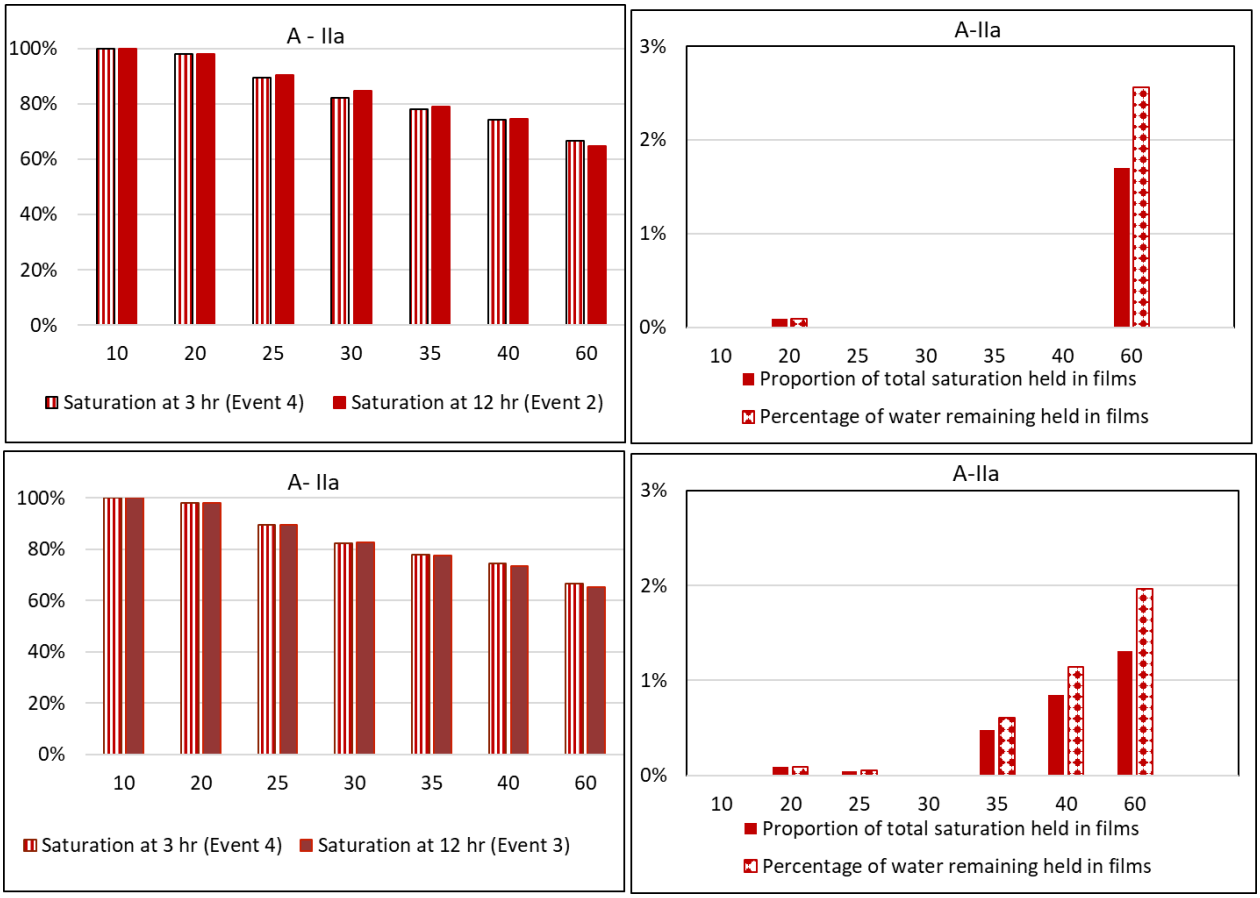

Figure 54. Alfalfa II abiotic (A-IIa) soil moisture drained by thinning films, post 3-hr equilibration time. Data from comparison of Events 4 and 2 shown in the top two figures; Events 4 and 3 are compared in the bottom two figures. Event 4 is the 3-hr data and Events 2 and 3 are the 12-hr runs, respectively. Left figures show saturation at the end of 3-hr and 12-hr times for different applied tensions relative to the saturation at the tension at 10 cm. The difference between the 3-hr and the 12-hr saturations [eq.24] is interpreted as the water drained by thinning films.

Alfalfa II biotic (A-IIb) has a larger proportion of water drained from films with the associated radius from the applied tension values of 30 cm to 60 cm yet no significant moisture drained from films with the associated radius from the tensions values below 30 cm (Figure 51). Note that the y-axis in Figure 51 extends to 5% whereas the following figures only extends to 3% (Figures 52-54). Alfalfa II biotic (A-IIb) had the largest percentage of water drained by films at each tension, except for that of 10 cm, after capillary drainage (Figure 52). The biotic treatment from Alfalfa I had a larger proportion of water drained from films when comparing Events 4 to 3

than when comparing Events 4 to 2 (Figure 53), indicating there was a difference between 12-hr runs for this treatment. The abiotic had a larger proportion of water draining from films with the associated radius from the applied tension value of 60 cm (Figure 54). Figure 54 also shows that there is a slight difference between 12-hr runs, similar to Alfalfa I biotic in Figure 53. It is reasonable to state that more moisture was drained from films during the comparison between Events 4 and 3 for all treatments. Since water is still draining from the pores after capillary drainage, given the opportunity to drain, it raises the question how long these films will continue to drain if allowed.

The volume of water lost between each change in tension value could indicate the proportion of pore space that is occupied by different pore radii, since pore radii are directly proportional with the capillary tension value. If there is a larger volume of water, it could be attributed to the soil having a large number of pores with that associated pore radii holding water (Figure 55).

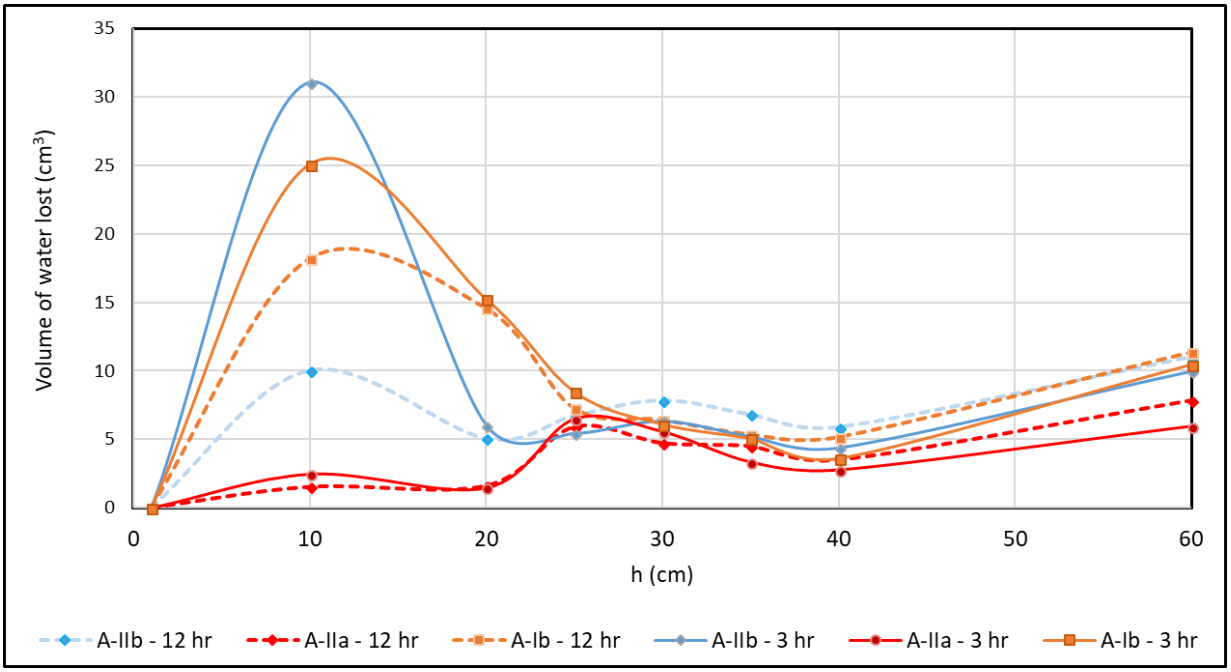

Figure 55. Volume of water drained at each tension for Alfalfa I biotic (A-Ib), Alfalfa II biotic (A-IIb), and Alfalfa II abiotic (A-IIa). Event 4 (3-hr equilibration time) and Event 2 (12-hr equilibration time) are compared.

For the same soil sample, if it is assumed that pore size distribution does not change between events, then differences in the volume of water draining between the two equilibration times, would indicate a different mechanism draining water (Figure 55 and 56). For different soil samples, however, water differences may be attributable to differences in pore size distribution as well as drainage mechanisms. Figure 57 compares Alfalfa II abiotic (A-IIa) to Alfalfa II biotic (A-IIb) for Events 3 and 4. The biotic treatment is draining an overall larger volume of water at each controlled tension value compared to the abiotic except at 25 cm of head (Figure 57). The biotic also shows a greater difference between the 3-hr hold time compared to the 12-hr hold time, whereas the abiotic is only showing a significant difference for the head value of 10 cm (Figure 57). Alfalfa I biotic (A-Ib) 3-hr and 12-hr increments also show different volumes of water lost at the 10 cm controlled tension value (Figure 58). These differences could be associated with biofilm growth in the pore as well as changes in pore geometry. All treatments show that the 12-hr increments are less saturated than the 3-hr increments, indicating that more moisture was drained from films after capillary drainage.

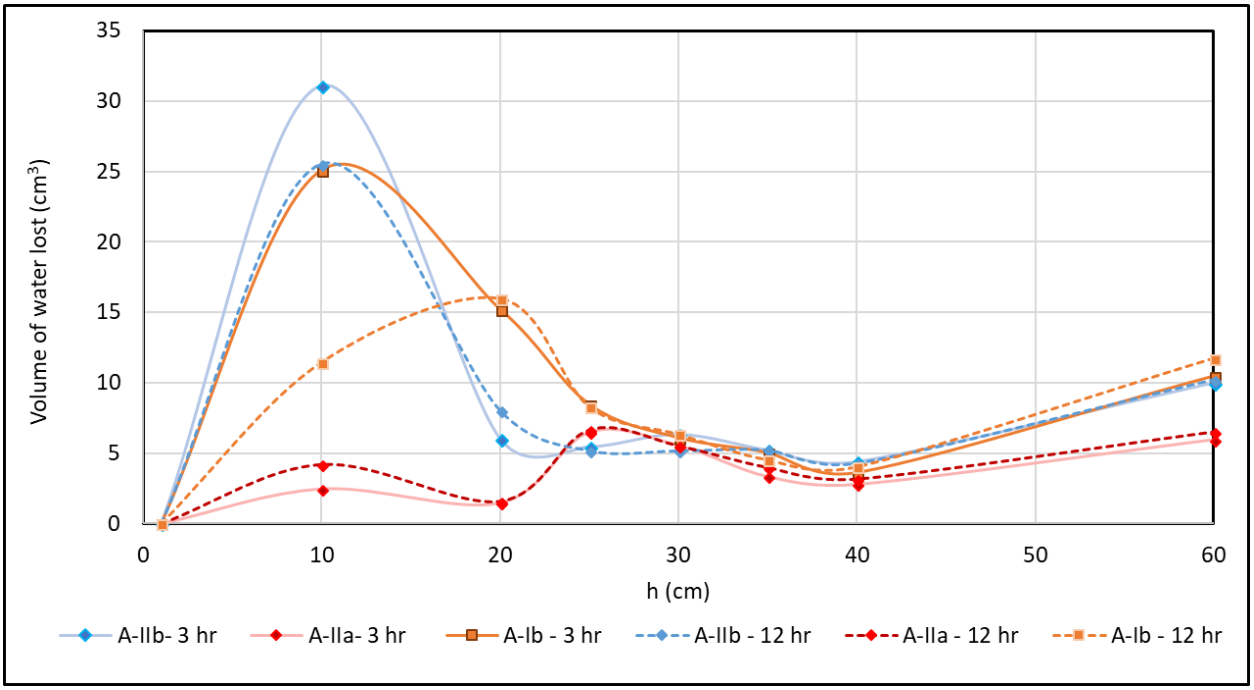

Figure 56. Volume of water drained at each controlled tension for Alfalfa I biotic (A-Ib), Alfalfa II biotic (A-IIb), and Alfalfa II abiotic (A-IIa). Event 4 (3-hr equilibration time) and Event 3 (12-hr equilibration time) are compared.

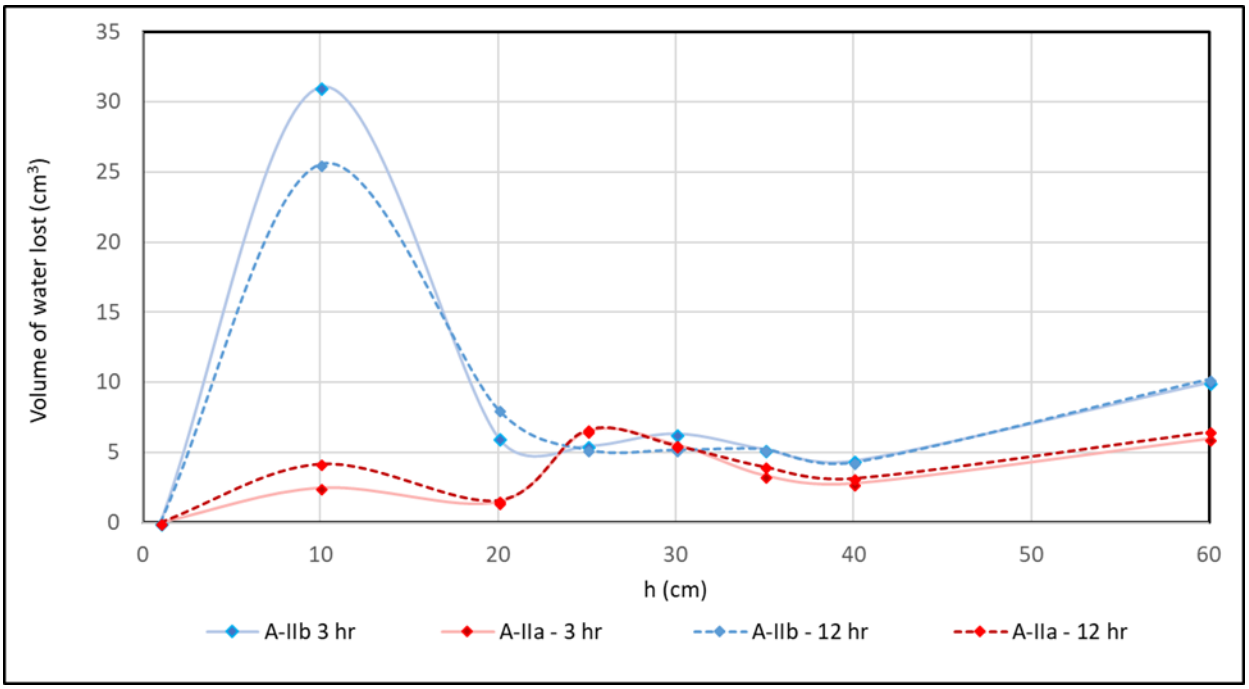

Figure 57. (Events 3 and 4) Volume of water drained for each controlled tension for Alfalfa II biotic (A-IIb) and Alfalfa II abiotic (A-IIa).

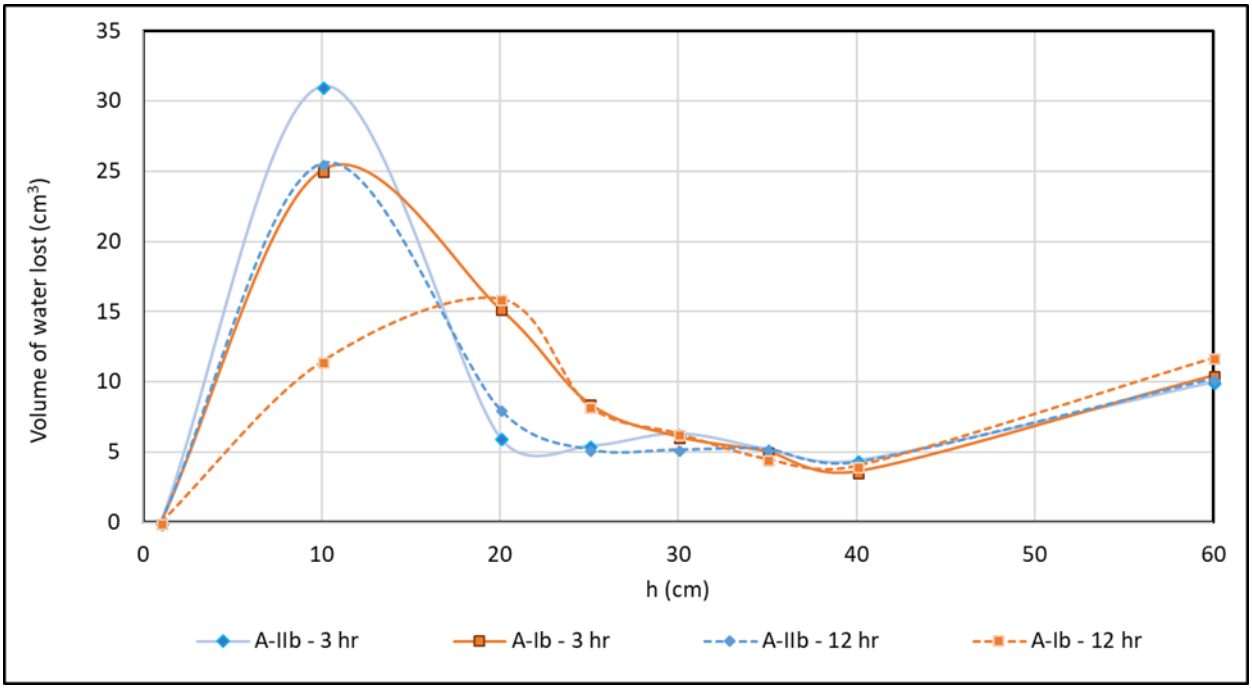

Figure 58. (Events 3 and 4) Volume of water drained for each controlled tension for Alfalfa II biotic (A-IIb) and Alfalfa I biotic (A-Ib)

3.7 Hydraulic Conductivity during drainage

The hydraulic conductivity of the Alfalfa II abiotic and biotic treatments during the static stepwise retention experiment was explored. The water released after the 3-hr hold time was associated with films due to the previous calculations made. This idea led us to believe that the hydraulic conductivity of capillary water could be different than the hydraulic conductivity of water drained by films. The hydraulic conductivity for the 3-hr hold time was calculated using equation 16 for both treatments and compared (Figures 59 and 60). As expected, the hydraulic conductivity varies at each controlled tension, since the water is moving through different sized pores. At all head values the biotic hydraulic conductivity is higher than the abiotic (Figure 59). This is seen during both the 3-hr and the 12-hr hold times.

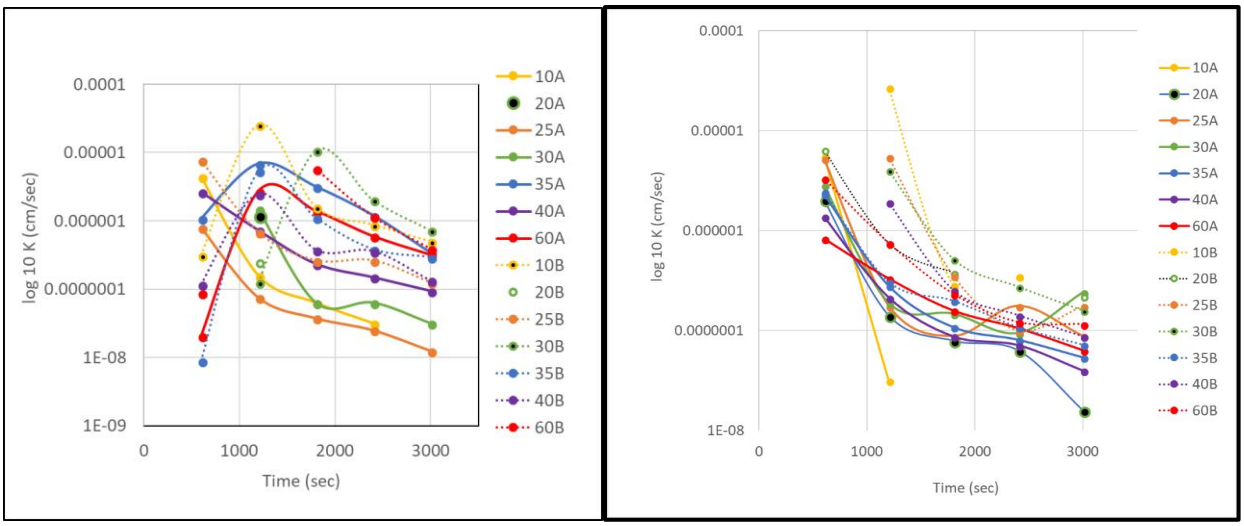

Figure 59. Hydraulic Conductivity (K) for 3-hr (left) and 12-hr (right) equilibration time for AII-a and AII-b. The legend shows the head value with the letter code A or B standing for abiotic or biotic, respectively. The graph on the right is the same as the graph on the left except the scale reads log base 10 for hydraulic conductivity.

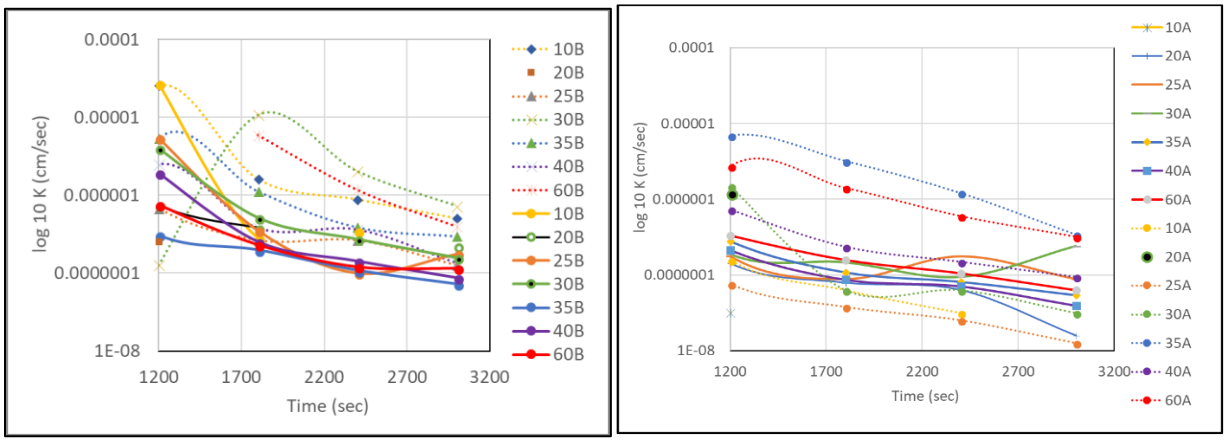

Figure 60. Alfalfa II biotic (A-IIb) shown on the left graph and Alfalfa II abiotic (A-IIa) shown on the right graph. The solid lines indicate the 12-hr hold time and the dotted lines indicate the 3-hr hold time.

In both cases the hydraulic conductivity decreases as drainage continues within the soil and pores begin to dry out. Most of the abiotic 12-hr hydraulic conductivities are also lower than the 3-hr increments (Figures 60). The K_{biotic} for the second 3-hr run shows the value at 10 cm tension to be lower than the value at greater tension. It is unclear if this is real or an artifact of calculations (Figure 61).

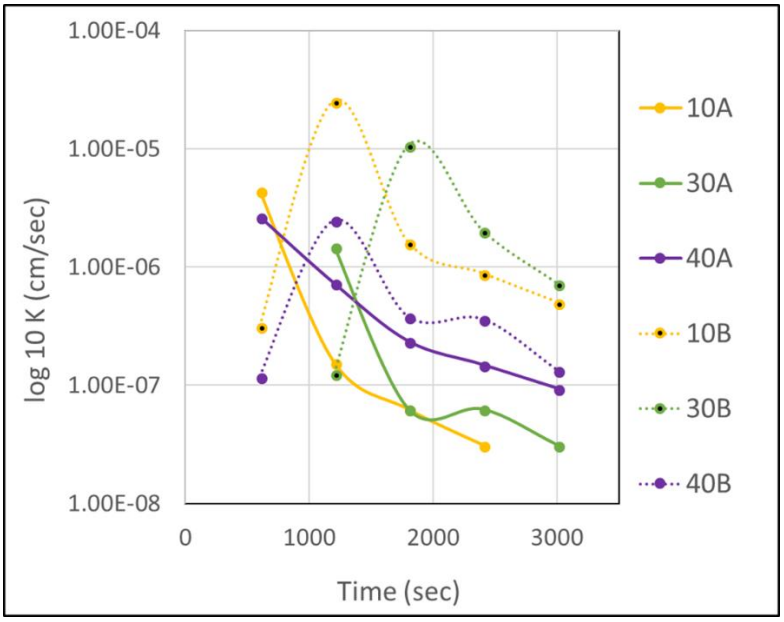

Figure 61. Hydraulic conductivity during Event 2 for the 3-hr equilibration time. Alfalfa II abiotic (solid) and Alfalfa II biotic (dotted); legend code shows applied tension in cm, with A and B referring to abiotic and biotic, respectively.

3.8 Dynamic Drainage at 60 cm

During the dynamic drainage experiments water could drain freely from the soil. It was expected that under free drainage the biotic treatments would release more moisture due to moisture being held in films. Data from the literature indicates that biofilms reduce the hydraulic conductivity of pores by either clogging pores thereby reducing pore size and increasing tortuosity and/or by changing the rheological properties of the water. This section examines a free drainage experiment using the hanging-water-column technique to investigate the two treatments of biotic and abiotic from Alfalfa II and the biotic treatment from Alfalfa I. The same soil samples used in the previous experiments, HyProp and Static Stepwise, were used. Five different drainage events were evaluated (Table 13) one with Alfalfa - Ib and Alfalfa - IIb, and the other four were abiotic and biotic treatments from Alfalfa II. Event 1 is different from the rest because the experiment only ran for 36 hours and begin immediately after the Static Stepwise

experiment. Event 2 only has data collected from the biotic treatments because the abiotic had issues with the equipment.

Table 13. Dynamic drainage experiments, where the run number is synonymous with the event number. Port I indicates the tension funnel for Alfalfa II abiotic treatment, Port IV indicates the biotic treatment for Alfalfa II and Port VII indicates the biotic treatment of Alfalfa I. The date the experiment took place on as well as the length of time the experiment was run for indicated by the hold time.

Event #:	1			2*			** Equipment Check	3			4			5		
Date:	3-Feb			26-Feb				2-Mar			6-Mar			13-Mar		
Hold Time:	36 Hours			72 Hours				72 Hour			72 Hours			72 Hours		
Port:	I	IV	VII	I	IV	VII		I	IV	VII	I	IV	VII	I	IV	VII

*Next to the event signifies contamination of abiotic soil specimen.
**Time reserved to sterilize equipment.

Note that the first figure is Event 1 where the data was collected differently from the other free drainage experiments, thus the results are different from the rest. The water reservoir was left at 60 cm to drain for 36 hours after completion of the Static Stepwise experiment. The water in Figure 60 is released slower compared to the other drainage experiments. This is caused from the fact that water had been released from each controlled head previously, changing the amount of water released at the 60 cm drainage.

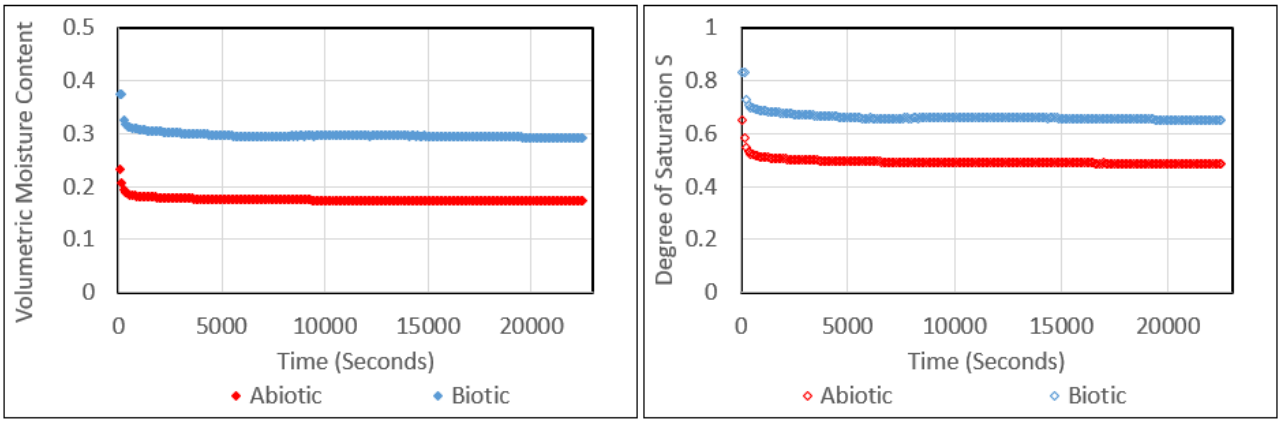

Figure 62. (Event 1) Free drainage for A-IIa and A-IIb. Time series of moisture content during drainage is shown in terms of volumetric moisture content (left) and saturation (right). For event data see Table 13.

Event 2 compared two different textures under biotic conditions, Alfalfa I and Alfalfa II. The two textures behaved similarly, except Alfalfa II had a larger initial saturated moisture content (Figure 61). The remaining three Events (3, 4 and 5) compared the Alfalfa II under biotic and abiotic conditions. In all cases, the biotic soil lost water more rapidly at early time (larger pores), and then drainage slowed down. The abiotic treatment lost water slowly in the beginning and then increased its drainage rate as time continued (Figure 62).

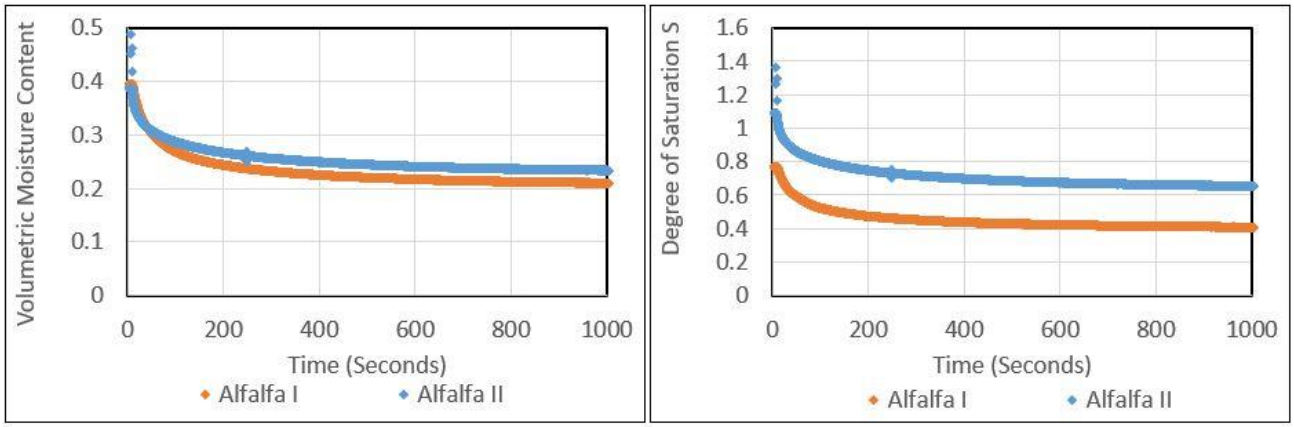

Figure 63. (Event 2) Free drainage for A-Ib and A-IIb. Time series of moisture content during drainage is shown in terms of volumetric moisture content (left) and saturation (right). For event data see Table 13.

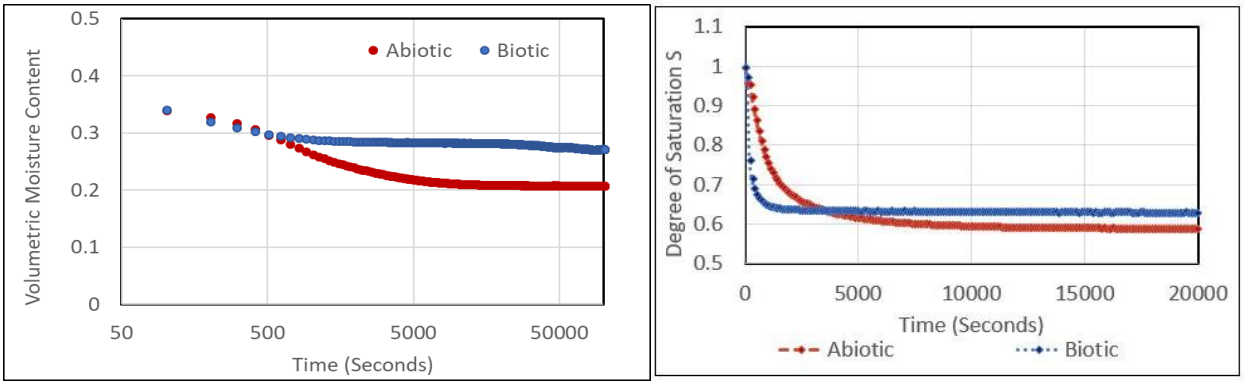

Figure 64. (Event 3) Free drainage for A-IIb and A-IIa. Time series of moisture content during drainage is shown in terms of volumetric moisture content (left) and saturation (right). For event data see Table 13.

Except for Event 1, Events 2-5 show a peculiar cross-over in the time series of the volumetric moisture content. While the cross over did not occur at the same time in all experiments, it did occur at similar moisture contents ranging from 28-32%. Below this moisture value, the biotic

soil loses water at much lower rates than the abiotic soil (Figures 63, 64 and 65). If the slope of the line represents the change in moisture content over time, then during free drainage it is approximately equal to the hydraulic conductivity. Event 3 (Figure 64), Alfalfa II biotic loses water rapidly but over time establishes an equilibrium of a higher saturated moisture content than the abiotic soil. Again, if the slope represents the hydraulic conductivity, in this case the (K) for the biotic is less than the abiotic. Event 4 shows both Alfalfa II abiotic and biotic losing water rapidly in the beginning then begins to drain water slowly (Figure 64).

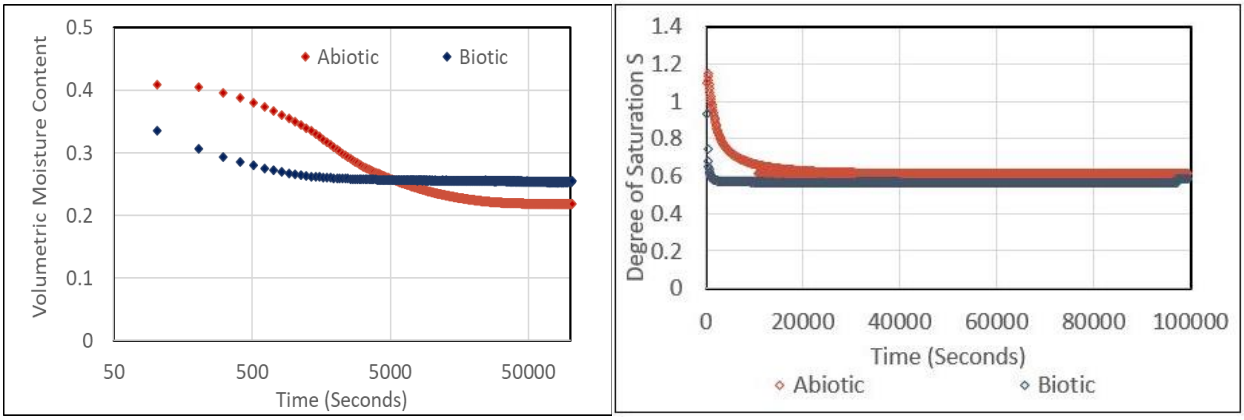

Figure 65. (Event 4) Free drainage for A-IIb and A-IIa. Time series of moisture content during drainage is shown in terms of volumetric moisture content (left) and saturation (right). For event data see Table 13.

Examining the degree of saturation, shows that the abiotic treatment may have been ponded at the start of the experiment which could have caused this treatment to have a higher degree of saturation compared to the biotic treatment (Figure 65). The final run was an extra experiment held for Alfalfa II abiotic and biotic treatments due to the fact that during event number 2 air entered beneath the ceramic plate of the abiotic tension funnel. Both treatments started at saturation and allowed to drain at 60 cm for 72 hours (Figure 66).

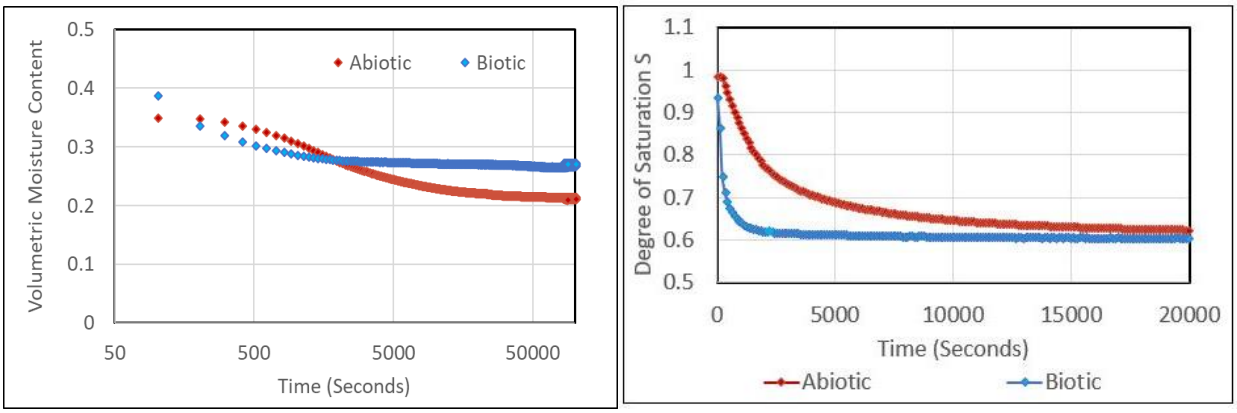

Figure 66. (Event 5) Free drainage for A-IIb and A-IIa. Time series of moisture content during drainage is shown in terms of volumetric moisture content (left) and saturation (right). For event data see Table 13.

Water is lost from both treatments rapidly, then the biotic remains at 27% volumetric moisture content and the abiotic remains at 21% (Figure 66). At the end of the experiment the biotic treatment ends at 60% saturation and the abiotic is extremely similar ending at 59% (Figure 66). In all cases, the hydraulic conductivity for the biotic and abiotic soils exhibit a crossover, with the biotic soil having much lower conductivity than the abiotic at long time. The higher hydraulic conductivity is interpreted as resulting from larger pores in the biotic soil.

3.9 Evaluation of Microbial Content and Activity

The content and activity of the microbiota were determined by fumigation extraction (Brookes *et al.* 1985) quantified with the Shimadzu TOC (Shimadzu Co., 2018) and by a 24-hour CO_2 burst test (Franzluebbers and Haney 1996). 160 grams of soil were provided for these analyses. Soil was incubated at 50% water filled pore space. CO_2 was evaluated using the Picarro Autoanalyzer (PICARRO Inc., 2018). Next, the Elementar Vario MACRO cube was used to analyze total carbon and total nitrogen content. Laboratory analysis were completed by CAL at Oregon State University (Table 13 and Table 14).

Table 14. Content and activity levels of the microbiota for Alfalfa II sample (A-IIb). D.S. indicates dry soil and MRC indicates microbial respiration carbon.

Microbial Biomass Carbon	Microbial Biomass Nitrogen	MBC:SOC Ratio	Community Respiration	Metabolic Quotient (qCO2)	Microbial Quotient	Total Dissolved C	Total Dissolved N
MBC	MBN	MBC:SOC		MRC:MBC	MBC: SOM	DOC	TDN
µg g^{-1} D.S.	µg g^{-1} D.S.		µg CO2-C /g D.S./day			µg g-1 D.S	µg g-1 D.S
2119.19	10.89	0.15	13.26	0.01	0.08	2337.84	163.27

Table 15. Total Carbon, Total Nitrogen and Total Soil Organic Matter content for both Alfalfa I (A-IIb) and Alfalfa II (A-IIb) samples corresponding to the two different alfalfa field site locations.

Sample:	Total C	Total N	SOM	C:N
	g C kg^{-1} D.S.	g N kg^{-1} D.S.	g SOM kg^{-1} D.S.	
Alfalfa I	15.1	1.59	28.69	9.50
Alfalfa II	14.43	1.57	27.42	9.19

The data was collected in order to assess what proportion of the soil organic matter (SOM) in these soils were of microbial biomass. The ratio of microbial biomass to the soil organic matter is about 8% and out of the soil organic carbon specifically, about 15% is of microbial biomass. Typically, the smaller the metabolic quotient the more efficient the microbial community is using carbon resources, yet this could also be influenced by laboratory conditions thus it is difficult to confirm that the community is efficient at using the carbon in the soil by this value alone. The low C:N ratio indicates that the material is being digested rapidly and nothing is being left in the system. The average C:N for soil microbes is around an 8 and in Table 14 both Alfalfa I and Alfalfa II have about a 9 C:N ratio.

Chapter 4: Discussion

4.1 Discussion of Results: Protocol for interpretation

The microbial biomass usually represents only 1% to 4% of the total soil organic carbon but can be affected by cropping systems and management techniques (Sparling 1992). Management practices influence microbial biomass almost immediately, making it a better predictor of changes to the total SOC pool (Powlson and Jenkinson 1981). The proportion of microbial biomass coming from the total SOC is surprisingly high at about 15% (Table 13) yet could be representative of the management techniques in practice (low tillage, cover crops, and yearly manure applications). Practices such as these will allow more labile organic substrates to be maintained within the soil (Balota *et al.* 2003). Less disturbance also favors the formation of micro-aggregates, protecting the habitat for the microbial community which will likely increase the total SOC pool and improve nutrient cycling (Awale *et al.* 2017). This will ultimately increase the amount of microbial biomass per unit of soil organic carbon, results shown in Table 13. It would be beneficial to examine another site which is under different management practices to compare these results. If the water retention capabilities are significantly different between the management styles, then it could be assumed that soil health, microbial biomass and water dynamics are tightly connected. Confirming that microbial biomass would be a good indicator for water retention capabilities in sandy soils. The ratio of microbial biomass to soil organic matter is around 8%. The question remains whether the impact on water retention is specifically caused from the MBC or the SOM in general. It is important to differentiate between the two, yet the results did not confirm either. The comparison between abiotic and biotic treatments was not suitable in providing enough evidence to support one organic matter pool over another, yet it did support previous research showing that SOM plays an important role on water retention

capabilities. Because the proportion of MBC was overall higher compared to other soils, it suggested that the effects of microbial exudates may still be relevant and considered when it comes to sandy soil hydrology. It is proposed that the dynamics of the biofilm will dominate as the soil dries, sustaining thinning films longer due to the water being held within the viscoelastic walls. During evaporation these films sustained at higher matric potentials supporting water transport and during drainage the films continued to release water at a slow rate for a longer period of time, all of which contributes to the water retention in the soil. In order to distinguish if the results witnessed in this study are attributed to biofilms specifically, more research is needed to truly confirm which factors are impacting water dynamics directly.

4.2 Challenges

Evaporation

The HyProp is a very accurate device for obtaining the moisture retention curve, as can clearly be seen in the overlap of the data obtained from the various runs. However, for obtaining evaporation data, the HyProp was found to be too sensitive to laboratory conditions, especially vibrations and temperature variations. Because we were exploring the physical properties of delicate films that connect the drying front to the evaporation surface within a soil, variation within the laboratory were found to sever those films, forcing early transitions between S-1 and S-2. The HyProp method did prove to be a wonderful technique to formulate the soil water characteristic curve, evaluate the hydraulic conductivity of the soil, and obtain the total energy potential of films. If the HyProp is used to evaluate evaporation in the future, it should be done in a temperature regulated and vibration free room. Furthermore, using the experiment at low temperature and in a dark room may prevent formation of surface bio-crusts.

Drainage

Surface ponding caused inconsistency in the calculation of moisture lost. Next series of experiments should set the first tension step at about 3 cm, sufficient tension to pull the excess ponded water but still be less than the air entry value of the soil. This would give a better initial moisture value. Our lowest tension applied was 10 cm which was used to correct for the ponding issue but at the cost of a valuable data point. When installing a new soil sample into a column, at least two wetting and drying cycles are necessary to establish the drainage pattern within the soil. Until that is established, results will not be consistent. Repeated wetting and drying cycles caused movement of the microbial community through the porous plate of the tension funnel. Considering the porous plate was 10 – 15 μm, some biotic components left the system and contaminated the tubing. The pore size of the porous plate in the tension funnel also set limitations for the maximum amount of head that could be applied. Only 60 cm could be maintained before air entry of the ceramic plate was reached. If the hanging-water-column method is used again then a finer porous plate should be used to eliminate these issues.

Contamination

The most important lesson learned is how difficult it is to sustain an abiotic sample throughout the experimental stages. The abiotic state is challenging to maintain, however, fortuitously gave us an excellent opportunity during the experiment to compare biotic and abiotic conditions for the same pore architecture and pore size distribution. It would beneficial to have multiple treatments to tease out the effects of microbial exudates. The abiotic sample was vastly different from the biotic, therefore it is difficult to pinpoint what is really causing the impact on water dynamics. Techniques such as fumigation or irradiation may be ways to obtain different abiotic treatments while not impacting soil structure.

4.3 Synthesis of Results

The data was analyzed in consideration of the limitations and capabilities of the experiments that are mentioned above. We have confidence in stating the following:

The HyProp

During evaporation, the soil moisture retention function revealed that a biological presence in the soil had a strong positive impact on the retention properties of a sandy soil which are visible in the water retention curves created with the HyProp data. The biotic soil always had a higher porosity and therefore a higher initial moisture content. At equivalent matric potentials, the biotic treatment held more moisture than the abiotic treatment. Although there was variability between runs and samples, in every case, the biotic soil held more moisture than the abiotic soil under the same tension and evaporative demand. The changes in retention cannot be directly attributed to water absorption by exudates because there is insufficient evidence to support this fact and it may be associated with by microbially induced changes to the pore geometry. The laboratory did give convincing evidence during the fourth run when the effect of biofilms on evaporation was discernable. Two key observations were made after reviewing these results. Biofilms permit a longer duration of S-1 evaporation thus extracting more water from the soil profile. This is presumably because the biological component is able to keep the film from thinning and snapping while sustaining a higher matric potential than an abiotic film. Microbial exudates allow the soil to extract water from deeper into the soil profile which is quantified by the ‘estimated’ drying depth. This depth is considered to be the thickness of the capillary fringe, where moisture is left in films and the drying zone is not completely dry. It is estimated that the biotic treatment would permit a much deeper drying depth, with more moisture remaining within this drying zone. Biofilms can sustain the necessary hydraulic conductivity to much drier

conditions relative to abiotic films. It is notable that the matric potential for the biotic soil began to increase a full day after the abiotic soil while the evaporation rate was the same. The data supports the model that biofilms with greater tensile strength are active in redistributing soil moisture through the cylinder towards the evaporation surface.

Hanging-water-column

The Static Stepwise experiments showed no significant difference between the 3-hr and the 12-hr moisture retention curves, yet at certain tensions there were slight differences indicating water was being released from films after capillary drainage. On the other hand, there was a significant difference between the biotic and abiotic treatments. The biotic treatment released a greater volume of water at each controlled tension compared to the abiotic. The biotic soils had a greater initial moisture content, but lost most of the water at low tensions, presumably from the existence of larger pores associated with formation of micro-aggregates. This was also evident during the Dynamic Drainage experiment. The tension was held at 60 cm, while each treatment was allowed to drain freely over a period. During this period, the biotic soils lost a large volume of water immediately. Again, presumably due to the formation of micro-aggregates caused by exudates cementing together particles within the biotic treatments. After the initial volume of water was lost out of the large pores, the biotic soil continued to drain slowly for a longer period of time. This was interpreted as being caused from the release of water from biofilms. As the soil is draining, the hydraulic conductivity during capillary drainage was higher in the biotic treatment and then reduces as drainage continues. The reduction is attributed to film drainage thus could represent the hydraulic conductivity of the film. As water movement slows and the hydraulic conductivity decreases, water is transported through biofilms as well as water films containing microbial exudates. It appears that during drainage both the micro-aggregate structure

and the presence of biotic films are causing changes to the water dynamics of sandy soil. It is important to note that the numerous wetting and drying cycles could have influenced biofilm growth causing pore clogging. This clogging could negatively affect water retention capabilities.

4.4 Conceptual Model

The Conceptual Model illustrates the biotic and abiotic treatments at two matric potentials, the first column at 0 kPa and the second column at -10 kPa. Water films are represented by dotted lines, teal indicates the biotic and grey the abiotic (Figure 67). As matric potential increases, there is a difference in the moisture content between the two treatments. The biofilms in the biotic treatment have a porosity created by the entangled components, allowing more moisture retained within this matrix. The water films within the biotic treatment are also thicker comparatively due to the presence of these exudates, sustaining a connected water phase through liquid bridges even at higher matric potentials which link pools of water throughout the soil. The abiotic treatment has films which have broken at this matric potential, leaving islands of water trapped between particles. Evaporation and drainage were both affected by the presence of these

thick films as well as the sustained films during further drying.

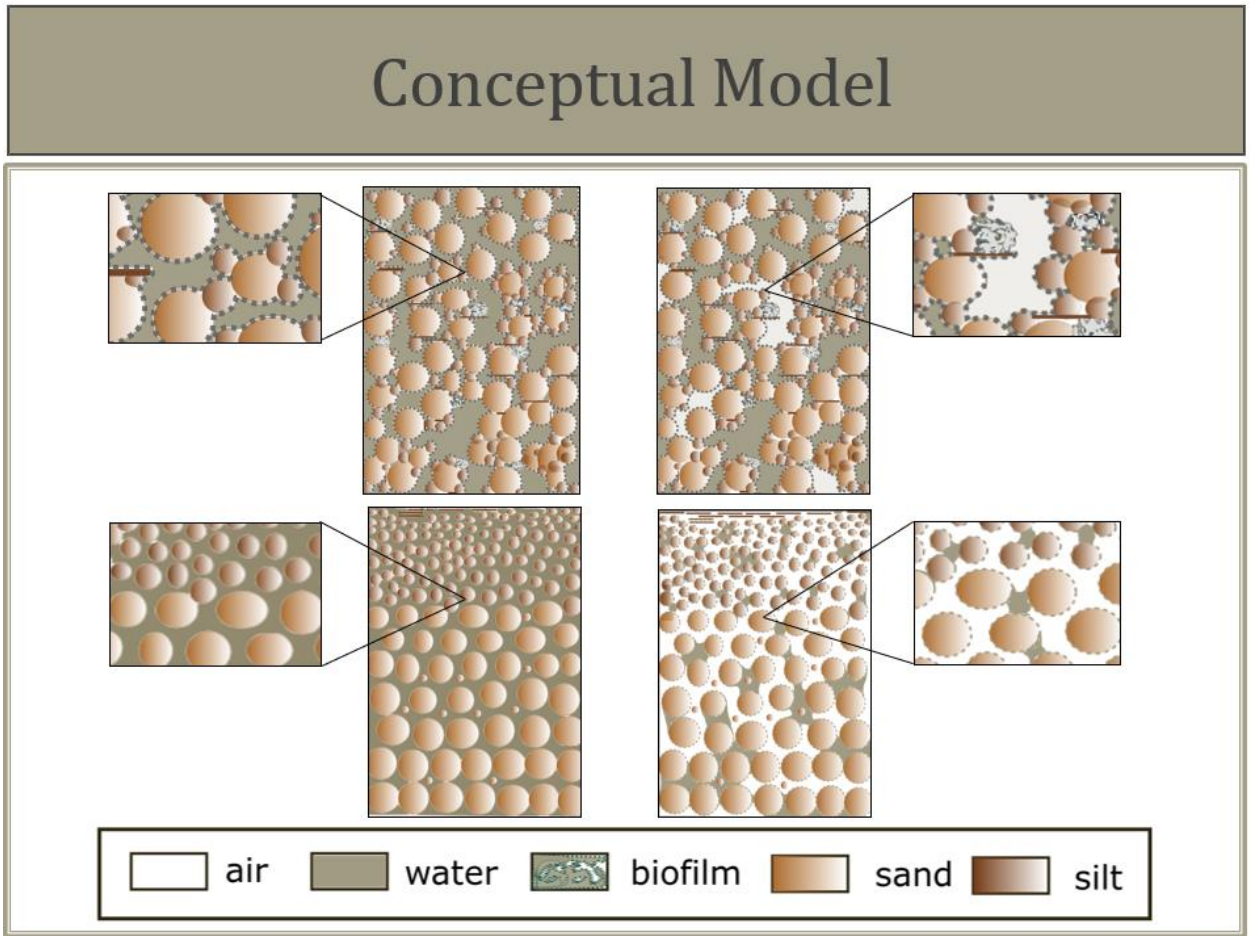

Figure 67. Conceptual Model of the impacts of microbial exudates on sandy soil hydrology during the drying cycle.

Chapter 5: Conclusion

Most sandy soils in arid to semi-arid agricultural regions have limited organic matter and the addition of organic matter is used to increase water retention. Organic matter influences soil properties by reducing the bulk density, increasing the porosity as well as the nutrient availability. This plays an important role in plant growth specifically by increasing water retention capabilities. It has been proven beneficial for optimal crop yield yet the mechanism responsible for this effect on water retention is truly unknown. Understanding the reason organic matter affects these properties is important to assess to improve agricultural management in areas that are subjected to drought. A certain proportion of organic matter comes from microbial biomass. This could be associated with the retention capabilities particularly because microbes produce exudates composed of polysaccharides (Flemming and Wingender 2010). In fact, it has been found that polysaccharides from exudates directly influence water dynamics (Read *et al.* 2003; Carminati *et al.* 2010; Carminati *et al.* 2011; Ahmed *et al.* 2014; Zarebanadkouki *et al.* 2014). Much of this research uses models to mimic the behavior of exudates which ultimately exaggerates the effects of these materials, leading to conclusions which may not accurately represent natural field conditions (Zhang *et al.* 2008; Moradi *et al.* 2011; Peng *et al.* 2011; Zarebanadkouki *et al.* 2012; Ahmed *et al.* 2016; Benard *et al.* 2018). The goal of this research was to investigate the water dynamics affected by the natural abundance of exudates found in the microbial biomass. The proportion of microbial biomass from organic matter content was quantified; which represented the natural abundance of microbial exudates. Microbial exudates are produced to form a matrix surrounding a community of cells called a biofilm. Water flows differently through the part of the pore without the biofilm than within. Inside the matrix of the biofilm there are entwined components of not only polysaccharides but also proteins, nucleic

acids, and lipids (Flemming and Wingender 2001a, 2001b) forming pores which have the capacity to retain and release water through viscoelastic walls (Stewart 1998; Billings *et al.* 2015b). Water dynamics of the biofilm are different than the water dynamics of the bulk soil, therefore an increase in biofilm growth and water retention capabilities are directly proportional. If biofilms have the capacity to grow uniformly throughout the pore, it could potentially cause pore clogging. If pore clogging occurs the water dynamics are affected differently, yet the natural abundance of biofilm did not 'diffuse homogenously' throughout the pore similarly to studies with root exudates (Carminati 2012). It appears that the lower abundance of microbial biomass results in a larger fraction of the pore volume which is not influenced by biofilms, assuming microbial biomass influences the amount of biofilm produced. The proportion of the pore without biofilm empties by the end of capillary drainage, while water remaining inside the biofilm continues to be released. As the soil continues to dry, either by means of evaporation or drainage, biofilm rheology begins to control water dynamics. The saturated hydraulic conductivity of the biofilm is reduced comparatively influencing water retention capabilities, yet as the soil continues to dry the hydraulic conductivity does not decrease rapidly compared to an abiotic film, allowing water transport within the soil profile. Redistribution of moisture through sustained films at high matric potentials is agronomically relevant by increasing the plant available water and increasing nutrient distribution in support of microbial communities. This becomes especially important during periods of drought. Organic matter also affects the pore size distribution by the formation of micro-aggregates which could be caused from exudates acting as cementing agents. The particles are glued together forming non-porous aggregates. The increased proportion of large particles form larger pore spaces affecting sandy soil hydrology by adjusting the water retention curve. The formation of micro-aggregates also provides a rougher

surface area in support of film development. The effects of the natural abundance of microbial exudates are in fact noteworthy, whether the cause is from the formation of micro-aggregates, biofilm dynamics or the combination of the two. It was found that microbial exudates affect sandy soil hydrology favorably. Although it was difficult to isolate the relative contribution from each mechanism with the two types of experiments selected for this study, it was clear that biofilms exhibit different hydrodynamics than abiotic films, that organic matter changes pore structure in hydrologically favorable direction, and that these advantages are of agronomic significance. Future research will be able to improve upon techniques to further isolate the mechanisms and processes behind these effects.

Bibliography

Ahmed, MA, Kroener, E, Benard, P, Zarebanadkouki, M, Kaestner, A, Carminati, A (2016) Drying of mucilage causes water repellency in the rhizosphere of maize: measurements and modelling. *Plant and Soil* **407** (1-2), 161-171. 10.1007/s11104-015-2749-1

Ahmed, MA, Kroener, E, Holz, M, Zarebanadkouki, M, Carminati, A (2014) Mucilage exudation facilitates root water uptake in dry soils. *Functional Plant Biology* **41** (10-11), 1129-1137. 10.1071/Fp13330

Awale, R, Emeson, MA, Machado, S (2017) Soil organic carbon pools as early indicators for soil organic matter stock changes under different tillage practices in inland Pacific Northwest. *Frontiers in Ecology and …*

Balota, EL, Colozzi-Filho, A, Andrade, DS, Dick, RP (2003) Microbial biomass in soils under different tillage and crop rotation systems. *Biology and Fertility of Soils* **38** (1), 15-20. 10.1007/s00374-003-0590-9

Barré, P, of Science, H-PD (2009) Rheological stabilization of wet soils by model root and fungal exudates depends on clay mineralogy. *European Journal of Soil Science* 10.1111/j.1365-2389.2009.01151.x

Bauer, A, Black, AL (1981) Soil Carbon, Nitrogen, and Bulk Density Comparisons in Two Cropland Tillage Systems after 25 Years and in Virgin Grassland 1. *Soil Science Society of America Journal*

Benard, P, Zarebanadkouki, M, Carminati, A (2018) Impact of Pore-Scale Wettability on Rhizosphere Rewetting. *Frontiers in Environmental Science* **6** 16. 10.3389/fenvs.2018.00016

Bengough, AG (2012) Water Dynamics of the Root Zone: Rhizosphere Biophysics and Its Control on Soil Hydrology. *Vadose Zone Journal* **11** (2), 10.2136/vzj2011.0111

Billings, N, Birjiniuk, A, Samad, TS, Doyle, PS, Ribbeck, K (2015a) Material properties of biofilms—a review of methods for understanding permeability and mechanics. *Reports on Progress in Physics* **78** (3), 36601.

Billings, N, Birjiniuk, A, Samad, TS, Doyle, PS, Ribbeck, K (2015b) Material properties of biofilms—a review of methods for understanding permeability and mechanics. *Reports on Progress in Physics* **78** (3), 36601.

Brookes, PC, Landman, A, Pruden, G, Jenkinson, DS (1985) Chloroform fumigation and the release of soil nitrogen: a rapid direct extraction method to measure microbial biomass nitrogen in soil. *Soil Biology and Biochemistry* **17** (6), 837-842.

Calhoun, FG, Hammond, LC, Caldwell, RE (1973) Influence of particle size and organic matter on water retention in selected Florida soils. *Proc Soil Crop Sci Soc Fla*

Carminati, A (2012) A Model of Root Water Uptake Coupled with Rhizosphere Dynamics. *Vadose Zone Journal* **11** (3), 10.2136/vzj2011.0106

Carminati, A, Benard, P, Ahmed, MA, M., Z (2017) Liquid bridges at the root-soil interface. *Springer* 10.3389/fenvs.2018.00016

Carminati, A, Moradi, AB, Vetterlein, D, Vontobel, P, Lehmann, E, Weller, U, Vogel, HJ, Oswald, SE (2010) Dynamics of soil water content in the rhizosphere. *Plant and Soil* **332** (1-2), 163-176. 10.1007/s11104-010-0283-8

Carminati, A, Schneider, CL, Moradi, AB, Zarebanadkouki, M, Vetterlein, D, Vogel, HJ, Hildebrandt, A, Weller, U, Schuler, L, Oswald, SE (2011) How the Rhizosphere May

Favor Water Availability to Roots. *Vadose Zone Journal* **10** (3), 988-998. 10.2136/vzj2010.0113

Carminati, A, Zarebanadkouki, M, Kroener, E, Ahmed, MA, Holz, M (2016) Biophysical rhizosphere processes affecting root water uptake. *Ann Bot* 10.1093/aob/mcw113

Carsel, RF, Parrish, RS (1988) Developing joint probability distributions of soil water retention characteristics. *Water Resources Research* 10.1029/WR024i005p00755

Carsel, RF, Research, P-RS (1988) Developing joint probability distributions of soil water retention characteristics. *Water Resources Research* 10.1029/WR024i005p00755

Chenu, C (1995) Extracellular polysaccharides: an interface between microorganisms and soil constituents. *Environmental impact of soil component interactions* **1** 217-233.

Cheshire, MV (1979) Nature and origin of carbohydrates in soils. *Nature and origin of carbohydrates in soils.*

Costerton, JW, Lewandowski, Z (1995) Microbial biofilms. *Annual Reviews in …*

Czarnes, S, Dexter, AR, Bartoli, F (2000) Wetting and drying cycles in the maize rhizosphere under controlled conditions. Mechanics of the root-adhering soil. *Plant and Soil* **221** (2), 253-271. Doi 10.1023/A:1004747323220

De Beer, D, Lewandowski, Z, Stoodley, P (1994) Liquid flow in heterogeneous biofilms. *Biotechnology and …*

De Beer, D, Stoodley, P (1995) Relation between the structure of an aerobic biofilm and transport phenomena. *Water Science and Technology*

Díaz-Zorita, M, Grosso, GA (2000) Effect of soil texture, organic carbon and water retention on the compactability of soils from the Argentinean pampas. *Soil and Tillage Research* **54** (1-2), 121-126. 10.1016/s0167-1987(00)00089-1

Donlan, RM (2002) Biofilms: microbial life on surfaces. *Emerg Infect Dis* **8** (9), 881-90. 10.3201/eid0809.020063

Flemming, HC, Wingender, J (2001a) Relevance of microbial extracellular polymeric substances (EPSs)--Part I: Structural and ecological aspects. *Water Sci Technol* **43** (6), 1-8.

Flemming, HC, Wingender, J (2001b) Relevance of microbial extracellular polymeric substances (EPSs)--Part II: Technical aspects. *Water Sci Technol* **43** (6), 9-16.

Flemming, HC, Wingender, J (2010) The biofilm matrix. *Nat Rev Microbiol* **8** (9), 623-33. 10.1038/nrmicro2415

Franzluebbers, AJ, Haney, RL (1996) Determination of microbial biomass and nitrogen mineralization following rewetting of dried soil. *Soil Science Society …*

Genuchten, VMT, Leij, FJ, Yates, SR (1991) The RETC code for quantifying the hydraulic functions of unsaturated soils. *The RETC code for quantifying the hydraulic functions of unsaturated soils*

Hillel, D (1998) Environmental soil physics: Fundamentals, applications, and environmental considerations. *Environmental soil physics: Fundamentals, applications, and environmental considerations*

Hillel, D (2012) Soil and water: physical principles and processes. *Soil and water: physical principles and processes*

Hollis, JM, Jones, RJA, Palmer, RC (1977) The effects of organic matter and particle size on the water-retention properties of some soils in the West Midlands of England. *Geoderma*

Jury, WA, Stolzy, LH (2018) Soil physics. *Handbook of Soils and Climate in Agriculture*

Kirkham, MB (2014) Principles of soil and plant water relations. *Principles of soil and plant water relations*

Minasny, B, McBratney, AB (2018) Limited effect of organic matter on soil available water capacity. *European Journal of Soil Science* **69** (1), 39-47. 10.1111/ejss.12475

Moradi, AB, Carminati, A, Vetterlein, D, Vontobel, P, Lehmann, E, Weller, U, Hopmans, JW, Vogel, HJ, Oswald, SE (2011) Three-dimensional visualization and quantification of water content in the rhizosphere. *New Phytol* **192** (3), 653-63. 10.1111/j.1469-8137.2011.03826.x

Mualem, Y (1976) A new model for predicting the hydraulic conductivity of unsaturated porous media. *Water Resources Research* 10.1029/WR012i003p00513

Naveed, M, Brown, LK, Raffan, AC, George, TS, Bengough, AG, Roose, T, Sinclair, I, Koebernick, N, Cooper, L, Hallett, PD (2018) Rhizosphere-Scale Quantification of Hydraulic and Mechanical Properties of Soil Impacted by Root and Seed Exudates. *Vadose Zone Journal* **17** (1), UNSP 170083

10.2136/vzj2017.04.0083

Nolasco, S (2018) Plot-Scale Field Investigations: Characterizing Water Motion in Sandy Agricultural Soils. *Oregon State University*

O'Toole, G, Kaplan, HB, Kolter, R (2000) Biofilm formation as microbial development. *Annual Reviews in Microbiology* **54** (1), 49-79.

Or, D, Phutane, S, Dechesne, A (2007) Extracellular Polymeric Substances Affecting Pore-Scale Hydrologic Conditions for Bacterial Activity in Unsaturated Soils. *Vadose Zone Journal* **6** (2), 298. 10.2136/vzj2006.0080

Peng, X, Hallett, PD, Zhang, B, Horn, R (2011) Physical response of rigid and non-rigid soils to analogues of biological exudates. *European Journal of Soil Science* **62** (5), 676-684. 10.1111/j.1365-2389.2011.01383.x

Pertassek, T, Peters, A, Durner, W (2011) HYPROP Data Evaluation Software User's Manual. *METER Group Inc.*

Peters, A, Iden, SC, Durner, W (2015) Revisiting the simplified evaporation method: Identification of hydraulic functions considering vapor, film and corner flow. *Journal of Hydrology* **527** 531-542. 10.1016/j.jhydrol.2015.05.020

Powlson, DS, Jenkinson, DS (1981) A comparison of the organic matter, biomass, adenosine triphosphate and mineralizable nitrogen contents of ploughed and direct-drilled soils. *The Journal of Agricultural Science* 10.1017/S0021859600037084

Rawls, WJ, Pachepsky, YA, Ritchie, JC, Sobecki, TM (2003) Effect of soil organic carbon on soil water retention. *Geoderma*

Read, DB, Bengough, AG, Gregory, PJ, Crawford, JW, Robinson, D, Scrimgeour, CM, Young, IM, Zhang, K, Zhang, X (2003) Plant roots release phospholipid surfactants that modify the physical and chemical properties of soil. *New Phytologist* **157** (2), 315-326. DOI 10.1046/j.1469-8137.2003.00665.x

Roberson, EB, Chenu, C, Firestone, MK (1993) Microstructural changes in bacterial exopolysaccharides during desiccation. *Soil Biology and Biochemistry*

Rosenzweig, R, Furman, A, Dosoretz, C, Shavit, U (2014) Modeling biofilm dynamics and hydraulic properties in variably saturated soils using a channel network model. *Water Resources Research* **50** (7), 5678-5697. 10.1002/2013wr015211

Sparling, GP (1992) Ratio of microbial biomass carbon to soil organic carbon as a sensitive indicator of changes in soil organic matter. *Soil Research* 10.1071/sr9920195

Stewart, PS (1998) A review of experimental measurements of effective diffusive permeabilities and effective diffusion coefficients in biofilms. *Biotechnology and Bioengineering* **59** (3), 261-272.

Stewart, PS (2003) Diffusion in biofilms. *Journal of bacteriology* 10.1128/JB.185.5.1485-1491.2003

Stewart, PS (2012) Mini-review: Convection around biofilms. *Biofouling* **28** (2), 187-198. 10.1080/08927014.2012.662641

Stewart, PS, Franklin, MJ (2008) Physiological heterogeneity in biofilms. *Nature Reviews Microbiology* **6** (3), 10.1038/nrmicro1838

Stoodley, P, De Beer, D, Lewandowski, Z (1994) Liquid flow in biofilm systems. *Applied and environmental …*

Traore, O, Groleau-Renaud, V, Plantureux, S, Tubeileh, A, Boeuf-Tremblay, V (2000) Effect of root mucilage and modelled root exudates on soil structure. *European Journal of Soil Science* **51** (4), 575-581. DOI 10.1111/j.1365-2389.2000.00348.x

Tuller, M, Or, D (2004) Retention of water in soil and the soil water characteristic curve. *Encyclopedia of Soils in the Environment* **4** 278-289.

Tuller, M, Or, D (2005) WATER RETENTION AND CHARACTERISTIC CURVE. *Elsevier*

Van Genuchten, MT (1980) A closed-form equation for predicting the hydraulic conductivity of unsaturated soils 1. *Soil Science Society of America Journal*

Vu, B, Chen, M, Crawford, RJ, Ivanova, EP (2009) Bacterial extracellular polysaccharides involved in biofilm formation. *Bacterial extracellular polysaccharides involved in biofilm formation* 10.3390/molecules14072535

Zacharias, S, Wessolek, G (2007) … Organic Matter Content from Pedotransfer Predictors of Soil Water Retention Abbreviations: MD, mean deviation; OM, organic matter content; PTF, pedotransfer …. *Soil Science Society of America …*

Zarebanadkouki, M, Kim, YX, Moradi, AB, Vogel, HJ, Kaestner, A, Carminati, A (2012) Quantification and Modeling of Local Root Water Uptake Using Neutron Radiography and Deuterated Water. *Vadose Zone Journal* **11** (3), 10.2136/vzj2011.0196

Zarebanadkouki, M, Kroener, E, Kaestner, A, Carminati, A (2014) Visualization of root water uptake: quantification of deuterated water transport in roots using neutron radiography and numerical modeling. *Plant Physiol* **166** (2), 487-99. 10.1104/pp.114.243212

Zhang, B, Hallett, PD, Zhang, G (2008) Increase in the fracture toughness and bond energy of clay by a root exudate. *European Journal of Soil Science* **59** (5), 855-862. 10.1111/j.1365-2389.2008.01045.x